University of New Mexico
UNM Digital Repository

Nuclear Engineering ETDs | Engineering ETDs

6-26-2015

SERPENT Modeling of the Transient Reactor Test Facility and Comparison with Measured Experimental Data

Joseph Templeton

Follow this and additional works at: https://digitalrepository.unm.edu/ne_etds

Recommended Citation
Templeton, Joseph. "SERPENT Modeling of the Transient Reactor Test Facility and Comparison with Measured Experimental Data." (2015). https://digitalrepository.unm.edu/ne_etds/45

This Thesis is brought to you for free and open access by the Engineering ETDs at UNM Digital Repository. It has been accepted for inclusion in Nuclear Engineering ETDs by an authorized administrator of UNM Digital Repository. For more information, please contact disc@unm.edu.

Joseph Paul Templeton
Candidate

Nuclear Engineering
Department

This thesis is approved, and it is acceptable in quality and form for publication:

Approved by the Thesis Committee:

Dr. Cassiano R.E. de Oliveira, Chairperson

Dr. Patrick McDaniel

Dr. Robert D. Busch

SERPENT MODELING OF THE TRANSIENT REACTOR TEST FACILITY AND COMPARISON WITH MEASURED EXPERIMENTAL DATA

BY

JOSEPH PAUL TEMPLETON

BSAST, NUCLEAR ENGINEERING TECHNOLOGY,
THOMAS EDISON STATE COLLEGE, 2012

THESIS

Submitted in Partial Fulfillment of the
Requirements for the Degree of

MASTER OF SCIENCE
NUCLEAR ENGINEERING

The University of New Mexico
Albuquerque, New Mexico

MAY 2015

DEDICATION

To Amanda, you have been there for me every step of the way. I can't thank you enough for not only the help you have provided. I would also like to dedicate this work to my parents and family, without you none of this would have been possible. I have been fortunate enough to have an amazing family, all of which has made a profound and lasting impression upon me for the better.

AKNOWLEDGMENTS

First and foremost I would like to thank Dr. Cassiano R.E. de Oliveira Chair of my Thesis Committee and my faculty advisor. You have given me room to work but always been there when I needed help. Without the cumbersome work collecting all the reference material this research may have never happened.

I would also like to thank the members of the Thesis Committee, Dr. Patrick McDaniel, your insight into the TREAT reactor has been invaluable. Dr. Robert Busch you have been there to help me whenever I've needed it. I am extremely grateful to have taken the laboratory class you taught. Actually performing such experiments as approach to criticality and control rod calibrations is a learning experience far beyond that of any book.

I would like to thank Dr. Mark DeHart for his guidance. Your advice in regards to the graphite and free carbon thermal neutron cross section ratios proved to be extremely important to modeling the reactor. Having you available to answer questions about the core as they arose has helped me immensely.

Finally I would like to thank all of the faculty that have taught me along the way. Dr. Forrest Brown your vast knowledge of Monte Carlo methods has given me an understanding of how Monte Carlo codes work in addition to the ability to use them. Dr. Adam Hecht, your passion for teaching and the enthusiasm you bring to the class room are unmatched. Dr. Gary Cooper you are an excellent teacher who is very concise while still being thorough. You have a way of explaining complicated things in a manner that is easy to understand. Dr Anil Prinja you raise your students to the standards you know they are capable of.

SERPENT MODELING OF THE TRANSIENT REACTOR TEST FACILITY AND COMPARISON WITH MEASURED EXPERIMENTAL DATA

by

Joseph Paul Templeton

BSAST, Nuclear Engineering Technology, Thomas Edison State College, 2012
M.S., Nuclear Engineering, University of New Mexico, 2015

ABSTRACT

Following the events at the Fukushima Daiichi nuclear power plant complex on March 11th 2011, there is an increased need for research into accident tolerant light water reactor fuels. In addition to the need for accident tolerant fuels testing there is a rising demand for clean renewable energy and the design of many generation IV reactors to fill the role which will require testing of such reactors and their fuels. Calculations and simulations are vital for the development and initial testing of these fuels, however ultimately experiments must be performed that push the fuels to the limits of their safety margins and beyond thus providing proof of concept. The Transient Reactor Test (TREAT) Facility is designed to perform transient testing to support a basic understanding of nuclear fuel behavior under such off-normal conditions (Idaho National Laboratory, 2009).

The TREAT Facility was an air cooled, graphite moderated, thermal spectrum reactor designed to test fast reactor fuels in over power and under cooling scenarios. The TREAT facility operated for 35 years. During this time the test facility conducted

thousands of transients and hundreds of tests for a wide variety of reactor development programs and fuel types, with a distinguished history of producing significant safety experiment results (Crawford et al., 1999). Return to operable condition and resumption of testing is currently under consideration by the Department of Energy. TREAT could provide a facility for testing of high-bumup LWR elements, CANDU reactor elements, and innovative fuel element designs for reactors of the future. (Crawford et al., 1998)

Reliable computer modeling of the TREAT reactor can be used to assist in the design and setup of experiments performed by the TREAT reactor. If transients can be accurately simulated using computer models then these can be compared to the current techniques for calculating the necessary parameters such as the number of fuel assemblies, control rod height and time required to achieve the desired total energy deposition in a test material. This additional information may help to confirm the validity of the predicted parameters. Additionally computer models of TREAT may be used in an effort to design LEU fuel assemblies to replace the HEU fuel assemblies currently used in the TREAT core.

TABLE OF CONTENTS

DEDICATION ..... **iii**

AKNOWLEDGMENTS ..... **iv**

TABLE OF CONTENTS ..... **vii**

LIST OF FIGURES ..... **x**

LIST OF TABLES ..... **xiii**

ACRONYMS AND OTHER NOTATIONS ..... **xiv**

CHAPTER 1: INTRODUCTION TO TREAT **1**

1.1 Design 3

1.1.1 Fuel 4

1.1.2 Assemblies 5

1.1.3 Control Rods 6

1.1.4 Permanent Reflector 8

1.1.5 Reactor Cooling 10

1.2 Operation 10

CHAPTER 2: SERPENT **14**

2.1 Monte Carlo 14

2.2 Serpent 2 18

CHAPTER 3: SERPENT MODEL OF TREAT **21**

3.1 Spatial Design 21

3.1.1 Spherical Model 21

3.1.2 Detailed Model 22

3.2 Various Changes to the Model 24

3.3 Homogenized Core 32

CHAPTER 4: REACTOR PHYSICS COMPARISONS 34

4.1 Temperature Coefficient of Reactivity 34

4.2 Control Rod Worth 44

4.3 Neutron Flux Distribution 46

4.4 Prompt and Delayed Neutronics 49

CHAPTER 5: CONCLUSION AND FUTURE WORK 53

5.1 Conclusion 53

5.2 Future Work 53

APPENDIX A: SPREADSHEETS AND CALCULATIONS 55

A.1 Number Density Calculations 55

A.2 Minimum Loading TREAT k-effective 57

A.3 Temperature Coefficient of Reactivity 58

A.4 Control Rod Worth 60

A.5 Neutron Flux Distribution 62

A.6 Effective Multiplication Factor Comparisons 67

A.7 Thermal Expansion 67

A.8 Homogenization 73

APPENDIX B: DIAGRAMS AND DRAWINGS 78

APPENDIX C: APPENDIX C: CODES 80

C.1 Spherical Model 80

C.2 Revision 0.0.....81

C.3 Revision 0.4.....84

C.4 Revision 4.....88

C.5 Revision n.....93

C.6 Revision p.....99

REFFERENCES 105

LIST OF FIGURES

Figure 1.1: Cutaway of the TREAT reactor. 1

Figure 1.2: TREAT various assemblies. 3

Figure 1.3: TREAT Standard Fuel Assembly 5

Figure 1.4: Shutdown Control Rod. 7

Figure 1.5: Radial cutaway of TREAT highlighting the permanent reflector. 9

Figure 1.6: TREAT air cooling system. 10

Figure 2.1: Fission source convergence. 19

Figure 2.2: Reaction rate mesh of TREAT spherical model. 20

Figure 3.1: Octa Serpent input. 22

Figure 3.2: TREAT assemblies lattice structures of various revisions.. 29

Figure 4.1: Cross section data for carbon and U-235. 35

Figure 4.2: Doppler-broadening of a resonance. 36

Figure 4.3: Comparison of temperature coefficients.. 40

Figure 4.4: Reactivity curve for TREAT using several values for neutron lifetime 44

Figure 4.5: Control rod 1 calibration. 45

Figure 4.6: Control rod 1 calibration comparisons. 46

Figure 4.7: Normalized radial flux measurements. 47

Figure 4.8: Normalized axial flux. 48

Figure 4.9: Normalized radial flux, with improper rod orientation. 49

Figure 4.10: Normalized radial flux, with proper rod orientation. 49

Figure 4.11: Effective delayed neutron parameters for TREAT. 50

Figure 4.12: Transfer function prompt neutron lifetime measurements. 51

Figure 4.13: Reactor physics parameter comparisons. 52

Figure A.1: Number densities used for all of the core materials with the exception of the B_4C and carbon steel of the control rods. 55

Figure A.2: Core graphite number densities. 56

Figure A.3: The calculations for the number densities of the B_4C and carbon steel of the control rods. 56

Figure A.4: Conversion of 60 inhr to the k-effective of 1.0015666. 57

Figure A.5: Revision p temperature coefficient calculations.....58

Figure A.6: Plots of change in k-effective vs temperature. 59

Figure A.7: Calculation and plot of control rod worth of revision p.. 60

Figure A.8: Critical rod height or rod height to achieve a desired reactivity can be easily estimated with rod position plotted against k-effective. 61

Figure A.9: Normalized neutron flux at various axial and radial points and their calculated uncertainties. 62

Figure A.10: Axial plot of normalized thermal flux for revision p. 63

Figure A.11: Normalized radial thermal neutron flux. 63

Figure A.12: Axial neutron flux extrapolation of data points from the plots provided in ANL-6173. 64

Figure A.13: Radial neutron flux extrapolation of data points from the plots provided in ANL-6173. 65

Figure A.14: Data points extrapolated from axial and radial thermal neutron plots. 66

Figure A.15: Effective multiplication factor of models 0.0 through 0.3. 67

Figure A.16: Effective multiplication factor of models 0.4 through k. 68

Figure A.17: Effective multiplication factor of models m through p. 69

Figure A.18: Change in planes perpendicular to z by thermal expansion. 70

Figure A.19: Change in density by thermal expansion.....71

Figure A.20: Temperature coefficient comparison with thermal expansion. 72

Figure A.21: Octagonal cylinder input. 73

Figure A.22: The calculated and serpent output volumes of the materials.....75

Figure A.23: Number densities of all homogenized assemblies and assembly sections. ..77

Figure B.1: Drawing of standard fuel assembly for revision 0.0 TREAT model.....78

Figure B.2: Radii for the octagonal cylinder surface input cards. 79

LIST OF TABLES

Table 3.1: HEU pertcentages of isotopes. 25

Table 4.1: Measured isothermal temperature coeficients of reactivty. 38

ACRONYMS AND OTHER NOTATIONS

Acronyms

ANL	Argone National Labratories
CANDU	Canada deuterium uranium reactor
CDF	cumulative distribution function
CP-2	Chicago Pile-2
HEU	highly enriched uranium
HTGR	high-temperature gas-cooled reactor
LEU	low-enriched uranium
IFP	iterated fission probability
INL	Idaho National Labratories
LMFBR	liquid metal fast breeder reactor
LWR	light water reactor
MFC	Materials and Fuels Complex
PDF	prbability distribution function
RAM	random access memory
RIA	reactivity initiated accident
TREAT	Transient Reactor Test Facility

Abbreviations

A	mass number
A/O	atomic weight percent
b	barns
B_4C	boron carbide

^{o}C	degrees celcius
cm	centimeters
E	energy
in.	inches
k	Boltzmann constant
K	kelvin
lbs.	pounds
m	mass
mil	0.001 inches
msec	milisecond
O.D.	outside diameter
ppm	parts per million
$\vec{r}$	position vector
t	time
T	temperature
U_3O_8	triuranium octoxide
UO_2	uranium dioxide
v	velocity (magnitude)
$\vec{v}$	velocity
V	volume
W/O	weight/percent
Z	atomic number

Notations

β	delayed neutron fraction
β_{eff}	effective delayed neutron fraction
Γ	total line width
Γ_D	Doppler width
Γ_γ	radiative line width
λ	decay constant
μ	cosine of the scatter angle
ν	average number of neutrons produced per fission event
ξ	random number
ρ	reactivity, (k-1)/k
σ	microscopic cross section
Σ	macroscopic cross section
$\vec{\Omega}$	direction (unit) vector
ℓ	prompt neutron lifetime
Δk	change in the effective multiplication factor

CHAPTER 1: INTRODUCTION TO TREAT

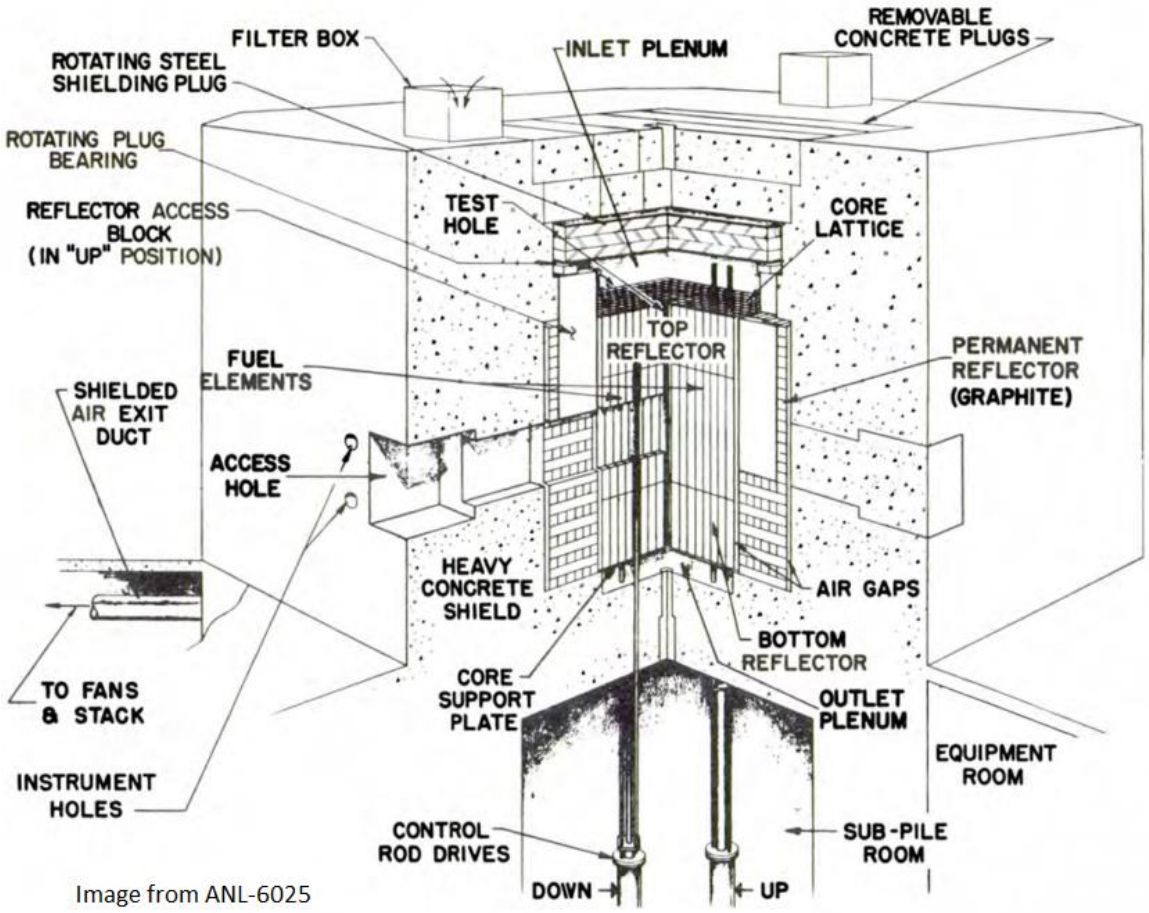


Figure 1.1: Cutaway of the TREAT reactor.

Argonne National Labs (ANL) originally constructed TREAT as part of its Argonne National Labs West Division which is now Idaho National Labs (INL). The TREAT facility is located 28 miles west of Idaho Falls, at the Materials and Fuels Complex (MFC) of INL. The MFC also houses facilities designed to handle and process irradiated nuclear fuel assemblies such as the Fuel Conditioning Facility, the Hot Fuel Examination Facility (post-irradiation examination) and the Fuel Manufacturing facility which puts TREAT in the perfect location to perform a multitude of fuel tests (Campbell).

In the 1980s TREAT underwent a major overhaul in order to increase its capability to support Liquid Metal Fast Breeder Reactor (LMFBR) safety program and provide a unique environment for testing thermal reactor design computational methods and data over spectral and temperature regimes that had not previously been encountered. (Bhattacharyya, 1982) Originally TREAT could not accommodate test clusters of size larger than 7 pins because of reactivity and size restrictions. Following the upgrade TREAT could test clusters of up to 37 pins (each pin having a .23”-.27” O.D.). Although TREAT was designed to evaluate fast reactor fuels, since the upgrade, it has also been used for light water reactor fuel testing as well as other exotic special purpose fuels (Ehresman).

The TREAT facility tested fuel by subjecting test materials to a neutron pulse that simulated conditions ranging from a mild upset to a severe reactor accident. The severity of the material conditions depended on such factors as core power, the power coupling factor and the amount of time the test material was subjected to the high neutron flux (the length of the transient). To test the material it was placed axially through the center of the core, the core was then brought to a power level substantial enough to heat the material to that of the normal operating conditions that the material would be subjected to. From there the transient rod was rapidly removed via pneumatics (later changed to hydraulics) thus simulating the reactivity initiated accident (RIA). The transient could be terminated after a predetermined amount of time by pneumatically inserting shutdown rods via the transient control system however rod insertion is not required in order to terminate the transient. Transients were self-limiting due to the very large temperature coefficient of reactivity thus a scram was not required to end the transient or to prevent damage to the

core. This inherent stability made the TREAT reactor exceptionally safe. The TREAT core itself was air cooled but during the short times of the transients air cooling was generally not used and would have had no relative effect. The core would not overheat due to its high carbon to Uranium 235 atomic ratio (10,000/1) as reported in ANL-6034. The high heat capacity of carbon in the uranium oxide-graphite matrix acted as an enormous heat sink and was an excellent thermal conductor.

1.1 Design

The TREAT core consisted of a square 19x19 (76”x76”) lattice structure of fuel, reflector, control rod and other various assemblies some of which are shown in figure 1.2 from ANL-6034. ANL-6034 has been my source for all design specifications, unless otherwise specified. All assemblies were 3.96”x3.96” with chamfered edges and a 0.04”

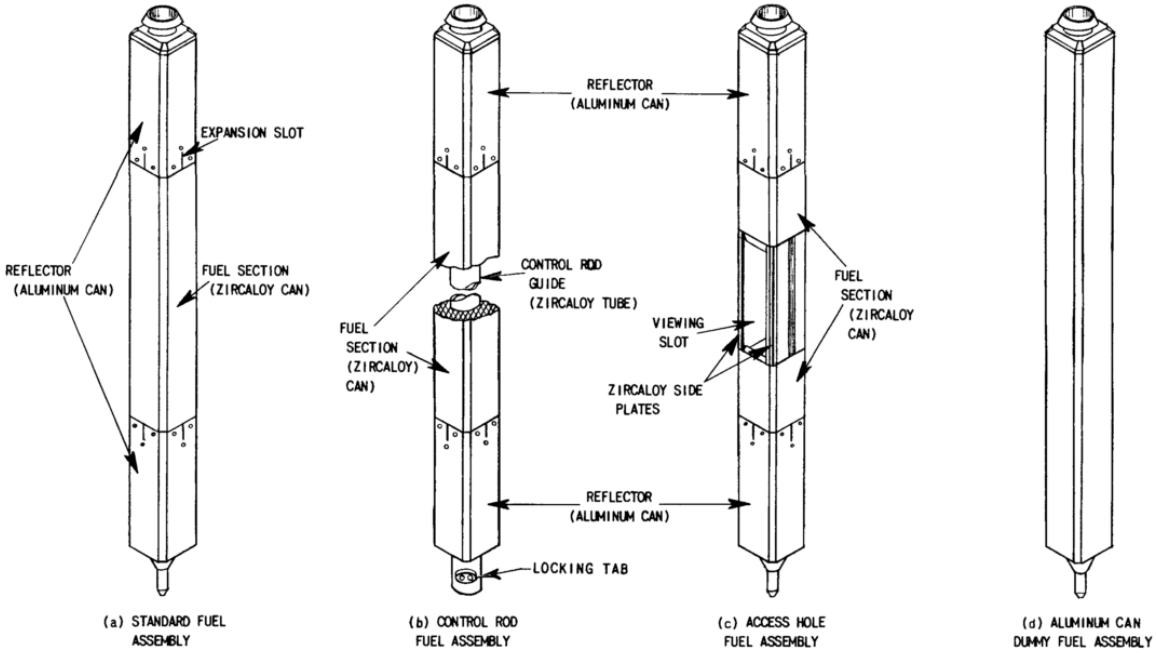


Figure 1.2: TREAT various assemblies.

gap between assemblies to allow for air flow. The chamfered edges form a $\frac{5}{8}$ in. square cooling channel at the corners of the elements when they were loaded in the core matrix.

Core assemblies were interchangeable with a minimum core loading of 133 fuel assemblies. All assemblies were eight feet tall however the fuel section of assemblies was four feet tall with 2 feet of reflector above and 2 feet of reflector below. Surrounding the core radially is two feet of permanent graphite reflector.

1.1.1 Fuel

The reactor fuel was made by mixing and grinding highly enriched uranium (93.1 W/O U-235) oxide (U_3O_8) with graphite flour and pitch which was then die pressed at 5000 psi and 100^{o}C into 3.809" square blocks that are 8" high with chamfered corners. After the blocks where formed they were then baked at 950^{o}C for two weeks which transforms the pitch to carbon and reduces the U_3O_8 to UO_2. It should be noted that this temperature is not high enough to attain a graphite crystal structure thus the carbon crystal structure is a complex mixture of graphite particles in a nongraphitized elemental carbon matrix (Swanson and Harrison, 1988). During the baking process borated stainless steel dividers were used between the blocks to reduce the risk of criticality however some boron diffused into the graphite. There are some discrepancies between the reports as to the exact boron content within the graphite-urania fuel blocks. The average boron concentration reported in ANL-5963, ANL-6034 and ANL-6174 was 6 ppm. ANL-6115, which reports specifically on the results of spectro-chemical and chemical analyses of the fuel, concludes that the boron content was 7.6 ppm. Although I have run calculations using both 6 ppm and 7.6 ppm the majority of my calculations were ran using 7.6 ppm boron concentration as I believe that to be the more correct of the two.

1.1.2 Assemblies

The fuel region of standard fuel assemblies was made of six 8 in. long fuel blocks placed within a zircaloy 3 clad can thus equating to a 4 foot high fuel region. The zircaloy cladding of the can was 25 mils thick around the sides with a 55 mils void between the fuel and the cladding. At the ends of the cans a $\frac{1}{4}$ in. ribbed zirconium spacer was placed in order to delay heat transfer from the fuel to the reflector. Finally $\frac{3}{32}$ in. zircaloy endcaps were welded on thus completing the fuel section of the fuel assembly. The fuel blocks were outgassed via an outgas tube that was attached a top the cans of fuel. This outgas tube remained in place for all fuel assemblies and in my model is represented as a void in the reflector above the fuel.

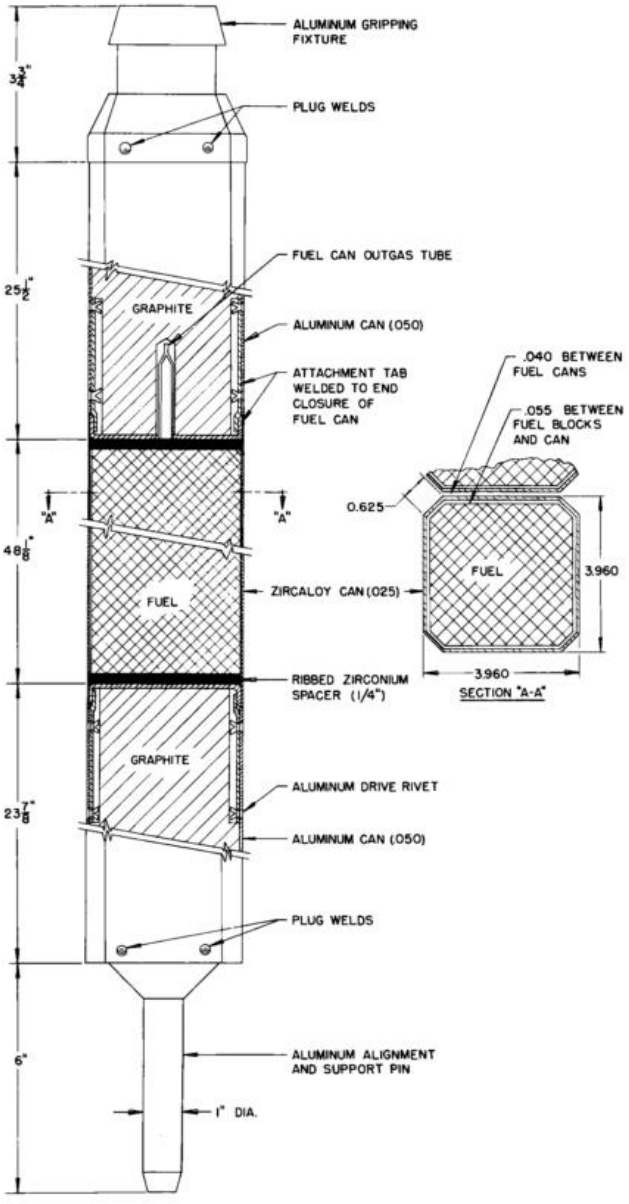


Figure 1.3: TREAT Standard Fuel Assembly

The reflector portions above and below the fuel of the fuel assemblies were graphite machined from the Chicago Pile-2 (CP-2) reactor. The graphite reflector was clad in aluminum 6063 cladding 50 mils thick. Riveted to the aluminum cladding were zircaloy tabs which

were then resistance welded to the fuel section of the fuel assemblies. In addition to a section of the graphite being machined out to provide space for the outgas tube, sections of graphite were also removed to account for the rivets and zircaloy tabs. I was not able to find any citable documentation defining these dimensions and I will discuss this further when I describe how I modeled the reactor in Chapter 3. As reported in ANL-6115 the boron content of the reflector graphite was also found to be higher than that originally specified at 1 ppm which is the concentration I used in my model. Figure 1.3 shows cutaways of a fuel assembly. In figure 1.3, from ANL-6034, it should be noted that there is a discrepancy from what is written in the report. The image portrays that the distance from the bottom of the lower zircaloy endcap of the fuel section to the top of the upper endcap as being $48\frac{1}{8}$ in. however I believe this distance should in fact be $48\frac{11}{16}$ in. given that the fuel is 48 in. each zirconium spacer is $\frac{1}{4}$ in. and each zircaloy endcap is $\frac{3}{32}$ in.

The control rod fuel assemblies were essentially identical to the standard fuel assemblies accept that a $\frac{1}{8}$ in. thick $2\frac{1}{4}$ in. O.D. zircaloy 2 guide tube ran through the axial center with a 40 mils thick void between the zircaloy guide tube and the fuel. This void is not mentioned in any text that I have access to and I will also discuss this issue further in Chapter 3.

1.1.3 Control Rods

The TREAT control rods were made up of three sections the first two of which were interchangeable depending on desired use. If the rod was desired to be used as a normal shutdown rod then the upper portion of the rod was boron carbide (B_4C) powder, compressed to a minimum density of 1.6 g/cc, housed within a $\frac{1}{8}$ in. thick carbon steel

tube with an O.D. of $1\frac{3}{4}$ in. The carbon steel tube was Kanigen nickel plated for corrosion resistance at elevated temperatures. This poison section of the rod was five feet long as was the zircaloy follower section. For normal shutdown rods the middle section was the zircaloy follower. The zircaloy follower section was made up of graphite rods housed within a $\frac{1}{8}$ in. thick zircaloy 2 tube with an O.D. of $1\frac{3}{4}$ in. If the control rod was desired to be used as a transient rod the poison and zircaloy sections are swapped thus the upper section was the zircaloy follower and the middle section was poison. The final section was the steel follower section and was seven feet of $\frac{1}{8}$ in. thick carbon steel tube with an O.D. of $1\frac{3}{4}$ in. The first two feet of which contained an extra-long (10 in.) male fitting to provide radiation shielding when the rod was in the shutdown position with the remainder of the two feet being comprised of graphite. The

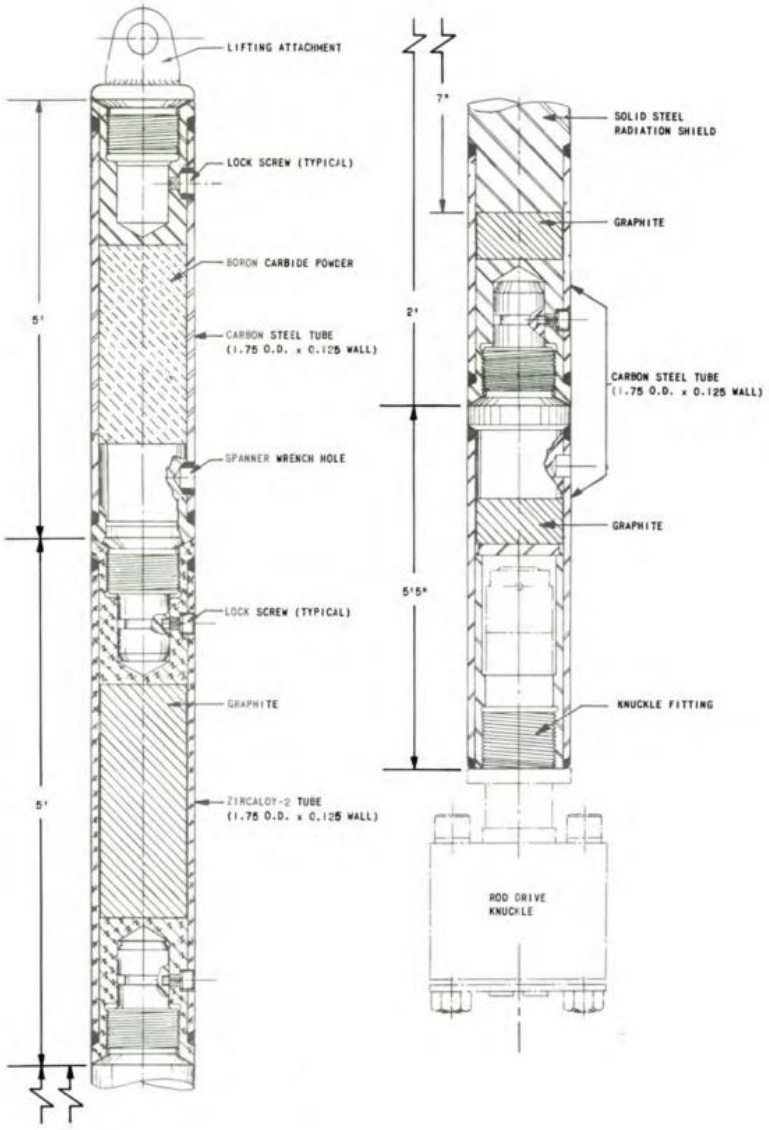


Figure 1.4: Shutdown Control Rod.

last five feet of the steel follower section was filled with graphite and the end plug was threaded to receive the drive knuckle. Figure 1.4 shows an axial cutaway of a control rod.

Besides standard fuel assemblies and control rod assemblies many other assemblies were manufactured for the core. Zircaloy clad dummy assemblies were made with the exact same specifications as the standard fuel assembly accept that reflector graphite was loaded into the fuel region instead of graphite-urania fuel blocks. The zircaloy clad dummy assemblies were located between the standard fuel assemblies and aluminum dummy assemblies to act as a thermal barrier for the aluminum clad assemblies. Aluminum clad dummy assemblies were made simply by placing reflector graphite fuel blocks into an eight foot long aluminum can. Additionally thermocouple fuel assemblies, access hole fuel assemblies, access hole dummy assemblies and shielding assemblies were manufactured, however since none of these were used in my model of the core I will not describe them here. Support and alignment of the various assemblies was provided by a 6 foot 7 inch grid plate machined to accommodate 32 control rod assemblies and 329 other various assemblies, again this grid plate is not part of my model and will not be described any further in this text. More information on the all of the assemblies and the grid plate support system can be found in ANL-6034.

1.1.4 Permanent Reflector

Surrounding the 19x19 structure of various assemblies was a 2 foot wide 7 foot 8 inch high permanent reflector comprised of stacked 4 inch square stingers. These graphite blocks also came from the CP-2 reactor however these blocks where not adequately protected from the elements. According to ANL-6115 moisture contents as high as 1.81 weight percent H_2O were measured however allowing the graphite blocks to sit in dry

circulated air would appreciably reduce the moisture content as indicated by the tests performed at Idaho where the highest moisture content was 0.035 weight percent H_2O. According to ANL-6115 the presumed moisture content was less than 1 percent. This possible moisture content should be small enough and should have dried enough at the time of the experiments that it should not be a concern and so I did not take it into consideration in my model.

Although not explicitly written or described, several drawings indicate that there were two 2 inch air gaps, one between the fuel and the permanent reflector and the other between the permanent reflector and the shielding. Several large removable graphite blocks also made up the permanent reflector in the areas which face viewing slots within the core. When it was desired to use a core viewing slot the 235 lbs. graphite could be vertically raised and held in place with an aluminum lifting bracket.

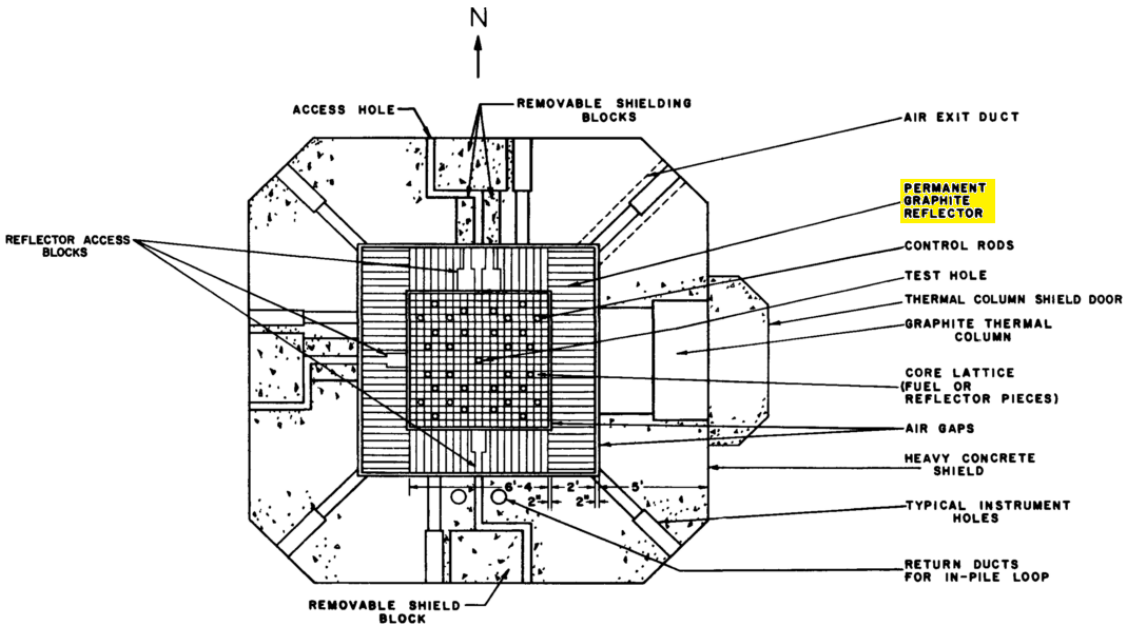


Figure 1.5: Radial cutaway of TREAT, from ANL-6174, highlighting the permanent reflector.

1.1.5 Reactor Cooling

The reactor cooling system was primarily installed to cool the reactor after a transient, the time for which varied depending on the transient however typically another transient could not take place until the reactor had cooled at least overnight. The TREAT reactor was air cooled via two parallel 40-HP Spencer Turbocombressors, each of which was rated for 3,250 cfm, and combined maintain about 6,000 cfm of airflow through the core. An induced draft air system was used keeping the core at a slightly negative pressure. Two filtered inlet plenums kept airborne contaminants from entering the core while exhaust filters kept potentially radioactive contaminants from exiting. To prevent damage to the exhaust filters a core bypass was installed and was automatically operated limiting the exhaust temperature to 250°C.

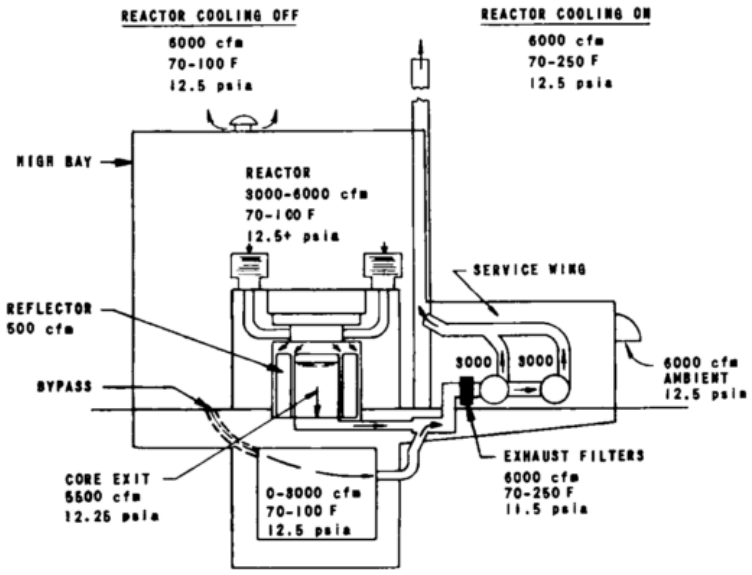


Figure 1.6: TREAT air cooling system (Freund et al., 1960).

1.2 Operation

With the exception of a few manual scram buttons at the reactor building all reactor controls were housed within the control building located half a mile from the reactor building. The control and instrumentations signal cables are ran underground between the two buildings. All control switches, indicators, and recorders required for

startup, steady-state, or transient operations are displayed on the control console in the control building.

In order to help understand transients it may be helpful to understand the orientation of the control rod. Initially I had the orientation backwards and this led to some confusion which required me to change my model. The control rod drive mechanism was in the sub-pile room, below the core. Shutdown rods were withdrawn fully when they were raised to their highest position above the core so that the bottom of the poison section was above the core. This means that the 5 feet of zircaloy follower ran through the core, the top of the zircaloy follower at 6 in. above the core and the bottom at 6 in. below the core. Below that was the steel follower. The poison section of shutdown rods was inserted by moving the rod downward into the core.

Transient rods had the poison section in the middle of the rod. The top section of the rod was the zircaloy follower section. The rod was considered fully withdrawn when the top of the poison section was 6 in. below the core. This means that the bottom of the 5 foot zircaloy follower was 6 in. below the core and the top of the zircaloy follower was 6 in. above the core. The transient rods poison section was inserted by moving the rod upward.

Transient operations were varied in initial temperature, peak power, length of transient and total energy deposited. Generally the reactor was brought critical at a power large enough to raise the test sample temperature to the standard operating temperature of the reactor fuel for which the sample was being tested. Some samples however could have been tested at a much lower or higher initial temperature and initial power level if desired. Control rod 1 would have been used to maintain criticality at the desired power

level. The control rods were positioned via a motor driven lead screw at a rate of 6 in./min. Control rod 1 was calibrated with all other rods fully withdrawn, as would be the state of the rods during the transient. Control rod 1 would be set as a standard shutdown rod i.e. the top section was poison and the middle section was the zircaloy follower. Based on the calibration of rod 1 it would be withdrawn, upwards, to a specific height which in turn increasing reactivity by a predetermined amount. Simultaneously control rod 2 would be inserted, upwards from below, thus maintaining criticality. Although control rod 2's position would influence the worth of control rod 1 when the transient is initiated control rod 2 is ejected and thus the calibration of rod 1 with all other rods withdrawn is valid.

With the control rods set and the test sample at the desired temperature the transient would be initiated and the transient control system would take control. Pneumatic air pressure would fully insert control rod 2, at a rate of up to 4 feet in 80 msec. with a maximum accelerating force of 5,000 lbs. The rod would be slowed towards the end of movement by the air it compresses into a dashpot as it moves. A relief valve set to 450 psi would provide enough resistance to stop the rod at the end of travel without causing bounce back. The final position of control rod 2 would be so that the top of the poison section is 6 in. below the core and the zircaloy follower section runs through the core. With control rod 2 no longer suppressing the positive reactivity caused by the elevated position of control rod 1 the transient begins.

Power would increase at a rate dependent on the reactor period which is of course dependent on the amount of positive reactivity. From this point a couple of different things could happen. The transient could be automatically terminated after a

predetermined time by the transient control system. If the transient is not set to automatically terminate then the operator could scram the reactor at any point or shim control rod 1 as desired to reduce or even increase power, although the self-limiting nature of the core will reduce reactivity and thus power as temperature rises. In the case of a self-limiting burst no operator action at all would be desired and the power level would only be controlled by the negative temperature coefficient of reactivity.

CHAPTER 2: SERPENT

2.1 Monte Carlo

A group of scientist in Los Alamos in the 1940s used the term Monte Carlo to describe a class of mathematical methods used on the development nuclear weapons (Kalos and Witlock, 2008). The Oxford Dictionary defines the Monte Carlo method as "A technique in which a large quantity of randomly generated numbers are studied using a probabilistic model to find an approximate solution to a numerical problem that would be difficult to solve by other methods." Although Monte Carlo methods can be used for many different scientific and economic purposes our primary interest here is its use in numerically solving the neutron transport equation.

$$\begin{aligned}&\frac{1}{\mathrm{v}}\frac{\partial \psi}{\partial t}\left(\vec{r},\vec{\Omega},t\right)+\vec{\Omega}\cdot\nabla\psi\left(\vec{r},\vec{\Omega},t\right)+\Sigma_t\left(r\right)\psi\left(\vec{r},\vec{\Omega},t\right)\\&=\int_{-1}^{1}d\mu_o\Sigma_s\left(\vec{r},\mu_o\right)\psi\left(\vec{r},\vec{\Omega}',t\right)\\&+\frac{1}{4\pi}\int_0^{4\pi}d\vec{\Omega}'\nu\Sigma_f\left(\vec{r}\right)\psi\left(\vec{r},\vec{\Omega}',t\right)+S\left(\vec{r},\vec{\Omega}\right)\end{aligned} \quad \textbf{(2.1)}$$

The Monte Carlo approach to solving the neutron transport equation entails the use of random numbers and probability density functions (PDF) in order to perform random sampling. For example the random sampling of the distance to collision in a material can be performed in the following way. Given that the PDF for distance to collision is:

$$f\left(x\right)=\Sigma_T e^{\left(-\Sigma_T\cdot x\right)} \quad \textbf{(2.2)}$$

Where x is the distance and is greater than zero and Σ_T is the total macroscopic cross section. From this PDF the cumulative distribution function (CDF) is derived.

$$F\left(x\right)=\int_0^x f\left(x'\right)dx'=1-e^{\left(-\Sigma_T\cdot x\right)} \quad \textbf{(2.3)}$$

Where $F(x)$ is the CDF. From here the method to producing the analytical formula for obtaining random samples is to set the CDF equal to a random number (ξ) and then solving for x.

$$\xi = 1 - e^{(-\Sigma_T \cdot x)} \Rightarrow x = -\ln(1-\xi)/\Sigma_T \quad \textbf{(2.4)}$$

1: Integrating the PDF from zero to x to obtain the CDF

2: Set the CDF equal to the random number.

3: Solve for x.

(Brown, 2005)

This same basic approach of can be used in determining other random variables such as cosine of the angle for which a neutron scatters (μ). All of these random variables from the birth of a neutron to its end can be simulated and tracked in this same manner including fissions and the production of new neutrons and when this is done with thousands of neutrons over hundreds of cycles it is easy to see how relevant statistical data can be accumulated.

Now that we have a general understanding of how the neutron lifecycle can be simulated and tracked we have to simulate the environment that the neutron interacts with. The simple way in which I understand this environment is that you define surfaces and materials, these surfaces and materials are used to define cells, cells are placed in a universe and universes can be replicated in a lattice structure in order to create a system. General surfaces include planes, spheres, cylinders and so on. One of the most important concepts to understand with surfaces is the "sense" of the surface. Dr. Brown describes sense in the following way.

For a given point in space, (x,y,z), and surface equation, F(x',y',z')=0, the sense of the point with respect to the surface is defined as:

Inside the surface,	sense < 0,	if F(x,y,z) < 0
Outside the surface,	sense > 0,	if F(x,y,z) > 0
On the surface,	sense = 0,	if F(x,y,z) = 0

(Brown, 2005)

As an example let's say we have a point at (1,1,1) and a sphere about the origin with a radius of 2 defined by:

$$x^2 + y^2 + z^2 - R^2 = 0 \quad \textbf{(2.5)}$$

Plugging in the numbers and applying the definition above:

$$1^2 + 1^2 + 1^2 - 2^2 = -1 \Rightarrow F(x, y, z) < 0 \quad \textbf{(2.6)}$$

We find that the sense is negative and the point is inside the circle. If possible, it is typically more efficient to visually picture if the point is inside or outside a surface but for complicated geometries or when in doubt this basic approach always works.

The input parameters for materials, as is also true with surfaces, will vary between different Monte Carlo codes, however for all codes an input parameter defining the cross section data library, typically ZAID, and density are required in material cards. The Z (atomic number) A (mass number) ID input as ZZZAAA defines the element and isotope for which pertaining cross section data will be looked up via the directory to the specific data library. Although multi-group data can be referenced for Monte Carlo simulations generally continuous-energy cross section data libraries are used. Continuous-energy meaning that for any discrete energy parameter a specific cross section data value is used, whereas multi-group data has specific cross section data for an entire range of energies.

As I mentioned cells are made up of surfaces and materials. The material of a cell may be set by referencing a material card. In addition cells material can be defined by certain pre-established parameters, for example in Serpent if the material name is set to "void" no interactions will occur with the neutron in the cell as if it were passing through a perfect vacuum. Another example is "outside" which terminates the neutron as soon as this region is entered, this is the same as setting a cells "importance" to 0 in MCNP. A cells geometry is defined by of one or more surfaces and the sense of those surfaces (placing it inside or outside of the surfaces). Cells are also defined by what universe they are in.

Universes containing one or more cells and have their own origin. Advanced geometry tools, such as lattices, are commonly used in Monte Carlo codes to replicate, rotate and translate universes. Using these tools a multitude of sub universes can be placed with in a larger universe, although the process can be repeated, ultimately the final system is formed in a single macroscopic universe, in Serpent this is always universe 0.

The initial cycles in a neutron transport Monte Carlo code are very influential, in a multiplying medium, for the first several cycles. Depending on the Monte Carlo code and user inputs the initial neutrons may be placed in random locations throughout the entirety of the system, only in fissionable material, or at a single point in the system either inside or outside of fissionable material. Other parameters such as energy and angular distribution can also be set depending on the code used. This initial source guess is very important and can have a major impact on the initial eigenvalue calculations. For example if all of the neutrons start out at a point outside of fissionable material then the k-effective calculation will be much lower than it would be in reality. For this reason a

value of "inactive" cycles must be established before calculations can be made. Monte Carlo codes track the history of were neutrons are most readily born and in proceeding cycles place the neutrons in these locations. In the first several cycles generally the spatial dependence of the placement of the neutrons varies as the neutron source shifts towards the locations in which the highest number of neutrons are produced in the material. This process is known as fission source entropy (Shannon entropy) and until convergence of the fission source is achieved it is important that the results of the eigenvalue and other calculations are discarded (Brown, 2009).

In order to decrease processing time and increase precision variance reduction Monte Carlo techniques can used (Booth, 1985). A very common example of a variance reduction technique is known as "Russian roulette". As an example of Russian roulette, a neutron is entering a cell away from a region of interest. When the neutron enters the cell the neutron can be removed by a probability of $1-v$, where $v<1$. If the neutron is removed less computational time is spent tracking it. However if the neutron survives its "weight", or the value it contributes to any tallies and results, is increased by a factor of v^{-1}. In this way less computational time is spent tracking neutrons that are traveling away from what you are interested in.

2.2 Serpent 2

Serpent 2 is a three-dimensional continuous-energy Monte Carlo reactor physics burnup calculation code. (VTT, 2007) This is a relatively new code, Serpent 1 was made available to the public in 2009. Currently there is no user's manual for Serpent 2, it is only available for Serpent 1 (Leppänen, 2013a). For this reason some of my references pertaining to particular information on Serpent 2 has come from the Serpent 2 forum as it

is currently the only place to obtain such information. As Serpent 2 is a Monte Carlo code surface cards and material cards make up cells housed in universes that can be put into lattice structures to make whole systems. As previously mentioned all other universes must ultimately go into universe zero.

The current installation package contains libraries based on JEF-2.2, JEFF-3.1, ENDF/B-VI.8 and ENDF/B-VII evaluated ACE format data files (Leppänen, 2013b). It should be noted that currently this does not include ENDF/B-VII.1 the newest ENDF data library. Thermal systems, such as TREAT, cannot be modelled using free-atom cross sections without introducing significant errors in the spectrum and results. Thermal scattering cross sections are used to replace the low-energy free-gas elastic scattering reactions for some important bound moderator nuclides, such as hydrogen in water or carbon in graphite (Leppänen, 2013b). The TREAT reactor graphite-urania fuel blocks pose an interesting complication in that they are not entirely graphite nor free carbon but both.

Generally fission source convergence using Serpent should happen very rapidly by default. According to the Serpent User's Manual "The initial source points are randomly selected inside the fissile cells in the geometry and no source input is needed from the user." Using the "set his 1" command (previously "set outfile 1" in Serpent 1) the rate of fission source convergence can be plotted to ensure convergence has occurred prior to the active cycles. For my model of TREAT

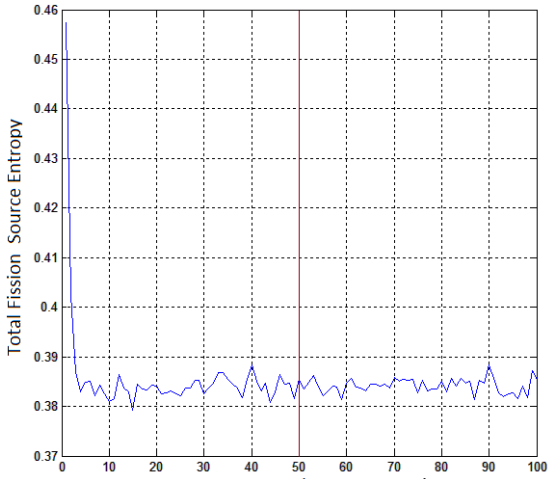


Figure 2.1: Fission source convergence.

convergence generally occurred within the first five to ten cycles, as can be seen in figure 2.1. This rapid convergence makes my fifty inactive cycles more than sufficient in ensuring fission source convergence (Leppänen, 2013a).

As previously mentioned variance reduction in Monte Carlo codes can reduce computational time and/or reduce uncertainty. According to Jaakko Leppänen on the Serpent 2 forum "The code doesn't have any real variance reduction techniques available at the moment, but implicit capture with Russian roulette was enabled in update 2.1.2" (Leppänen, 2013c). For the simulations I have ran, the implicit (using variance reduction) results are generally within the uncertainties of the analog (not using variance reduction) calculations and the implicit data generally has lower uncertainty.

Serpent 2 uses geometric plotters in yz, xz, and xy. These plots default to the origin and the boundary values unless otherwise specified. Plots output as .png files. If left undefined in the materials card colors are selected randomly for the cells. In addition to the geometric plotter Serpent 2 has a reaction rate mesh plotter. The inputs and defaults of the plotter are similar to that of the geometric plotter. The color scheme of the output file consists of yellow to red, representing relative fission power and white to blue, representing relative thermal flux (Leppänen, 2013c). Figure 2.2 is a reaction rate mesh plot of the spherical model of the TREAT reactor.

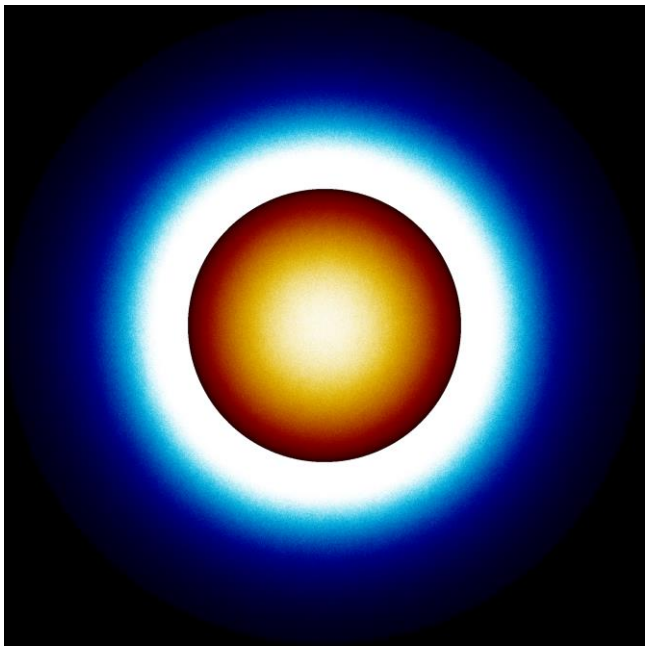


Figure 2.2: Reaction rate mesh of TREAT spherical model.

CHAPTER 3: SERPENT MODEL OF TREAT

3.1 Spatial Design

3.1.1 Spherical Model

When I began working on this model of the reactor I had never used Serpent or any other Monte Carlo code. In order to familiarize myself with the code and how it worked I started with the most basic model I could find. ANL-6174 describes an eigenvalue calculation for a homogenized spherical representation of the reactor which contains two regions, a central core region and an outer reflector region. Additionally all atomic number densities are provided in the report. This geometrically simple design allowed me to obtain my first calculation of an analog k-effective as 1.00942 ± .00052 using 10,000 source neutrons for 50 inactive cycles and 500 active. Although I have varied the number of source neutrons and active cycles unless otherwise specified all k-effective data I present in this thesis will be analog with 50 inactive cycles. As reported in ANL-6174 their results for the same model but using various group cross section data (the use of continuous energy codes being limited by computational speed in the early 1960's) varied between 1.005 and 1.028. With the minimum core loading of TREAT the actual measured value of k-effective was 1.00157.

This effective multiplication factor value of 1.00942 was calculated using graphite thermal neutron cross section data for 100% of the carbon atoms in the fuel. I found that using free gas thermal neutron cross sections yielded a k-effective of 1.03020 ± 0.00060. In the early models I made of the core, although I knew that the consistency of the graphite-urania fuel blocks was a mixture of graphite particles in a nongraphitized elemental carbon matrix. I did not know how to adequately represent such a material with

respect to the neutronics calculations. Initially I made two copies of each model, one using free carbon thermal neutron cross sections for all of the fuel carbon atoms and the other using graphite. I eventually found the graphite cross sections seemed more representative of the actual physics measurements from reports on TREAT experiments and for a few models used only graphite thermal neutron cross section data. It turns out that neither approach is the most representative as I will describe shortly.

3.1.2 Detailed Model

After running the spherical model of TREAT I began creating as detailed of a model as possible primarily using the Design Summary Report, ANL-6034. The major challenge in this first detailed model was defining all of the surfaces and cells of the fuel assembly. I made a relatively simple drawing on note book paper in order to keep track of each cell and the surrounding surfaces, a scanned copy of this is available in Appendix B. Fortunately Serpent takes surface inputs of octagonal infinite cylinders as the assemblies are when you consider the chamfered edges. The only difficulty in this was that input parameters of radius to the square portion and radius to the chamfered edge must be defined and the design report only defines the length of the chamfer. Figure 3.1 shows the Serpent surface input parameters. Drawing the assembly and doing some basic trigonometry calculations I was able to determine the radius. Spatial drawings of my model including all radii inputs can be found in Appendix B. For this first detailed model I did not include any control rods and thus the control rod

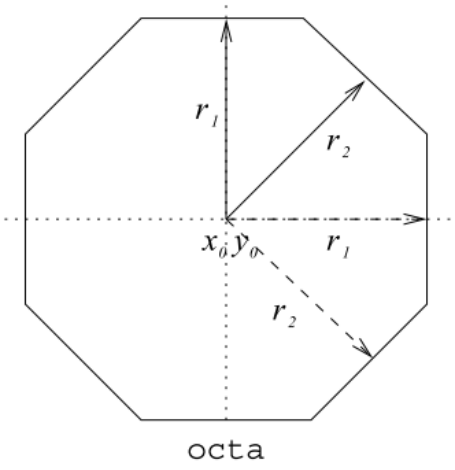


Figure 3.1: Octa Serpent input.

fuel assemblies were standard fuel assemblies with a $1\frac{3}{4}$ in. void running axially through the center. In addition to this model not having control rods there was also no 2 in. air gap between the core and the permanent reflector, although I had seen a gap in some figures in the reports I had not seen anything actually written about the gap and decided to wait to include it until I had a better understanding of its exact dimensions.

Each assembly was made with in its own universe, initially there were four universes: standard fuel assembly, control rod fuel assembly, aluminum clad reflector assembly and zircaloy clad reflector assembly. When I added control rods to the model I separated the control rod fuel assemblies into: control rod 1, control rod 2 and shutdown control rods. All the various assemblies were put into universe zero via a 19x19 lattice structure thus allowing the core loading to be easily changed. The zero universe also contained the permanent reflector cell and defined all areas outside of the permanent reflector as "outside". This first revision of the detailed TREAT model is provided in Appendix C.

My model initially consisted of six material records: fuel, coolant, air, zircaloy, aluminum and reflector. When I added control rods to my model I made two more material cards: steel and poison. All number densities in the materials cards were input in atoms/(b·cm). Although the coolant of the core is air and thus far I have used the same number densities for both I did want to distinguish between the two. The coolant is only the air that would flow through the channels. Other gaps that would have air in them but no flow, for example the gap between the reflector and the aluminum, used the air material card. I calculated the number densities for air based on airs density of 0.0012937 g/cm^3 at standard temperature and pressure (273 K and 101.325 kPa) (Engineering

Toolbox, 2015b). Given the relatively low effect of air on k-effective which I found to be an approximate increase of 0.001Δk with the removal of air in my model I concluded that it would only be necessary to include the number densities for the nitrogen and oxygen content which constitute 99.06 atomic percent of the air. The actual calculations are provided in the spreadsheets in Appendix A.

The number densities for the remainder of the materials were calculated based on ANL-6174 which provides a volume fraction for each element of a given material. Additionally this report provides atomic concentrations at the specified reference densities. This made calculation of number densities as simple as multiplying the volume fractions and the atomic concentrations. It was not necessary for me to calculate the atomic concentrations of each isotope for the elements, as they appear in nature, since Serpent can do this automatically. It was however necessary to do this for boron-10 and boron-11 since boron does not have a natural abundance cross section data library.

3.2 Various Changes to the Model

As my work continued and I read through more reports and reread others I slowly found small mistakes within my original model and so the process of refining the model to be as representative of the actual TREAT reactor began. For every change I have made to my model I have recalculated the change in the eigenvalue thus giving me an idea of the magnitude of effect. For every several changes or when I have made changes to the model that I suspect may have a relative impact on the reactor physics calculations, such as the effect of changing free gas and thermal neutron cross section ratios on the temperature coefficient of reactivity, I have ran all the various calculations necessary to compare to all of the reactor physics measurements that I have evaluated thus far. This

has added excellent insight into physical nature of the core in terms of neutronics, for every change I have made I have tried to predict the results and for each time I have been wrong I have had to think through what has happened in the life of the neutrons that may have adversely affected my predictions.

The next detail I added to my model was control rods, which despite being 6 in. above the core did cause a noticeable change in the effective multiplication factor reducing it by 0.004 Δk. Initially I placed the rods above the core fuel with a void going through the core so the rods would go down when inserted. I quickly realized this was wrong because the control rod drive mechanisms are in the sub-pile room below the core repositioned the rods below the core so that they would rise up when inserted. As it turns out both of these scenarios were right depending if it was a shutdown rod or transient rod, however both cases were also wrong in using a void through the core. In the most recent revision I believe I finally got the rod orientation correct and I will discuss this towards the end of this section. Switching the orientation of rods but leaving a void through the core with rods withdrawn had no effect on the calculations outside of the 68% confidence interval.

The next major change to my model, as recommended by Dr. Patrick McDaniel, was the boron impurity in the fuel which I changed from 6 ppm as is reported in ANL-6034 to 7.6 ppm as is reported in ANL-6115. Although this change in the model did decrease the effective multiplication factor by 0.014 Δk, a rather substantial change as expected, it did not affect any other reactor physics calculations. Next I changed the concentrations of my HEU, based on data provided for HEU in high-temperature gas-

cooled reactor (Knief, 2008), to include U-234 and U-236 instead of just U-235 U-238 by the following atomic percentages.

Table 3.1: HEU pertcentages of isotopes.

Isotope	Original W/O	New W/O	New A/O
U-234	0%	1.0%	1.0050%
U-235	93.1%	93.0%	93.0649%
U-236	0%	0.2%	0.1993%
U-238	6.9%	5.8%	5.7309%

Following the addition of the uranium isotopes, I next added the 2 in. air gap between the assemblies and the permanent reflector. Finally I changed the zircaloy clad reflector assemblies from being a single can of graphite reflector, clad in zircaloy like the aluminum clad reflectors, to be exactly the same as a standard fuel assembly except with CP-2 reflector graphite in place of the graphite-urania blocks (aluminum clad reflector for the top and bottom 2 feet and zircaloy clad reflector for the middle 4 feet). Each of these changes reduced k-effective by a relatively small amount as can be seen in Appendix A.6. In total the effective multiplication factor (which was 1.00355 ± 0.00030 following the change from 6 ppm boron to 7.6 ppm) dropped to 0.99156 ± 0.00027 which is still relatively close to the measured value of k-effective of 1.00157.

While visiting INL and talking to a few research professors there, particularly Dr. Mark DeHart, I was informed of a report (Swanson and Harrison, 1988) which actually describes the free carbon to graphite ratio as being 41% free carbon and 59% graphite. Making this change to the model required me to use two separate carbon data libraries which is not normally feasible however in serpent carbon happens to have two separate data libraries. The ZIADs for which are 6000 for natural carbon and 6012 for carbon-12 since natural carbon is almost entirely carbon-12 using either should be acceptable. As

expected this change not only increased k-effective when compared to the 100% graphite model but also changed the temperature coefficient of reactivity as I will discuss further in the next chapter. While changing the carbon number density I happened to notice that I had used the incorrect number density for zirconium in the zircaloy. Changing this to the correct number density significantly increased the effective multiplication factor, even more than the change in carbon to graphite ratio resulting in a k-effective of 1.03654 ± 0.00033.

After my visit to INL Dr. Mark DeHart provided me with the Serpent model of TREAT they had been using. Attempting to run the code was not possible due to a lack of the required RAM for the vast number of data libraries referenced in the materials cards, however it did provide me with many much needed dimensions of several components described in the reports but to which no physical dimensions were provided, for example the dimensions of the outgas tube. In the model from INL there were many additional elements in the material cards not mentioned in any reports I had read, particularly in the reflector graphite, zircaloy and aluminum. In order to measure how such impurities would affect my model I wanted to add these to my material cards however adding all of them would require too much RAM. Ultimately I decided to add only impurities above a certain number density and/or high absorption cross sections. The addition of these impurities did reduce k-effective by about -0.01 Δk, which is not as much as I expected but still a significant change. Although I regrettably did not run all of the reactor physics calculations after this change later, in the most recent revision of my model I removed all of these additional elements and I will discuss this shortly.

From the INL model I was able to finally get the dimensions for the cladding and void of the control rod fuel assemblies between the control rods and the fuel. This change replaced a moderate amount of fuel with void and cladding and thusly obviously reduced k-effective but only by about -0.007 Δk.

I also noticed a distinct difference in the number densities of the boron and carbon for the B_4C in the control rod. As mentioned earlier the density of the compacted B_4C is a minimum reported value and no average value is provided. Assuming the number density used in the INL model is the average density this would be the correct value to use. This change actually contributed no measurable change in control rod worth and had a very minimal effect on the effective multiplication factor.

For the next two models I wanted to evaluate changing the positions of the aluminum clad reflector and zircaloy clad reflector. The reports describing minimum core loading generally make no mention of the positions of the aluminum and zircaloy clad reflectors however ANL- 6034 says that "these assemblies are installed in fuel positions immediately adjacent to the active core". Unfortunately this description could be considered to be up to some interpretation. To me this means only assemblies where the sides touch but it is not inconceivable that this could also include assemblies where corners are in contact. My initial models put zircaloy clad assemblies in positions where two corners where in "contact" with the fuel assemblies. The next model I made put zircaloy clad reflectors where any corner would be next to the corner of a fuel assembly. The final model only put zircaloy clad reflectors where the sides were in contact with the fuel assemblies or at least this was my intent however I missed three assemblies and did

not catch this mistake until several revisions latter. An illustration of these lattice structures is shown in figure 3.2.

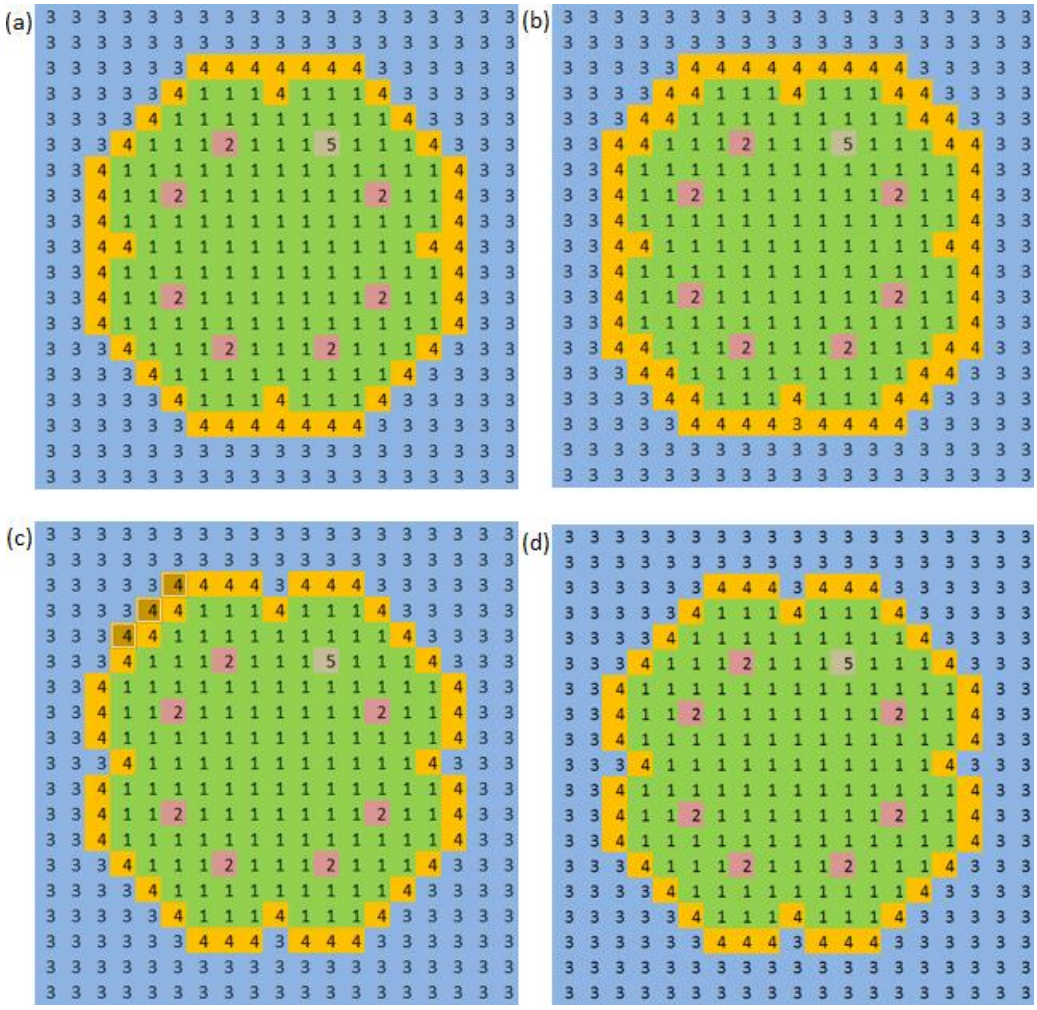


Figure 3.2: TREAT assemblies lattice structures of various revisions: (a) revision f (b) revision g (c) revision h (d) revision o.

Again, the next several changes were things that I suspected I needed but the reports did not define dimensions for. One of the changes was the addition of the outgas tube. The INL model represented this as a voided space in the graphite above the fuel. Although I predicted the reduction in reflector material would increase leakage and reduce the eigenvalue it actually had no distinguishable affect outside of the uncertainties.

I had presumed that there was a gap between the reflector graphite and the aluminum cladding to allow for the difference in thermal expansion between the two materials, however none of the reports I had read described such spacing or gave dimensions. From the INL model these dimensions were defined. I assume all dimensions that have come from their reports are from the original design or as-built drawings which I have asked for access to, but have yet to obtain. With the new knowledge of these dimensions I changed my model to include the addition of a gap between the reflector and the aluminum. Initially I did this for the top and bottoms of the standard fuel assemblies, control rod fuel assemblies and zircaloy clad reflector assemblies. This reduced k-effective by approximately -0.01 Δk most likely due to an increase in leakage. I next added the same space between the reflector and aluminum to the aluminum reflector assemblies. This reduced k-effective by about -0.003 Δk to which the decreased reduction in the effective multiplication factor can be contributed to the fact that this reduction in reflective material is an areas that are further from the core. Finally I added aluminum endcaps to the aluminum reflector assemblies assuming that the endcap is the same thickness as the cladding. I did not expect to see any change in k-effective due to the distance from the fissile region and did not see any measurable difference in the calculation.

From this point several small fixes were made to my model. As previously mentioned I overlooked three zircaloy clad reflector assemblies that need to be changed to aluminum clad reflector assemblies so I did this. Additionally I noticed I had put the number density for titanium in both the aluminum and reflector material cards so I removed the repeats. These changes slightly reduced k-effective. Finally I changed the

rod fully withdrawn position to be exactly 6 in. above the fuel, before this the rods were set to be exactly 6 in. above the top of the zircaloy endcap. As expected this change had no impact on the effective multiplication factor.

In one of the recent changes I've made I finally got the rod orientation correct. While any transient rods would still rise up from below the core upon insertion I set the shutdown rods and control rod 1 to drop in from above the core. Additionally I placed the zircaloy follower in the core when rods are withdrawn. Replacing the void with the zircaloy follower through the core did produce an increase in k-effective by about 0.001 (overlap in these uncertainties is only seen in the 95% confidence interval). I initially expected to see a larger increase in k-effective however I now believe that because of the large carbon to U-235 ratio adding more moderator to the core has very little relative influence. The presence of the zircaloy follower would reduce leakage to some degree and this reduction in leakage may even have more effect on reactivity then its contribution as a moderator, however the zircaloy cladding has more impurities then the graphite reflector and much lower moderating capacity. Additionally the zircaloy follower cladding is over twice the thickness as the cladding around the fuel assemblies. My final conclusion is that the small increase in moderation and reduction in leakage was mostly offset by the increased absorption thus resulting in a small increase that is only distinguishable within the 95% confidence interval.

The final change that I have made to the model was to change the number densities back to those I had calculated using ANL-6174. This includes changing the B_4C number densities back to the ones I had calculated. I found that the removal of these impurities does not seem to affect any reactor physics parameters besides k-effective

which was an increase of about 0.01, the same magnitude as adding the additional elements from the INL model.

3.3 Homogenized Core

In an attempt to speed up calculations I had made a separate model with each assembly homogenized. The premise being that if a homogenized core in Serpent still performed calculations representative of the real reactor physics measurements then a deterministic model set up the same way should perform similarly. Additionally if it was found that the homogenized model ran much faster than potentially Serpent model could be used. This would allow time dependent calculations to be performed with the neutron transport code coupled with a thermo-hydraulics code and each assembly could still have a defined/calculated average temperature, giving the core a basic temperature distribution.

In order to perform this homogenization I calculated the volume of each material within an assembly by hand. Serpent is capable to outputting volume fractions of each material in an output file and I used this to check and compare the results of my calculations. In order to have serpent calculate volume fractions of assemblies I took the universe for each assembly and made it into its own separate code so that the volumes of a material would not be calculated with the volumes of the same material in a different assembly. After verifying the volume fractions I calculated and the ones Serpent calculated matched I multiplied all of the original material atomic number densities times their corresponding material volume fraction thus giving me the new number density for each element. All of these newly calculated number densities went into a new material card appropriately named for the corresponding assembly. Thus each assembly and its

corresponding universe now had only one cell, with the exception of control rod fuel assemblies which maintained all of their original cells up to the cladding between the fuel and the control rod. Beyond said cladding the rest was homogenized.

The effect of this homogenization was far more profound then I expected, reducing k-effective down to 0.97200 ± 0.00023 from 1.00617 ± 0.00039. I believe this drastic reduction to be caused by the homogenization of all of the impurities from the cladding into the fuel. After returning all standard and control fuel assemblies to their original configuration and leaving all reflector assemblies homogenized which increased k-effective to 1.01429 ± 0.00031. However in none of these models did I notice a significant decrease in computational time and thusly I do not see any advantage in running any sort of homogenized model with Serpent. I suspect that there was no significant change in run time, despite the reduced number of regions, is because of the Monte Carlo coding technique of tracking what types of collisions occur with what material and "rolling the dice" for the most probable interactions first when passing into a new region.

The results of this homogenization model seem to imply that although some simplifications can be performed which would greatly help in the creation of a fast deterministic model the fuel or control rod regions should probably remain homogenized which adds some geometric difficulties.

CHAPTER 4: REACTOR PHYSICS COMPARISONS

4.1 Temperature Coefficient of Reactivity

There are many factors that can contribute to a changing temperatures effect on reactivity and can be separated into categories based on the material in which the temperature changes and the parameter effected by the changing temperature. For thermal reactors, such as TREAT, we tend to divide temperature coefficient of reactivity into two material categories, fuel and moderator (Lamarsh and Baratta, 2001). Although TREAT has its fuel and moderator homogenized together it is still easy to look at temperatures effect on uranium and carbon separately. Within these material categories such factors as Doppler broadening, hardening of the neutron spectrum and thermal expansion contribute in varying degrees to temperature coefficient of reactivity, depending on the design of the core.

For the TREAT reactor there is a significantly greater portion of the reactor that is moderator than fuel stemming from the 10,000/1 carbon to U-235 ratio. It can be logically concluded that the primary factor in the temperature coefficient of the materials of the TREAT reactor is the hardening of the neutron spectrum. With an increase in temperature the energy spectrum of the neutrons is shifted so that the average neutron energy is greater. This increase in energy tends to reduce absorption and scattering cross sections as they typically follow the inverse of velocity in the thermal region. The temperatures I used in my calculations ranged from 296-1999 K which, using the Boltzmann constant, equates to an average thermal neutron energy of 0.0255-0.1726 eV. In figure 4.1 you can see how increasing temperature reduces the total scatter cross section of carbon by a few tenths of a barn and the total absorption cross section of U-235

from nearly 700 b to nearly 250 b. For the total scatter cross section of carbon because the energy range is just beyond the $1/v$ region the cross section changes considerably less than the absorption cross section of U-235, however considering the very large carbon ratio this affect may be much greater than initially anticipated.

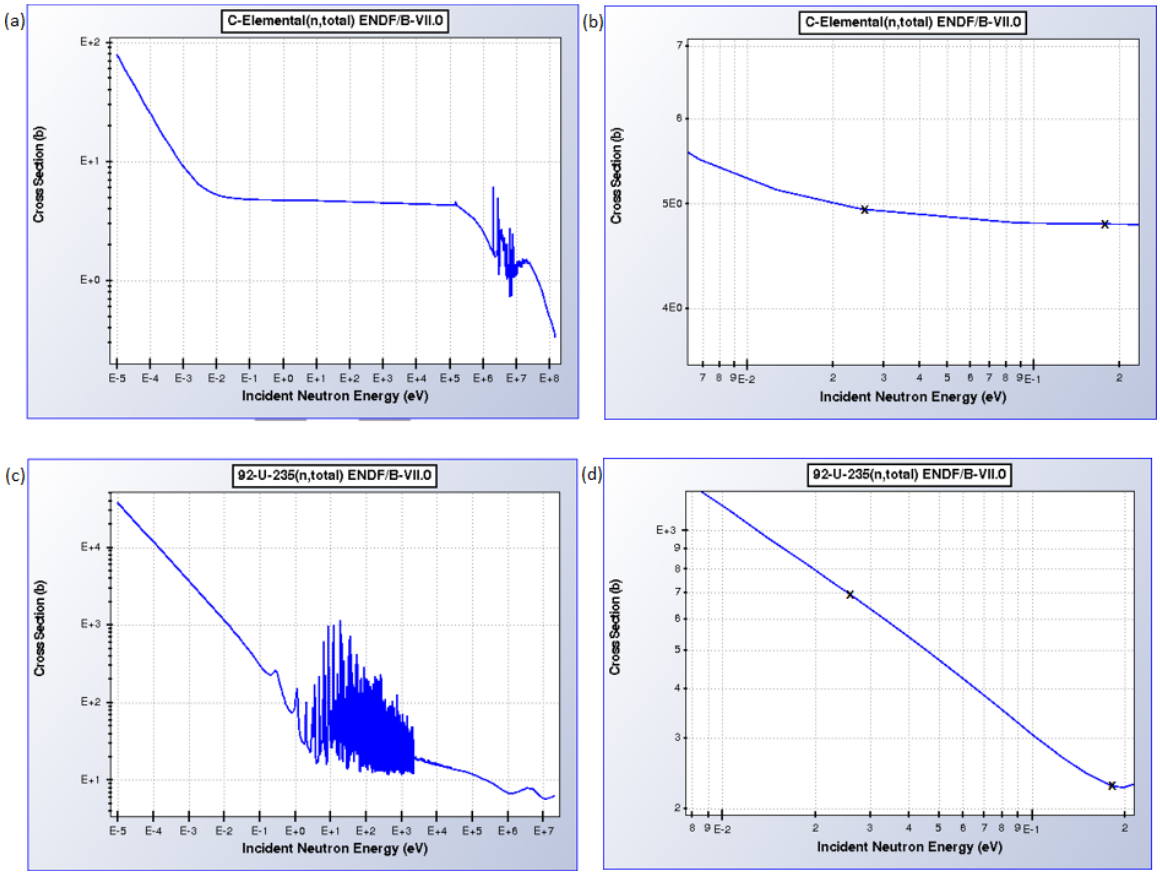


Figure 4.1: Cross section data for carbon and U-235 (Heman, 2011). (a) Total cross section for a neutron in carbon (b) Neutron cross section in carbon over 0.01-0.2 eV (c) Total cross section for a neutron in U-235 (d) Neutron cross section in U-235 over 0.01-0.2 eV.

Using a mesh view of the reactions provided by Serpent one can actually see that as temperature rises the reactions occur less densely towards the center of the core and spread out to the edges. It is difficult to make this distinction by comparing the images side by side and instead the images must be displayed like an animated GIF or flip book in order to clearly see the spreading of the reactions. This spreading of the reaction rate clearly represents fewer central neutron interactions and displays how hardening of the

neutron spectrum reduces moderation and absorption therefore increasing leakage and thusly reducing k-effective.

Doppler broadening also known as the nuclear Doppler effect is an increase in the Doppler width of the resonance and can be expressed as (Duderstadt and Hamilton, 1976):

$$\Gamma_D \equiv \left(\frac{4E_o kT}{A} \right)^{1/2} \tag{4.1}$$

It can be seen that increasing the temperature T will increase the Doppler width Γ_D. This Doppler width changes the shape of the resonance as:

$$\overline{\sigma}_\gamma (E,T) = \sigma_o \frac{\Gamma_\gamma}{\Gamma} \left(\frac{E_o}{E} \right)^{1/2} \Psi(\zeta, x) \tag{4.2}$$

Where:

$$x \equiv 2(E - E_o)/\Gamma \quad \textbf{and} \quad \zeta \equiv \Gamma/\Gamma_D \tag{4.3}$$

$$\Psi(\zeta, x) \equiv \frac{\zeta}{2} \int_{-2E/\Gamma}^{\infty} \frac{dy}{1+y^2} \left[\exp\left(-\frac{(\mathrm{v} - \mathrm{v}_r)^2}{2\mathrm{v}_{th}^2} \right) - \exp\left(-\frac{(\mathrm{v} + \mathrm{v}_r)^2}{2\mathrm{v}_{th}^2} \right) \right] \tag{4.4}$$

Figure 4.2 shows how varying T changes the value of $\overline{\sigma}$ in equation 4.2.

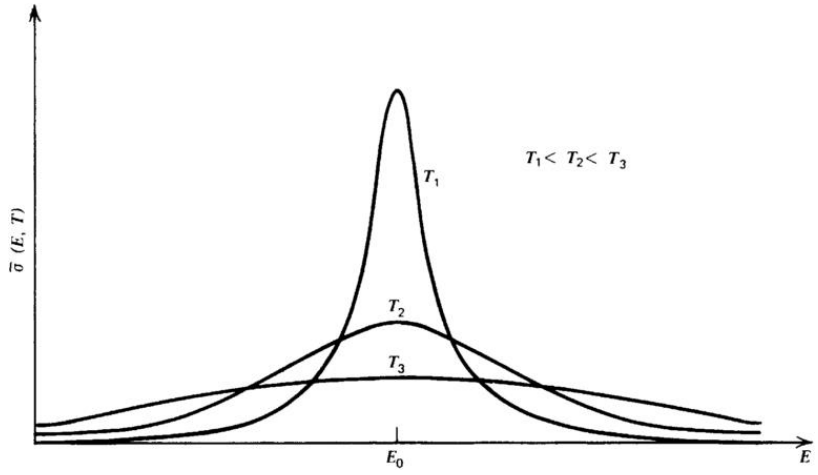


Figure 4.2: Doppler-broadening of a resonance (Duderstadt and Hamilton, 1976).

Although the broadening of the resonance region does not increase the area under the resonance (Lamarsh and Baratta, 2001). A resonance can be thought of as having an infinitesimally high cross section meaning that any neutron with an energy

within the range of the resonance will almost certainly be absorbed. Considering that neutrons have a discrete energy following each collision a neutron may easily skip over a resonance region entirely. If however the resonance is broader than it is more likely that a neutron will have an energy within a resonance region following a collision as it down scatters in energy. The concept of broadening of a resonance region increasing absorption rate is similar to that of the self-shielding effects of control rods in that the dense poison has such a strong absorption cross section that few neutrons make it very far into the rod and so very few neutrons are absorbed in the center of the rod. If the control rod were divided into several much smaller rods and spread out, thus its surface area increased, it would absorb far more neutrons for the same amount of material.

The nuclear Doppler effect on the temperature coefficient of reactivity is most likely not very strong for TREAT however. This is because carbon has no resonances and because the TREAT fuel is HEU. In a core with LEU the Doppler effect increases absorption in resonance regions of U-238 and thus decreases the resonance escape probability, thereby decreasing the effective multiplication factor and therefore reactivity. With far less U-238 in the HEU this change in the effective multiplication factor is much less. The Doppler effect will however have some impact on parasitic absorption in structural materials, particularly those that have many resonances such as zirconium, iron, and tin.

The effect of thermal expansion is of primary consequence with in reactors that possess a liquid moderator where the expansion of the moderator reduces the density and actually removes some of the total mass of the moderator from the core. Since the TREAT is moderated by a solid graphite/carbon material its thermal expansion is

relatively limited. The effects of radial expansion would most likely be very small, if decipherable at all, because the graphite would expand into the void between the cladding and the fuel material. Axial expansion however does slightly change the shape of the core as it actually becomes slightly taller as it heats up. This may increase geometric buckling thereby increasing neutron leakage from the core and reducing k-effective.

All of my calculations of temperature coefficient of reactivity were isothermal measurements, meaning that the entire core is set to be the same temperature. The thermal neutron cross sections for graphite can only be set to specific temperature increments (296, 400, 500, 600, 700, 800, 1000, 1200, 1600 and 1999 Kelvin) and for this reason I calculated the eigenvalue only for these temperatures. Free-atom cross section data libraries are provided in 300K intervals starting at 300K up to 1800K. Doppler broadening corrections can be made to these cross section data using the "tmp" entry in the material card thus allowing the cross section data of free-atoms to be corrected to any temperature (Leppänen, 2013b). The serpent manual states that the "closest temperature below the broadened value is used as the basis" and so I have done this in all of my calculations.

ANL-6173 describes isothermal temperature coefficient measurement made on the TREAT reactor. To summarize the reactor was brought critical after circulating cold outside air through the core and again after circulating warm inside air through the reactor. The temperature coefficient was determined with both long and short rods. Long rods being the standard rods used in the reactor and short rods were used early on to obtain as clean of a reactor as possible for initial physics measurements. Short control rods were not used in any of my models so I will not go on to further describe them

however additional data on them can be found in ANL-6173. Table 4.1 below shows the resulting data collected for TREATs isothermal temperature coefficient.

Table 4.1: Measured isothermal temperature coeficients of reactivty.

Rods	**Temperature**		**Δk**	**Temperature Coefficient**	
	Hot (^{o}C)	Cold (^{o}C)	(inhr)	(inhr/^{o}C)	(Δk /^{o}C)
Short	35.0	15.5	131	6.74	1.8 ± 0.2 x 10-4
Long	37.5	22.0	104.5	6.76	1.8 ± 0.2 x 10-4

The uncertainty of these measurements is very high because of the relatively small temperature change. Additionally this assumes linearity of the temperature coefficient which is not the case, as temperature rises the temperature coefficient will actually decrease. Furthermore ANL-6173 does mention an approximate 4-8^{o}C temperature difference between the core and the permanent reflector, which I did not replicate in my model.

I calculated the temperature coefficient of reactivity of my model after various significant changes that were made. As the temperature coefficient decreases as temperature rises I will present my calculations only for the lowest temperature increment that I am able to measure, from 23 ^{o}C to 127 ^{o}C. In my early model of TREAT (rev. 0.3) which contained 6 ppm boron impurity and was comprised of 100% graphite for the thermal neutron cross section in the fuel I calculated the temperature coefficient of reactivity to be 1.075 x 10^{-4} Δk /^{o}C. It should be noted that for this calculation only 5,000 source neutrons were used over 500 cycles, for the calculations with rev 0.4 15,000 source neutrons were used over 500 cycles and for all calculation there after 30,000 source neutrons were used over 500 cycles. After changing my boron impurity concentration in the fuel graphite to 7.6 ppm I again calculated temperature coefficient

and found it to be 1.004 x 10^{-4} Δk /ºC. As can be seen in figure 4.3 changing the boron concentration had relatively no effect on the temperature coefficient, most likely because there are no resonances in boron-10 for Doppler broadening to occur.

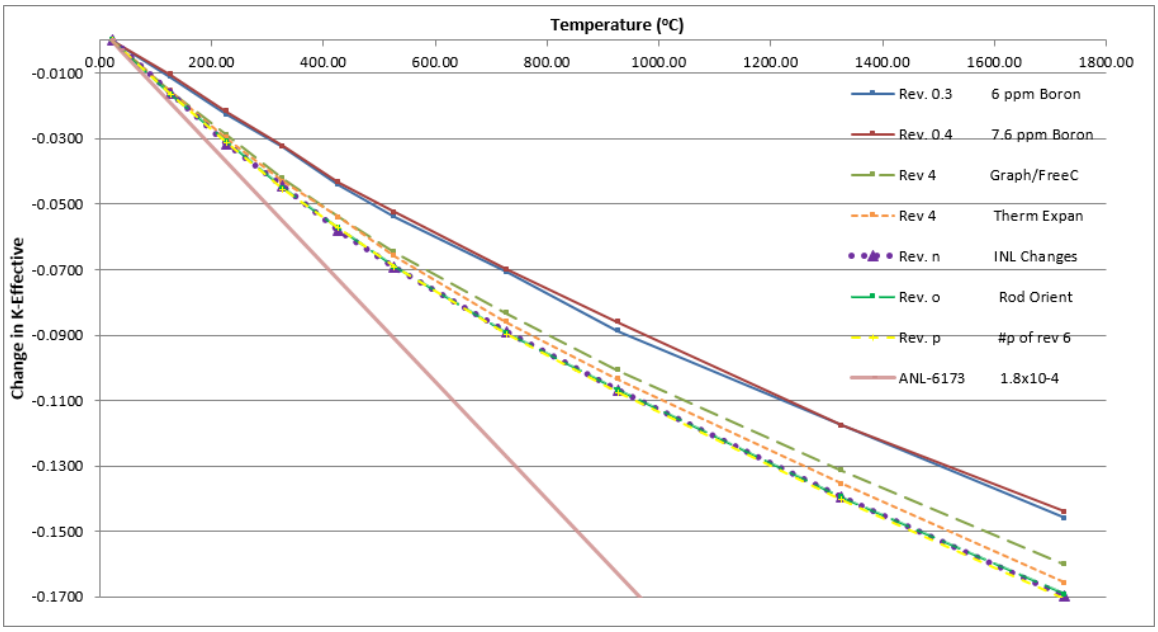


Figure 4.3: Comparison of temperature coefficients. Revisions n, o and p all plot very closely together and are difficult to distinguish from one another.

The next major change I made was setting the graphite to free carbon thermal neutron cross section ratio. I initially made this ratio 60% graphite and 40% free carbon and later changed it to the correct values of 59% graphite and 41% free carbon. After changing the values to 60/40 in rev. 4 (with a few other minor changes that can be seen in the list of revisions in appendix C) I calculated a temperature coefficient of 1.498 x 10^{-4} Δk /ºC. This is a considerable change in the temperature coefficient of reactivity and can be contributed to the rather complex nature of thermal scattering off of a free carbon atom versus a carbon atom within a crystalline graphite structure.

I next attempted to account for thermal expansion, still using rev. 4 as the model however all planes (PZ) were changed in order to account for the thermal expansion of the graphite. I only accounted for the axial thermal expansion of the graphite and used the

maximum expansion coefficient of the data I was able to find 6 x 10-6 m/mK or cm/cm^{o}C. (Engineering Toolbox, 2015a) In total 10 planes were changed 9 times and so the exact calculations can be found in the corresponding spreadsheet in Appendix A.7. As the dimensions change with temperature so do the volumes however the total number of atoms does not and so density decreases. All number densities in the fuel and reflector regions were recalculated at each temperature increment which is over 100 different number densities whose calculations will also be listed in Appendix A.7 as well as the changes in volume.

In spite of the tedious work required to determine the new dimensions and number densities and incorporate all of them in the code I found the effect to be relatively minuscule especially in the lower temperature range. From 296 to 400 K I found the temperature coefficient to be 1.489 x 10^{-4} Δk /^{o}C with uncertainties, an indistinguishable change. As the temperature increases the thermal expansion does have a more prominent effect, yet these temperatures tend to exceed the peak transient temperatures of TREAT and so realistically these data are not very useful. Additionally this was the maximum value of the thermal expansion coefficient of graphite which ranged from 2 – 6 x 10^{-6} m/mK meaning the effects may be even less then my calculations predict. When considering the effort involved in accounting for thermal expansion and the relatively insignificant change in the region of interest I subsequently did not take thermal expansion into account in any proceeding calculations.

In the following calculation of the temperature coefficient I had made several changes to the core between rev. 4 and rev. n. Although changing the thermal cross section ration of graphite/carbon from 60/40 to 59/41 would have had some effect the

change was undoubtedly very small. I do not know exactly what caused the change in the temperature coefficient. Initially I thought broadening of resonances in the impurities however when I later removed elements added from the INL model temperature coefficient did not change. Most of the other changes involved the removal of graphite reflector from regions so I assume that somehow that brought the temperature coefficient closer to the measured values reported in ANL-6173 of $1.8 \pm 0.2 \times 10^{-4}$ Δk. With the new number densities as well as several other changes that can be seen in Appendix C the calculated temperature coefficient for rev. n came out to be 1.562×10^{-4} Δk /^{o}C, almost with in the uncertainty of the measured value and seemingly a very good result.

For the change to rev. o I expected a more substantial increase in temperature coefficient then I actually found. The calculated temperature coefficient in the 23 ^{o}C to 127 ^{o}C range was only 1.575×10^{-4} Δk /^{o}C and tracked nearly identically to the rev. n model in the full temperature range from 23 ^{o}C to 1726 ^{o}C as can be seen in figure 4.3. The change to rev. o switched the position of the rods to be above the core and more importantly replaced what had been void/air through the core (when the rods are fully withdrawn) with reflector graphite. I expected this to change the temperature coefficient in two ways. First, increasing the negative effect temperature coefficient of reactivity because the additional moderator/graphite would have a reduced scatter cross section as temperature increased and the spectrum hardened. I think however this may be very small due to the relatively small volume of graphite introduced and because the change in scattering cross section of carbon is not in the $1/v$ region and thus only changes by a couple tenths of a barn.

The other effect I expected to stem from all of the impurities introduced in the form of the zircaloy cladding of the zircaloy follower. I expected to see Doppler broadening particularly in the zirconium, however the effect seemed to be limited, I assume because the zircaloy cladding possess a relatively small volume when compared to the core. Additionally the spacing of the rods may have an effect. The zircaloy fuel cladding is far thicker between the fuel and the rods then it is between fuel assemblies (five times the thickness). I believe there is a self-shielding effect from the cladding as I have seen in my homogenized model in which homogenizing the zircaloy cladding into the fuel assembly greatly reduced k-effective. It would not be surprising to see that this effect could mean a diminished neutron flux with in all zircaloy interfaces but especially the much thicker zircaloy cladding between the fuel and the rods. A decrease in neutron flux in the zircaloy cladding of the zircaloy follower would imply that the Doppler broadening of the zircaloy in this particular region would have a decreased impact on the temperature coefficient of reactivity.

Finally, in revision p, I changed the number densities back to those calculated from ANL-6174, thus removing any additional elements added based off the INL model. This change included returning to my originally calculated number densities for the poison in the control rods. As mentioned earlier I had originally thought that the addition of these elemental impurities from the INL model increased temperature coefficient however the removal had no effect on temperature coefficient so I must conclude that neither did their addition.

4.2 Control Rod Worth

The control rod worth as determined by control rod calibration is extremely important when performing transient operations on the reactor, particularly for control rod 1. The expected positive reactivity added to the core upon initiation of a transient is calculated based on the position of control rod 1 at the start of the transient. Since period and peak power calculations are dependent on reactivity subsequently these calculations are also based off of the position of control rod 1 and its calibration. ANL-6173 describes the calibration of the control rods, this includes both long and short rods, however since short rods were never used in my model I will not discuss that here.

As stated in ANL-6173 incremental changes in control rod position were made and the corresponding period was used to calibrate the control rod. Control rod 1 was calibrated over nearly half of its range, from fully withdrawn to insertion to 25 in. The addition of fuel however does change the flux distribution of the core, increasing control rod worth if elements are added near the rod by increasing the flux near the rod and vice versa when elements are added farther away from the rod. Additionally in order to perform rod calibration another rod must be repositioned which changes the flux profile of the core. The error due to the method of control rod calibration and depending on the fuel assembly loading is described to be as much as 5% of the total Δk. Control rod calibrations were made based off of an effective delayed neutron fraction (β_{eff}) of 0.0072 and a neutron lifetime (ℓ) of 9.0×10^{-4}

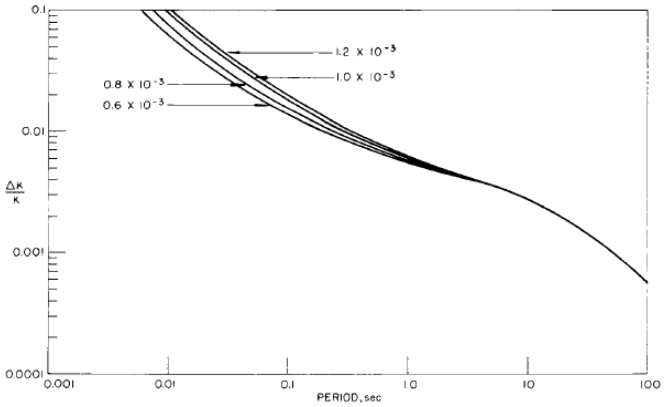


Figure 4.4: Reactivity curve for TREAT using several values for neutron lifetime (Kirn et al,. 1960).

sec. Thus allowing for the calculations in figure 4.4. ANL-6173 does not report any numerical data on the results of the calibration of control rod 1 but instead presents only the plot shown in figure 4.5. In figure 4.5 I have extrapolated the plot into numerical data for comparison against my calculations.

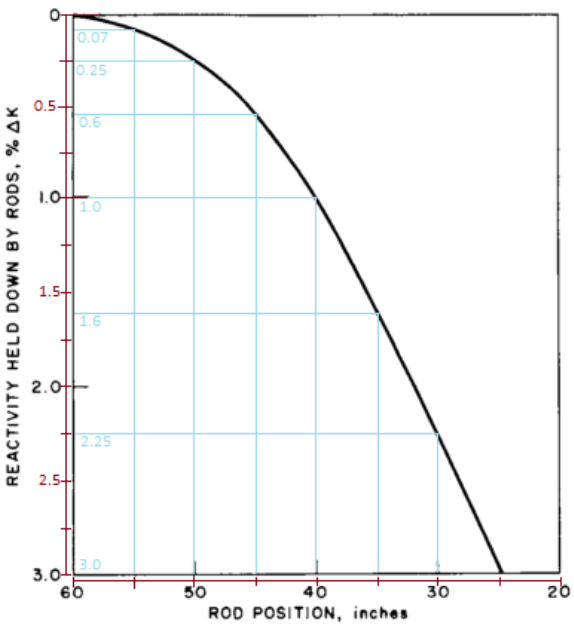


Figure 4.5: Control rod 1 calibration (Kirn et al,. 1960).

Calibration of control rods using Serpent is fairly straight forward, the height of control rod 1 is changed in the model by changing two planes. For each increment of rod height the code is ran and a calculation of the corresponding eigenvalue is output.

I ran a full set of control rod worth calculations on four various models and saw no substantial difference in any of them. The first model was revision 0.4 which was after the change to a boron impurity of 7.6 ppm in the fuel graphite. In the next model, revision 4, I changed the thermal cross section ratios of graphite/free C to 60/40. I was uncertain if this might have an effect on the control rod worth but it did not. After making several changes based on the INL model, particularly changing the B_4C density from the reported minimum value of 1.6 g/cm^3 to slightly higher densities provided in the INL model, I expected to see an increase in the control rod worth. I believe the change in density was too small to see any sort of distinguishable change. Revision n however yielded very similar results to the previous two. Finally in revision o I changed the control rod

orientation so that a zircaloy clad reflector replaced what was void/air through the core when the rod was fully withdrawn. This time I expected the reflector to provide positive reactivity when compared to the void. If that had been the case I would have expected the insertion of the control rod to not only remove the positive reactivity provided by the graphite, but simultaneously add the negative reactivity associated with the poison, which would have increased control rod worth. I found however that the positive reactivity provided by having the zircaloy follower in the core in place of air/void was very small and thus this change had no effect on control rod worth. Figure 4.6 provides a comparison of the various revisions and their corresponding rod worth curves.

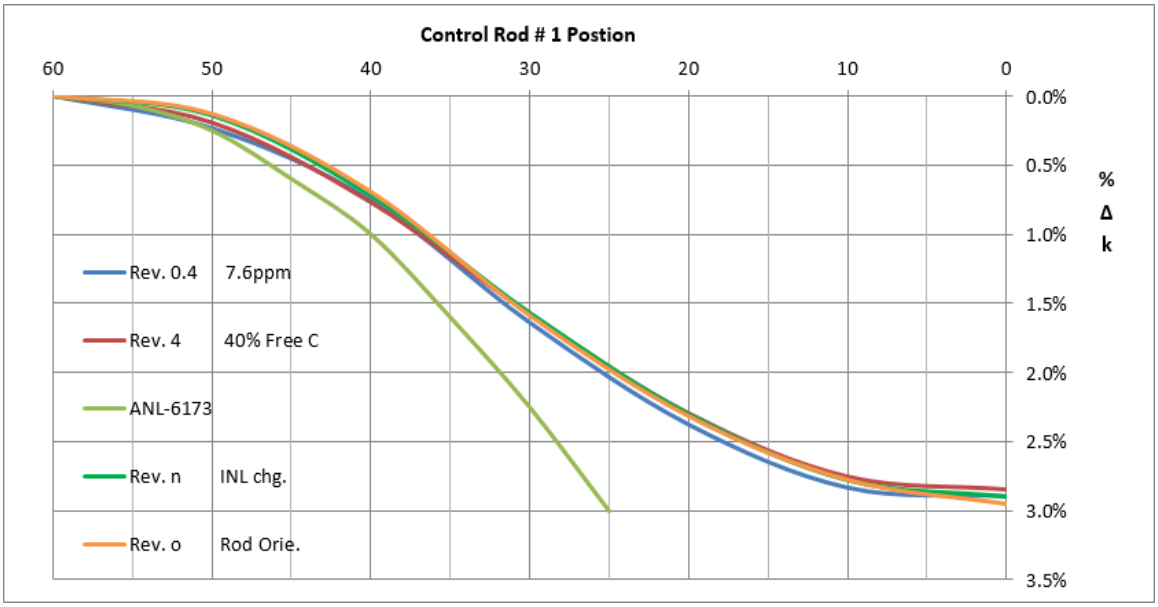


Figure 4.6: Control rod 1 calibration comparisons. It can be seen that for all four models the control rod worths follow the same path.

4.3 Neutron Flux Distribution

The neutron flux distribution of TREAT is very important to the operation of the reactor, particularly as it pertains to the power coupling factor. Although I did not replicate any power coupling calibrations using my model I did compare my flux calculations against that provided in ANL-6173. The fluxes reported in ANL-6173 were

measured using U-235, Pu-239 and gold foils, one square centimeter by one mil, as well as using a fission counter. These measurements were taken with control rod 1 maintaining the reactor critical at a position between 47.5 and 49.5 in. thusly for my model I placed control rod 1 at 48.5 in. For my comparisons I have used the data from the U-235 foils which when compared to the fission counter measurements radially are in good agreement. Just as with the control rod worth all data is presented only in plots which required some extrapolation inevitably leading to some uncertainty beyond that of the original measurements. No uncertainties in measurements were reported in ANL-6173 and so any error bars that I present pertaining to ANL-6173 measurements are meant to be my best estimate of uncertainty based on potential error in my extrapolation process, as well as the deviation from expected values or deviation between measurements. Figure 4.7 shows how the extrapolation for radial flux was obtained.

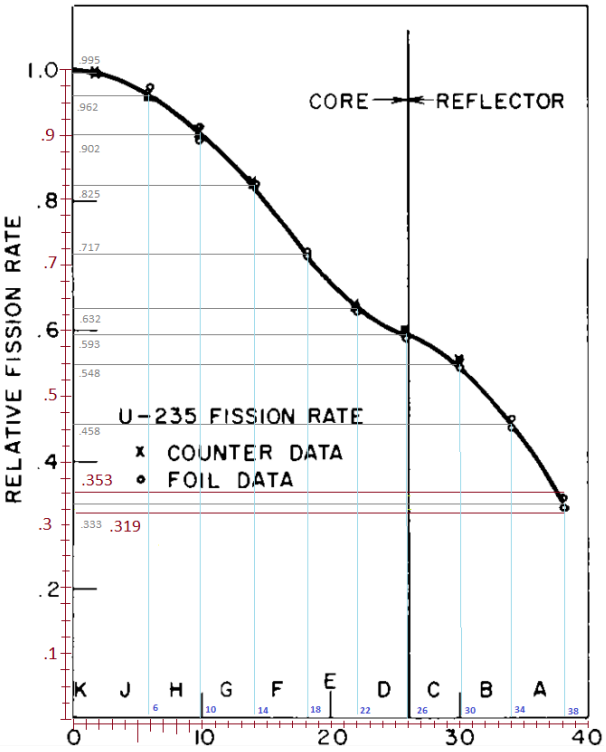


Figure 4.7: Normalized radial flux measurements (Kirn et al,. 1960).

In my calculations both axial and radial fluxes were greater than that reported in ANL-6173. I do not believe these to be significantly greater than the uncertainties in the measurements however. I found that for the various models there were only two changes that made a distinguishable difference. The first major change that effected flux was the change in the graphite to free carbon thermal neutron cross sections

ratios to 60/40 percent (59/41 in later models). This change actually slightly reduced the average radial thermal neutron flux, but did not seem to have a significant impact on the axial flux. Figure 4.8 illustrates the comparison between the models and their calculated radial fluxes.

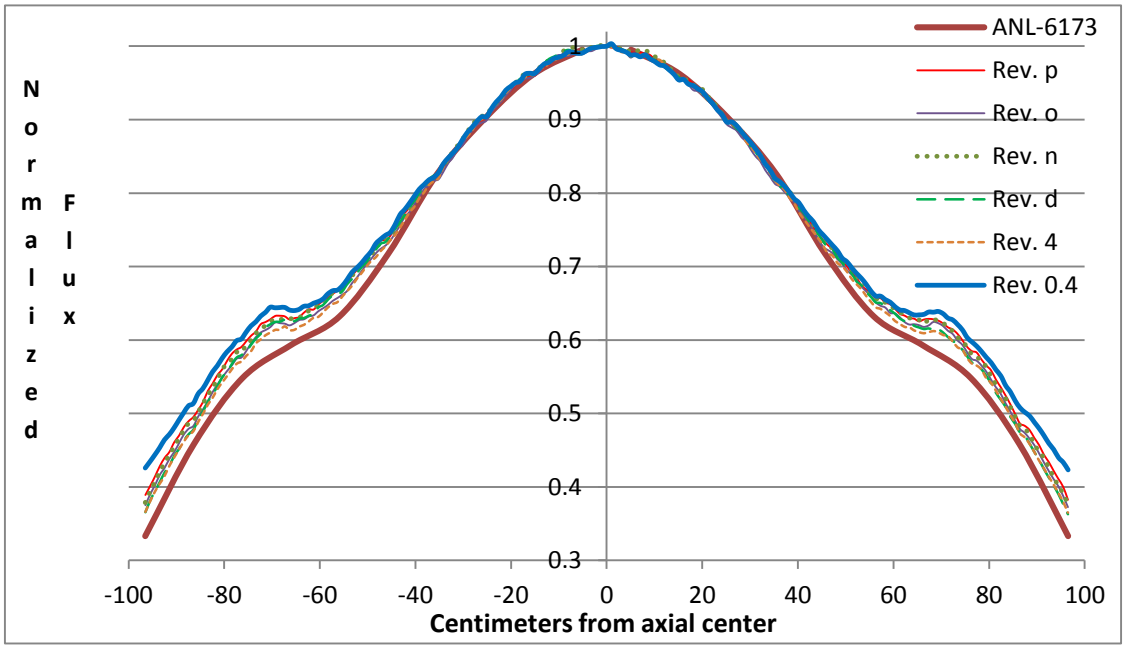


Figure 4.8: Normalized axial flux. Revision 4 though p are all compare closely and are hard to distinguish from one another, however revision 0.4 stands out having a slightly higher average flux.

The other significant change pertained to rod orientation and axial flux. In early models I had noticed axial flux plotted peculiarly in that the average for the lower half of the core compared well on average but the plots did not actually track well. In the upper half of the core the average flux for my calculations was much higher than that of the ANL-6173 measurements. Eventually I realized that if I flipped the orientation of the detectors the plots tracked much more closely. Given that the top and bottoms of my model are symmetric with the exception of the control rods this made me realize that the orientation of my control rods was obviously incorrect and after changing the orientation

the comparison in flux plots tracked far better. Figures 4.9 and 4.10 illustrate the comparison between the models and their calculated axial fluxes.

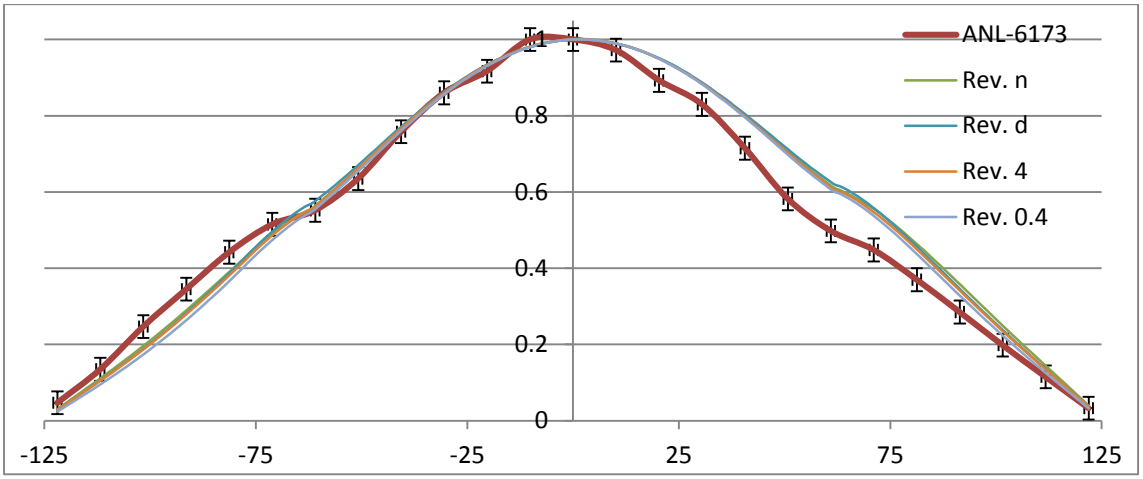


Figure 4.9: Normalized radial flux, with improper rod orientation. Revisions 4, d and n all track very closely and are hard to distinguish from one another, but differ greatly from the reported measurements.

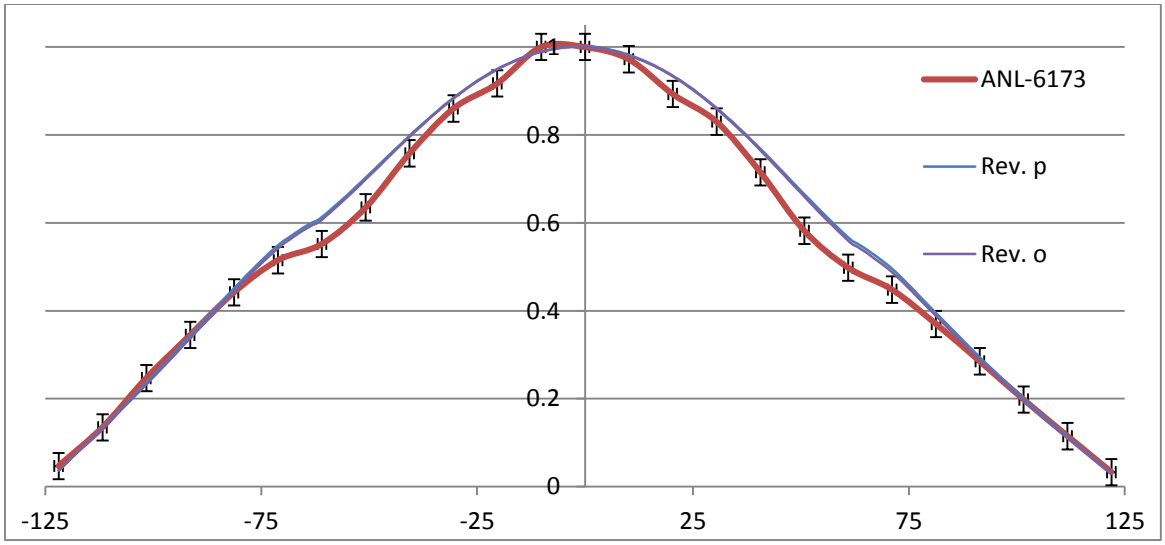


Figure 4.10: Normalized radial flux, with proper rod orientation. Revisions o and p track very closely and compare far better with the measurements reported in ANL-6173.

4.4 Prompt and Delayed Neutronics

As reported in ANL-6173 the prompt neutron lifetime measurements were made in three ways: Rossi-alpha, transfer function and super-prompt critical methods. All three of these methods depend on the effective delayed neutron fractions and their corresponding decay constants, the uncertainties of which may have caused some errors

in all calculations. The reported values of the neutron fractions and decay constants are presented in figure 4.11 from ANL-6173.

Neutron Group, i	Decay Constant, λ_i	Effective Delayed Neutron Fraction, β_i
1	0.0124	0.000244
2	0.0305	0.001567
3	0.1110	0.001411
4	0.3010	0.002828
5	1.1300	0.000826
6	3.000	0.000302

$$\beta_{eff} = \Sigma(\beta_i)_{eff} = 0.007178$$

Figure 4.11: Effective delayed neutron parameters for TREAT (Kirn et al,. 1960).

The report also describes the theory and methodology behind each measurement in some detail.

The results of the transfer function approach are reported to most likely be 9.0 x 10^{-4} sec and almost certainly to fall between 8.8 x 10^{-4} and 9.2 x 10^{-4} sec. Figure 4.12 shows the results of the data for the transfer function method from ANL-6173. For the Rossi-alpha method of measuring prompt neutron lifetime seven separate measurements were made the results of which ranged from 8.23 x 10^{-4} and 10.16 x 10^{-4} sec. The value reported to be the best was 8.8 x 10^{-4} sec with an uncertainty probably within five percent, neglecting the uncertainty related to β_{eff}. Finally super-prompt critical measurements were found to differ greatly from the other two methods, with reported values of 7.0, 7.0 and 8.1 x 10^{-4} sec which was attributed to the method of rod calibration and changes in core loading between transients, the effects of which are previously mentioned in the discussion on control rod worth. Based on the results from the three methods the value for the prompt neutron lifetime was thusly concluded to be 9.0 x 10^{-4} sec.

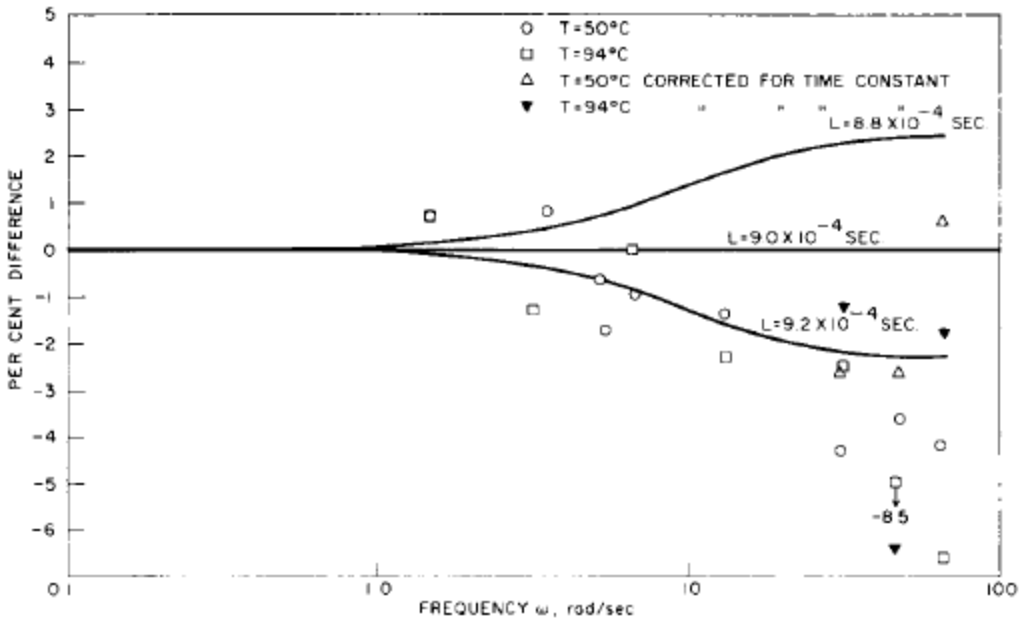


Figure 4.12: Transfer function prompt neutron lifetime measurements (Kirn et al,. 1960).

Serpent 2 uses several methods in order to determine the adjoint-weighted time constants. Initially I was not certain which to use however after reading through the Serpent 2 forum I found a post by Jaakko Leppänen recommending the use of the iterated fission probability method "The IFP estimators are new, and they should produce the best values for the time constants" (Leppänen, 2013d). Although all of the methods seem to produce very similar results all the data I present has come from the IFP method. All in all I have not seen any significant change in any of the prompt neutron lifetimes or delayed neutron fractions between the various models, which is not surprising considering I have not changed the fuel composition significantly in any of the models. The data provided by the calculations of my model for prompt neutron lifetimes and delayed neutron fractions seems to compare very well with that provided in ANL-6173. To summarize the data for prompt and delayed neutronics as well as the other data described in this chapter Figure 4.13 lists the various revisions and how their calculated physics parameters compare to the data in the ANL reports.

	Serpent Rev. 0.3 6 ppm (Free C)		Serpent Rev. 0.3 6 ppm (Graphite)		Serpent Rev. 0.4 7.6 ppm Boron		Serpent Rev. 4 Graph/FreeC		Serpent Rev. n INL Changes		Serpent Rev. o Rod Orientation		Serpent Rev. p Rod Orientation		ANL Reports	
Temperature Coefficient			-1.08E-04		-1.00E-04		-1.50E-04		-1.56E-04		-1.58E-04		-1.57E-04		-1.80E-04	
Prompt Neutron Lifetime	9.35E-04		9.54E-04		9.45E-04		9.10E-04		9.36E-04		9.29E-04		9.46E-04		9.00E-04	
Delayed Neutron Groups:	λ	β	λ	β	λ	β	λ	β	λ	β	λ	β	λ	β	λ	β
1	0.0125	2.46E-04	0.0125	2.52E-04	0.0125	2.27E-04	0.0125	2.47E-04	0.0125	2.41E-04	0.0125	2.25E-04	0.0125	2.05E-04	0.0124	2.44E-04
2	0.0318	1.09E-03	0.0318	1.16E-03	0.0318	1.09E-03	0.0318	1.10E-03	0.0318	1.12E-03	0.0318	1.17E-03	0.0318	1.19E-03	0.0305	1.57E-03
3	0.1094	1.13E-03	0.1094	1.22E-03	0.1094	1.13E-03	0.1094	1.10E-03	0.1094	1.13E-03	0.1094	1.12E-03	0.1094	1.10E-03	0.111	1.41E-03
4	0.3170	3.21E-03	0.3170	3.15E-03	0.3170	3.18E-03	0.3170	3.24E-03	0.3170	3.25E-03	0.3170	3.15E-03	0.3170	3.11E-03	0.301	2.83E-03
5	1.3540	9.81E-04	1.3540	9.06E-04	1.3540	9.04E-04	1.3540	9.42E-04	1.3540	9.40E-04	1.3540	9.59E-04	1.3540	9.62E-04	1.13	8.26E-04
6	8.6364	3.12E-04	8.6364	3.63E-04	8.6364	3.11E-04	8.6364	3.25E-04	8.6364	3.02E-04	8.6364	3.26E-04	8.6364	3.55E-04	3	3.02E-04
Effective	0.7437	6.97E-03	0.7928	7.05E-03	0.7398	6.85E-03	0.7597	6.94E-03	7.25E-01	6.98E-03	7.62E-01	6.95E-03	7.99E-01	6.91E-03		7.18E-03
Control Rod Worths	(Δk/inch)		(Δk/inch)		(Δk/inch)		(Δk/inch)		(Δk/inch)		(Δk/inch)		(Δk/inch)		(Δk/inch)	
60-50 inches					0.0237%		0.0226%		0.0163%		0.0144%		0.0250%		0.0250%	
50-40 inches					0.0535%		0.0557%		0.0552%		0.0561%		0.0505%		0.0750%	
40-30 inches					0.0825%		0.0804%		0.0878%		0.0829%		0.0848%		0.1250%	
K-Effective	1.04013		1.01795		1.00355		1.005760		1.00571		1.00651		1.01698		1.00157	

Figure 4.13: Reactor physics parameter comparisons.

CHAPTER 5: CONCLUSION AND FUTURE WORK

5.1 Conclusion

The model I have developed is quite capable of easily and accurately performing steady state calculations of the TREAT reactor under a multitude of different scenarios. Simplifying this model into something that still accurately calculates reactor physics parameters with respect to those measured may still be a bit of a challenge however. It would seem that homogenizing the cladding of the fuel into the fuel has an adverse effect on the calculations and for obvious reasons homogenizing the control rods into the fuel assembly would greatly change calculations as well. The inability to homogenize these regions complicates geometry and although it does not significantly affect computing time for Serpent calculations it may prove to be a challenge for running time dependent deterministic calculations.

5.2 Future Work

Unfortunately I was unable to model the upgraded TREAT reactor. I do not have enough reference material to know exactly what changes were made in order to make these changes and I do not have measurements of any reactor physics parameters to compare the results of these changes to. Modeling the TREAT reactor, post upgrade, however is far more relevant and I believe is one of the biggest priorities in terms of future work.

Beyond modeling the upgraded TREAT reactor the next major priority would be performing time dependent calculations. In order to perform time dependent calculations a simple, fast and representative model must be made. The seemingly reasonable way of doing this is by using a deterministic neutron transport solving code. Multi-group cross

section data can be calculated using Serpent for the deterministic code. The deterministic code would need to be coupled with a heat transfer code in order to perform the time dependent calculations as they pertain to transient operations.

In addition to time dependent calculations there are still many steady state calculations that could be performed in order to better understand the TREAT reactor. One example of such research pertains to the boron impurity in the fuel. Although we can be fairly certain the average impurity is about 7.6 ppm it may very well be that the boron concentration near the surfaces of the graphite blocks is higher. If it were the case that the boron concentration is higher near the surface this could affect reactor physics calculations. Similarly I still felt unclear on the exact density of the B_4C in the control rods. Calculations could be run with varying densities of the B_4C in order to determine the effects on control rod worth and possibly determine the density in which the calculations accurately reproduce the measurements taken in ANL-6173.

APPENDIX A: SPREADSHEETS AND CALCULATIONS

A.1 Number Density Calculations

Element	Material											N at Stan. Density
	Core Graphite (Fuel)		6 to 7.6 ppm correction.	Reflector Graphite		Zircaloy		Al6063-S Alloy		Coolant		
	Vol Frac	N		Vol Frac	N	Vol Frac	N	Vol Frac	N	N		
Carbon I	0.999585	0.086239196	8.457								Carbon I	0.086275
Boron	4.21E-006	5.74E-007	7.29565E-07	1.36E-006	1.8553E-07						Boron	0.136419
B-10		1.14865E-07	1.45913E-07		3.7106E-08							
B-11		4.59459E-07	5.83652E-07		1.48424E-07							
Iron	2.19E-004	1.85516E-05		2.13E-004	1.80175E-05	2.00E-003	0.000169924	0.005172	0.00043852		Iron	0.084788
U 235	1.79E-004	8.65408E-06									U 235	0.048428
U238	1.32E-005	6.31316E-07									U238	0.047827
Tin						2.35E-003	7.7674E-05				Tin	0.032991
Zirconium						0.995642	0.042084792				Zirconium	0.042269
Aluminum								0.994828	0.05995729		Aluminum	0.060269
Carbon II				0.999786	0.083749074						Carbon II	0.083767
Nitrogen										1.0201E-05		
Oxygen										4.3433E-05		

Figure A.1: Number densities used for all of the core materials with the exception of the B_4C and carbon steel of the control rods.

The volume fractions and atomic number densities at standard density come from ANL-6174. The number densities are calculated by multiplying volume fraction times the number density at standard density. Number densities are in atoms/(b•cm).

	Core Graphite (Fuel)		6 to 7.6		N at Stan.	Weight % -----> Atomic %				
Element	Vol Frac	N	ppm		Density	Elements	A	W%	m	A%
Carbon I	0.999585	8.6239196E-02	correction.			U-234	234	1.0%	4.27E-05	1.0050%
Graph	0.59	5.08811256E-02		Carbon I	0.086275	U-235	235	93.0%	0.003957	93.0641%
Free C	0.41	3.53580703E-02		Boron	0.136419	U-236	235	0.2%	8.51E-06	0.2001%
Boron	4.21E-006	5.7432399E-07	7.296E-07			U-238	238	5.8%	0.000244	5.7308%
B-10		1.1486480E-07	1.459E-07			Total	942	100.0000%	0.004252	100.0000%
B-11		4.5945919E-07	5.837E-07	Iron	0.084788					
Iron	2.19E-004	1.8551614E-05		U 235	0.048428					
U 235	1.79E-004	8.6540836E-06		U238	0.047827					
U238	1.32E-005	6.3131640E-07		Tin	0.032991					
U total		9.2854000E-06		Zirconium	0.042269					
	A%			Aluminum	0.060269					
U-234	1.0050%	9.3315046E-08		Carbon II	0.083767					
U-235	93.0641%	8.6413704E-06								
U-236	0.2001%	1.8583592E-08								
U-238	5.7308%	5.3213101E-07								
U total		9.2854000E-06								

Figure A.2: Core graphite number densities.

The number densities for the uranium isotopes were recalculated to include U-234 and U-236 from weight percentages (Knief, 2008) which were converted in to atomic percentages and then multiplied by the total atomic number densities for U-235 and U-238 that I previously had.

	E	F	G	H	I	J	K	L
58		A	A_t	A(x)	Avo/b	Dense	%	N (per(b*cm))
59	B_4C	55.2507	55.2507	1	0.60221	1.6	100%	1.74394642E-02
60	Boron	10.81	55.2507	4	0.60221	1.6	100%	6.97578569E-02
61	B-10						20%	1.39515714E-02
62	B-11						80%	5.58062855E-02
63	Carbon	12.0107	55.2507	1	0.60221	1.6	100%	1.74394642E-02
64	N="=J59*I59*H59/G59"							
65	Carbon Steel							
66		A	A_t	A(x)	Avo/b	Dense	%	N (per(b*cm))
67	Fe	54.9380	54.9380	1	0.60221	7.85	99%	8.51888875E-02
68	Mn	55.845	55.8450	1	0.60221	7.85	1%	8.46518204E-04

Figure A.3: The calculations for the number densities of the B_4C and carbon steel of the control rods.

A.2 Minimum Loading TREAT k-effective

Parameter	Value	Reference	Neutron Groups:	λ_i	β_i	β_i/λ_i
			1	0.0124	2.440E-04	1.9677E-02
excess ρ=	60 inhr	ANL-6115 pg 4	2	0.0305	1.567E-03	5.1377E-02
β effective=	0.007178	ANL-6173 pg 34	3	0.111	1.411E-03	1.2712E-02
$\Sigma(\beta_i/\lambda_i)$=	0.093993		4	0.301	2.828E-03	9.3953E-03
$T_{1\ inhr}$=	3600		5	1.13	8.260E-04	7.3097E-04
$\rho_{1\ inhr}$=	2.6109E-05	ρ=Σ(βi/λi)/T	6	3	3.020E-04	1.0067E-04
$\rho_{60\ inhr}$=	0.0015666			Eff.	7.178E-03	9.3993E-02
K-Eff=	1.0015666					

Figure A.4: Conversion of 60 inhr to the k-effective of 1.0015666.

This calculation is based off of the effective delayed neutron fractions provided in ANL-6173. The reactivity calculation is based off of equation A.1 (Lamarsh and Baratta, 2001).

$$T = \frac{1}{\rho}\sum_i \beta_i \bar{t}_i \qquad \textbf{(A.1)}$$

Where $\bar{t}_i = 1/\lambda_i$ and by solving for reactivity eq. A.1 can be rewritten as eq. A.2.

$$\rho = \frac{1}{T}\sum_i \beta_i/\lambda_i \qquad \textbf{(A.2)}$$

Knowing the period (T) for one INHR is 1 hour or 3,600 seconds and the effective delayed neutron fractions from ANL-6173 reactivity can easily be calculated. Using this value for reactivity k-effective can be very closely approximated as one plus reactivity.

A.3 Temperature Coefficient of Reactivity

	A	B	C	D	E	F	G	H	I	J
1	ANL-6173 Temp. Coef.				Rev. p Temp. Coef.					
2	K	°C	Δ K-eff by -1.8×10^{-4} dk/°C	Uncert. of $\pm 0.2\times10^{-4}$	K	°C	TREAT Serpent K_{eff}	Δ K-eff	Temp. Range (K)	Isothermal α_T Over Temp. Range
3	295.15	22	0.00015	0.00002	296	22.85	1.016630	0.0000		
4	296	22.85	0.00000	0.00000	400	126.85	1.000310	-0.0163	296-400	-1.5692E-04
5	310.65	37.5	-0.00264	0.00029	500	226.85	0.985450	-0.0312	296-500	-1.5284E-04
6	400	126.85	-0.01872	0.00208	600	326.85	0.971071	-0.0456	296-600	-1.4987E-04
7	450	176.85	-0.02772	0.00308	700	426.85	0.959239	-0.0574		
8	500	226.85	-0.03672	0.00408	800	526.85	0.947440	-0.0692	296-800	-1.3728E-04
9	593.15	320	-0.05349	0.00594	1000	726.85	0.926889	-0.0897		
10	600	326.85	-0.05472	0.00608	1200	926.85	0.909061	-0.1076	296-1200	-1.1899E-04
11	700	426.85	-0.07272	0.00808	1600	1326.85	0.876411	-0.1402		
12	800	526.85	-0.09072	0.01008	1999	1725.85	0.845928	-0.1707	296-1999	-1.0024E-04
13	811.15	538	-0.09273	0.01030					°C	
14	1000	726.85	-0.12672	0.01408					127-527	-1.3218E-04
15	1088.15	815	-0.14259	0.01584					527-927	-9.5947E-05
16	1200	926.85	-0.16272	0.01808					927-1726	-7.9015E-05
17	1600	1326.85	-0.23472	0.02608						
18	1999	1725.85	-0.30654	0.03406						

Figure A.5: Revision p temperature coefficient calculations.

The temperature coefficient calculations compare changes in k-effective as temperature changes. These are all isothermal meaning the entire core is at one constant temperature. The other TREAT model revisions were calculated in the same manner.

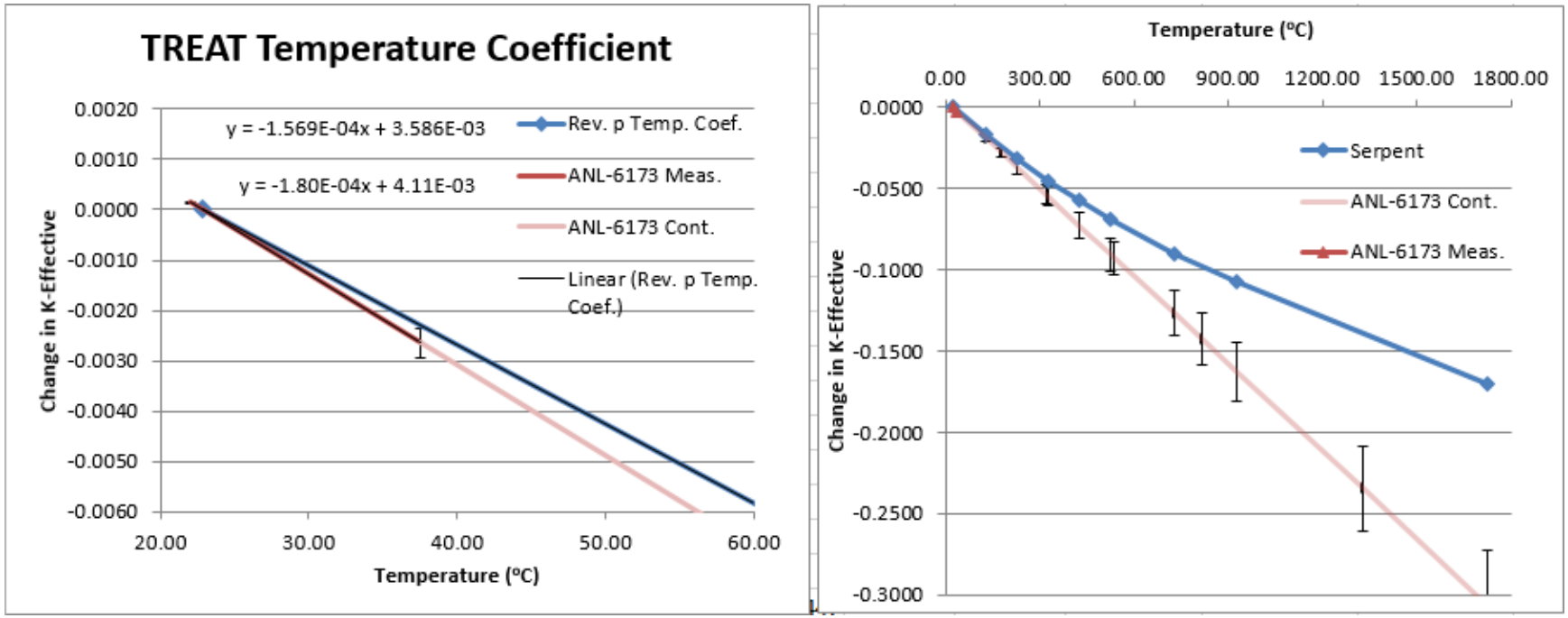


Figure A.6: Plots of change in k-effective vs temperature.

To emphasize how small of a temperature change was made in the measurements reported in ANL-6173 the left plot is blown up to show this region. As can be seen on the right this linear approximation diverges as temperature and thus the comparable data is limited.

A.4 Control Rod Worth

Rev. p (Returned number densities to rev. 6 values.)									70,000 sn 300 cycles			
Lattice with 133 fuel assemblies and 8 control rod assemblies												
	K-eff				Control Rod Worths				Control Rod Worths			
	Analog		Implicit		Analog				Implicit			
Rod 1 Postion	k-eff	uncert	k-eff	uncert	Δk/k	%Δk/k	%Δk	Uncert	Δk/k	%Δk/k	%Δk	Uncert
60	1.01698	0.00027	1.01714	0.00021	0	0	0.000%	0.038%	0	0.000%	0.000%	0.030%
50	1.01448	0.00030	1.01455	0.00027	0.002464	0.246%	0.250%	0.040%	0.002553	0.255%	0.259%	0.034%
40	1.00943	0.00029	1.00938	0.00025	0.007479	0.748%	0.755%	0.040%	0.007688	0.769%	0.776%	0.033%
30	1.00095	0.00027	1.00083	0.00022	0.016015	1.601%	1.603%	0.038%	0.016296	1.630%	1.631%	0.030%
20	0.99300	0.00031	0.99300	0.00019	0.024149	2.415%	2.398%	0.041%	0.02431	2.431%	2.414%	0.028%
10	0.98825	0.00032	0.98848	0.00025	0.029073	2.907%	2.873%	0.042%	0.02899	2.899%	2.866%	0.033%
0	0.98714	0.00025	0.98712	0.00022	0.030234	3.023%	2.985%	0.037%	0.030416	3.042%	3.002%	0.030%

Control Rod Worths			
ANL-6173			
Rod 1 Postion	%Δk	Uncert	%Δk/inch
60	0.00%	0	
55	0.07%	0.000035	0.014%
50	0.25%	0.000125	0.025%
45	0.60%	0.0003	0.040%
40	1.00%	0.0005	0.050%
35	1.60%	0.0008	0.064%
30	2.25%	0.001125	0.075%
25	3.00%	0.0015	0.086%
		Average:	0.051%

		%Δk	
		Serpent	ANL-6173
	60-50	0.0250%	0.0250%
	50-40	0.0505%	0.0750%
	40-30	0.0848%	0.1250%
	30-20	0.0795%	
	20-10	0.0475%	
	10-00	0.0111%	

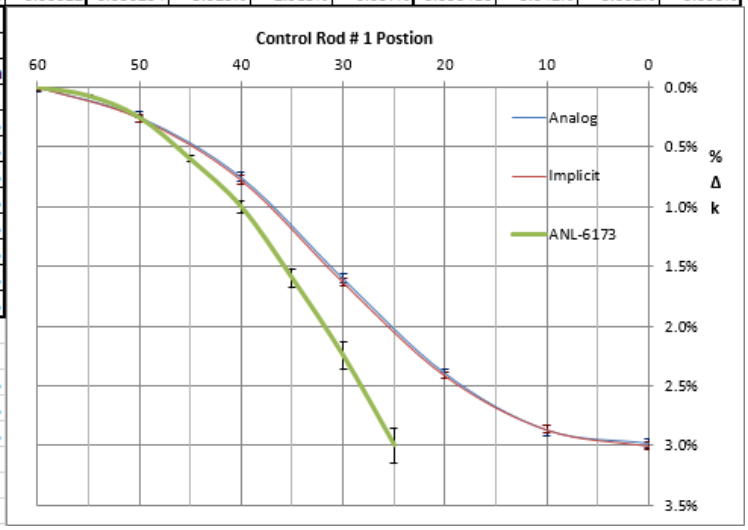


Figure A.7: Calculation and plot of control rod worth of revision p. I have included implicit calculations for comparison as well as uncertainties.

Similarly to the temperature coefficient, control rod worth calculations compare changes in k-effective as rod height changes. The change in k-effective measured in temperature coefficient is nearly five times that of the control rod worth calculations. For this reason I did not include uncertainties, nor implicit data, with temperature coefficient calculations. The variations are relatively indistinguishable. With control rod worth calculations however the effects of the uncertainties become more pronounced as can be seen with the control rod at 50 in. Uncertainties were calculated based on equation A.3 (Knoll, 2010).

$$\sigma_u^2 = \left(\frac{\partial u}{dx}\right)^2 \sigma_x^2 + \left(\frac{\partial u}{dy}\right)^2 \sigma_y^2 + \left(\frac{\partial u}{dz}\right)^2 \sigma_z^2 + \ldots \qquad \textbf{(A.3)}$$

Where u is the change in k-effective and thus x and y are the initial and final values of k-effective at the various rod positons. Thus equation A.3 can be written as equation A.4.

$$\sigma_{\Delta k} = \sqrt{\sigma_{k_{\text{intial}}}^2 + \sigma_{k_{\text{final}}}^2} \qquad \textbf{(A.4)}$$

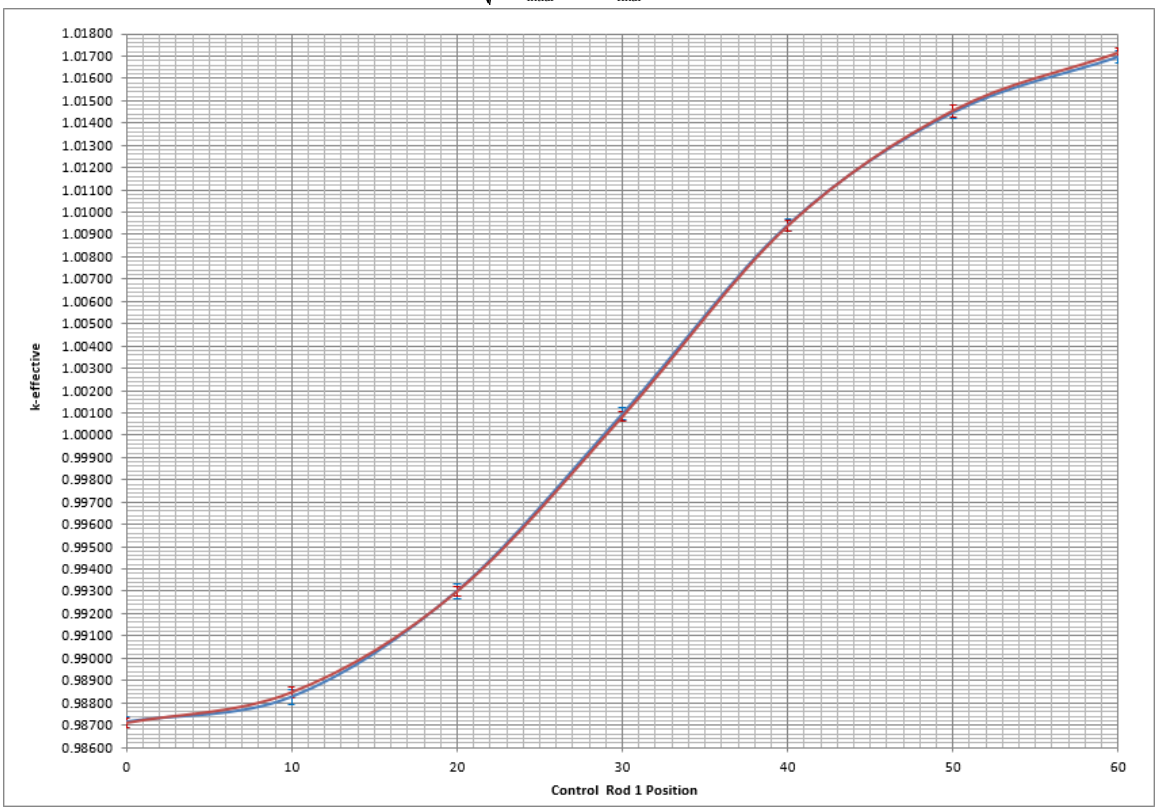


Figure A.8: Critical rod height or rod height to achieve a desired reactivity can be easily estimated with rod position plotted against k-effective.

A.5 Neutron Flux Distribution

Radial rev. p Serpent Data						Axial rev. p Serpent Data					
det	cm	Flux	% Uncert.	Normal	Uncert.	det	cm	Flux	% Uncert.	Normal	Uncert.
1	-96.52	3.303E-02	0.00356	0.38922	0.00139	1	-121.9	1.243E-01	0.00183	0.03703	0.00007
2	-95.51	3.407E-02	0.00345	0.40158	0.00139	2	-120.9	1.582E-01	0.00204	0.04711	0.00010
3	-94.51	3.516E-02	0.00348	0.41442	0.00144	3	-119.9	1.915E-01	0.00177	0.05704	0.00010
4	-93.50	3.636E-02	0.00321	0.42852	0.00138	4	-118.9	2.243E-01	0.00168	0.06679	0.00011
5	-92.50	3.731E-02	0.00297	0.43977	0.00131	5	-117.9	2.569E-01	0.00146	0.07651	0.00011
6	-91.49	3.800E-02	0.00346	0.44784	0.00155	6	-116.9	2.893E-01	0.00143	0.08614	0.00012
7	-90.49	3.911E-02	0.00333	0.46097	0.00154	7	-115.9	3.222E-01	0.00151	0.09595	0.00014
8	-89.48	3.988E-02	0.00300	0.46995	0.00141	8	-114.9	3.547E-01	0.00144	0.10564	0.00015
9	-88.48	4.086E-02	0.00303	0.48161	0.00146	9	-113.9	3.872E-01	0.00141	0.11530	0.00016
10	-87.47	4.155E-02	0.00337	0.48972	0.00165	10	-112.9	4.206E-01	0.00136	0.12528	0.00017
11	-86.47	4.204E-02	0.00329	0.49545	0.00163	11	-111.9	4.528E-01	0.00143	0.13487	0.00019
12	-85.46	4.287E-02	0.00329	0.50525	0.00166	12	-110.9	4.847E-01	0.00134	0.14435	0.00019
13	-84.46	4.377E-02	0.00322	0.51586	0.00166	13	-109.9	5.171E-01	0.00136	0.15400	0.00021
14	-83.45	4.504E-02	0.00284	0.53086	0.00151	14	-108.9	5.498E-01	0.00137	0.16375	0.00022
15	-82.44	4.590E-02	0.00266	0.54097	0.00144	15	-107.9	5.832E-01	0.00122	0.17370	0.00021

Figure A.9: Normalized neutron flux at various axial and radial points and their calculated uncertainties.

Here I have only included calculations for the first 15 points of the axial and radial fluxes. Serpent 2 outputs the Flux and percent uncertainty. I have normalized the fluxes by dividing all by the centerline flux (maximum). Although equation A.3 could be used to in the calculation of uncertainty it is not necessary since normalization is division by a constant. The uncertainty listed is the percent uncertainty multiplied by the normalized flux value.

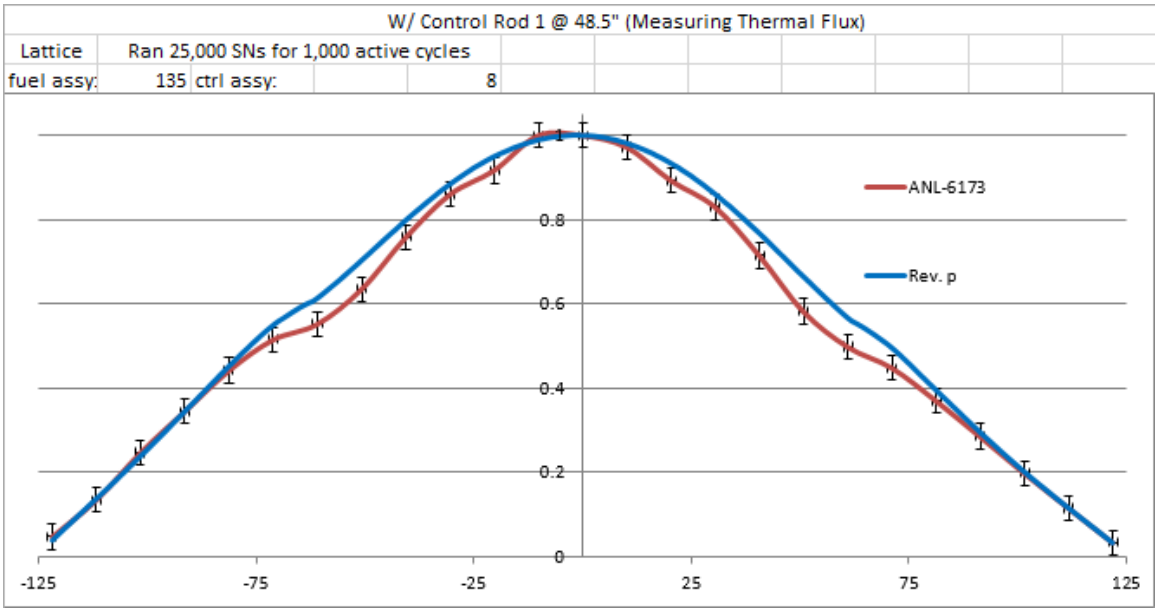


Figure A.10: Axial plot of normalized thermal flux for revision p.

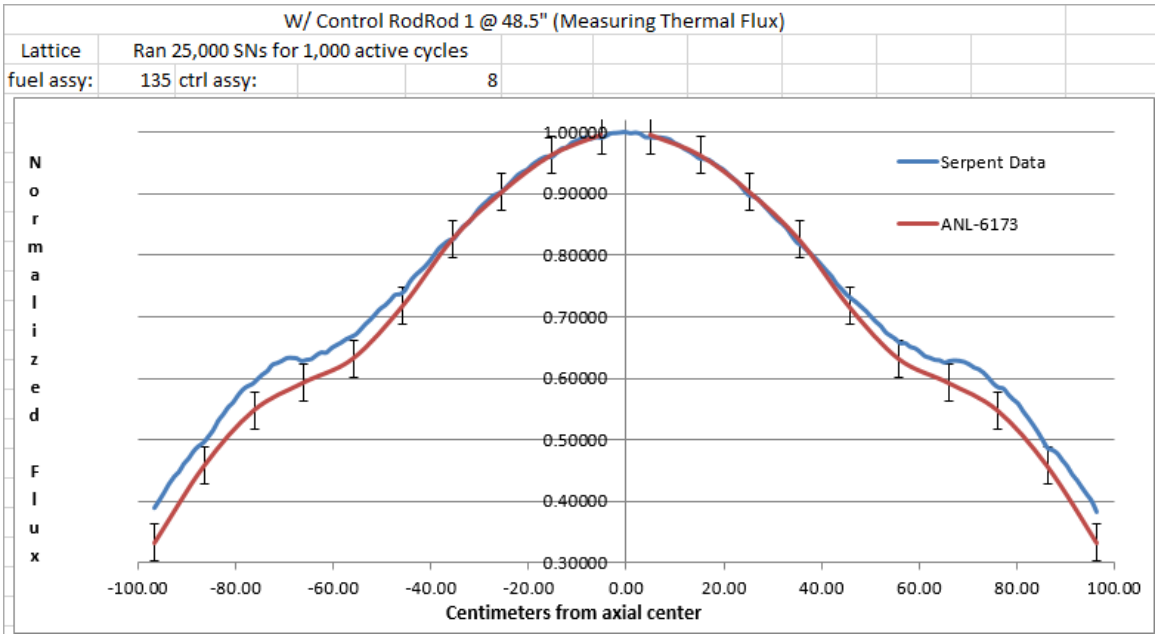


Figure A.11: Normalized radial thermal neutron flux.

I have not included uncertainty bars for my calculations because the uncertainties are very small and for the multitude of data points they only obscure the plot.

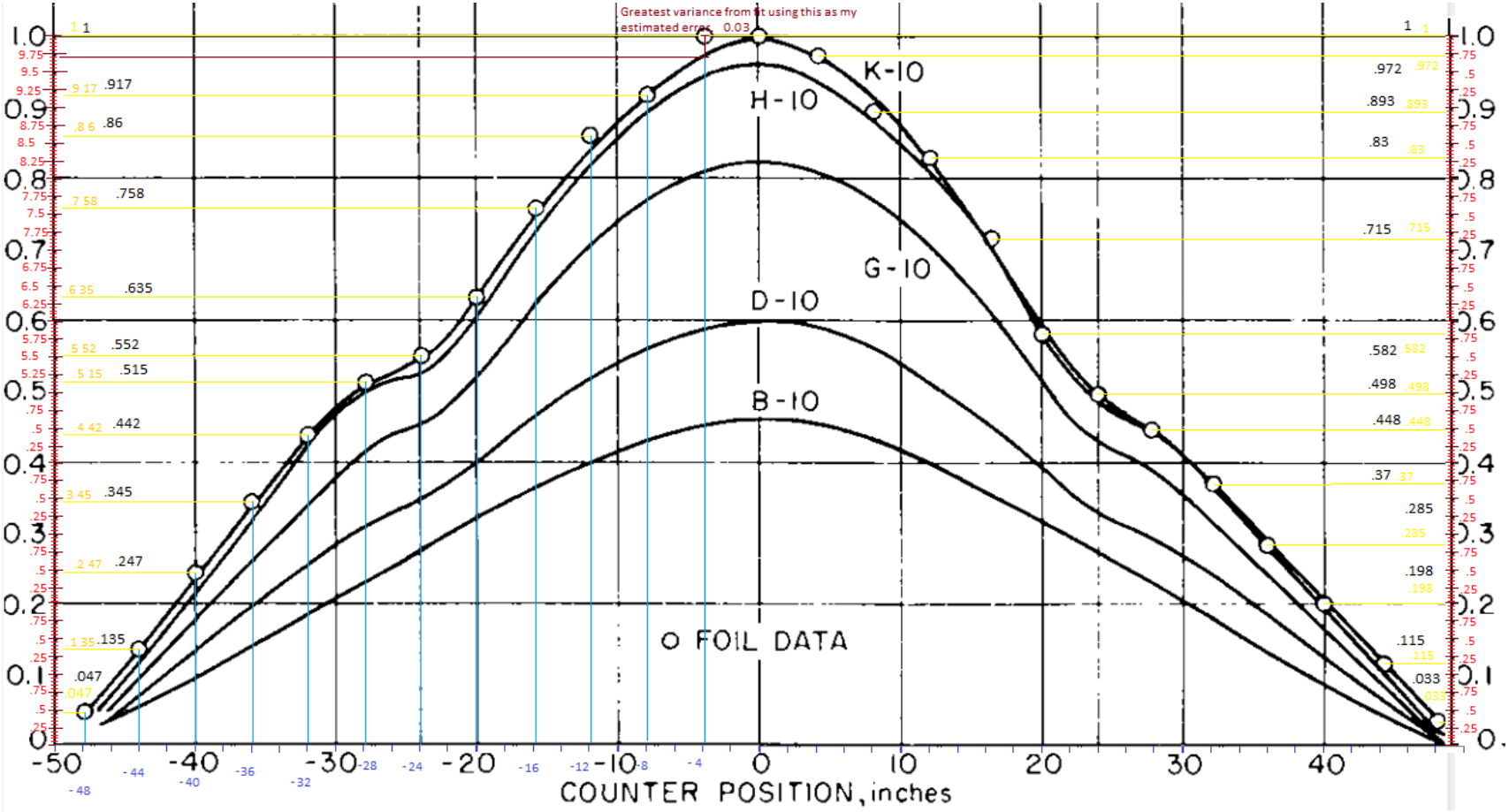


Figure A.12: Axial neutron flux extrapolation of data points from the plots provided in ANL-6173.

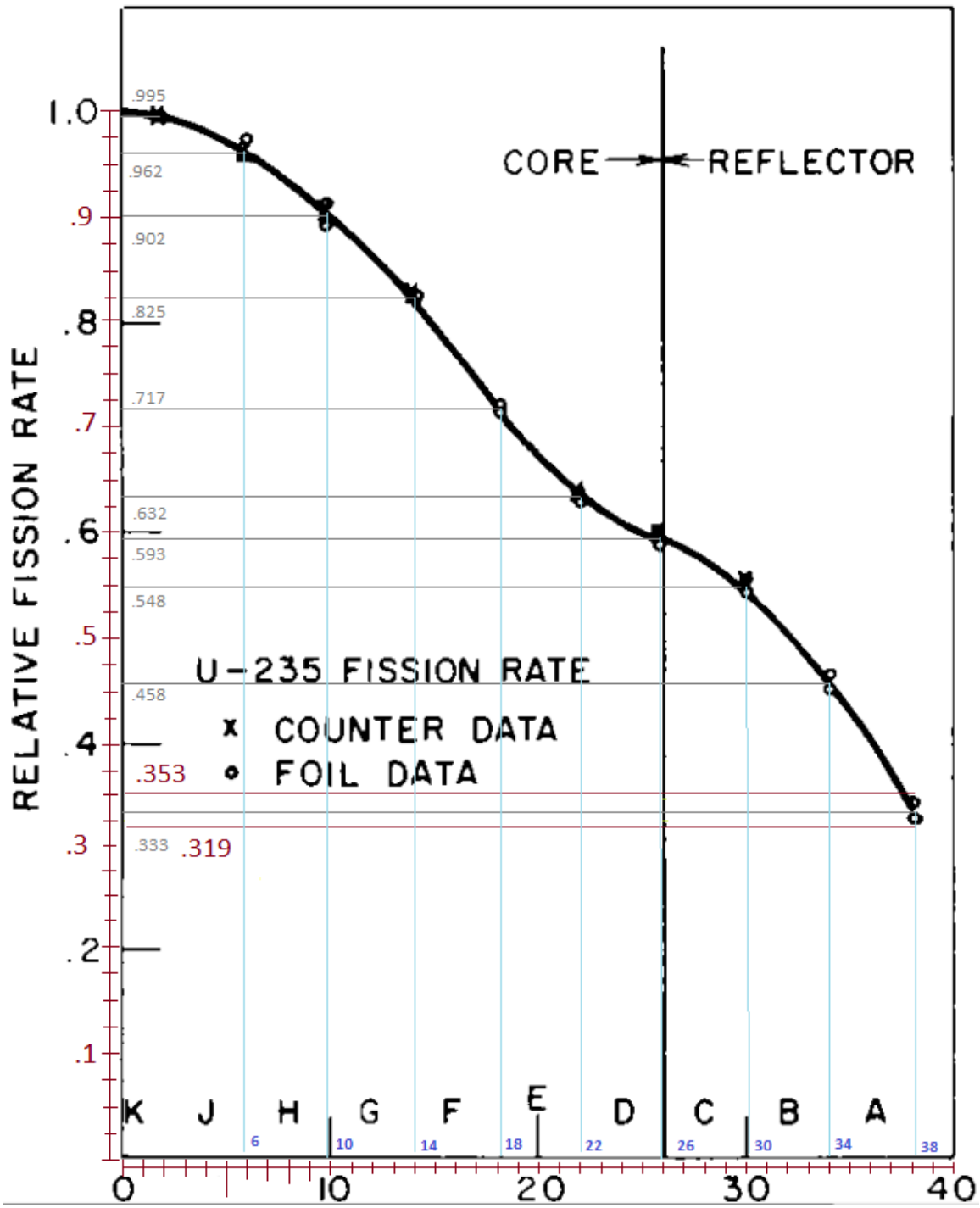


Figure A.13: Radial neutron flux extrapolation of data points from the plots provided in ANL-6173.

ANL-6173 Radial				ANL-6173 Axial			
in	cm	Nomral	Uncert.	inches	cm	Nomal	
2	5.08	0.995	0.034	-48	-121.92	0.047	0.03
6	15.24	0.962	0.034	-44	-111.76	0.135	0.03
10	25.4	0.902	0.034	-40	-101.6	0.247	0.03
14	35.56	0.825	0.034	-36	-91.44	0.345	0.03
18	45.72	0.717	0.034	-32	-81.28	0.442	0.03
22	55.88	0.632	0.034	-28	-71.12	0.515	0.03
26	66.04	0.593	0.034	-24	-60.96	0.552	0.03
30	76.2	0.548	0.034	-20	-50.8	0.635	0.03
34	86.36	0.458	0.034	-16	-40.64	0.758	0.03
38	96.52	0.333	0.034	-12	-30.48	0.86	0.03
				-8	-20.32	0.917	0.03
-2	-5.08	0.995	0.034	-4	-10.16	1	0.03
-6	-15.24	0.962	0.034	0	0	1	0.03
-10	-25.4	0.902	0.034	4	10.16	0.972	0.03
-14	-35.56	0.825	0.034	8	20.32	0.893	0.03
-18	-45.72	0.717	0.034	12	30.48	0.83	0.03
-22	-55.88	0.632	0.034	16	40.64	0.715	0.03
-26	-66.04	0.593	0.034	20	50.8	0.582	0.03
-30	-76.2	0.548	0.034	24	60.96	0.498	0.03
-34	-86.36	0.458	0.034	28	71.12	0.448	0.03
-38	-96.52	0.333	0.034	32	81.28	0.37	0.03
				36	91.44	0.285	0.03
				40	101.6	0.198	0.03
				44	111.76	0.115	0.03
				48	121.92	0.033	0.03

Figure A.14: Data points extrapolated from axial and radial thermal neutron plots.

Radial uncertainty used is based off of the variation in the two measurements at 38 in. Axial uncertainty used is based off of the deviation from expected values of the measurement at - 4 in. Since radial flux is only plotted in one direction (from center westward) I have duplicated this in both directions radially. I assume this radial traverse was away from control rod 1 to limit its impact on flux but have had some difficulty determining the location of control rod 1.

A.6 Effective Multiplication Factor Comparisons

These are all the values for k-effective that I have collected for all the revisions I have created in order of revision. The revision is to the left of the data sets and a brief description of the changes made is provided above the data.

Shpere						
	run	keff analog	uncertainty	keff implicit	uncertainty	source n's
Graphite	1	1.00816	0.00156	1.00937	0.00104	2000
	2	1.00942	0.00052	1.00974	0.00043	10000
Free Carbon	1	1.03068	0.00117	1.02882	0.00096	2000
	2	1.0302	0.0006	1.03017	0.00049	10000
Pre 7.6ppm Era (6ppm)						
500 cycles with the first 50 removed for all calculations above.						

0.0	Detailed Model (no rods)						
		run	keff analog	uncertainty	keff implicit	uncertainty	source n's
	Graphite	1	1.02494	0.00051	1.02506	0.00041	10000
	Free Carbon	1	1.04289	0.00061	1.04233	0.00037	10000

0.1	Detailed Model (Rods above)						
		run	keff analog	uncertainty	keff implicit	uncertainty	source n's
	Graphite	1	1.02088	0.00041	1.02117	0.00029	20000
	Free Carbon	1	1.04247	0.00036	1.04221	0.00032	20000

0.2	Detailed Model (Rods above, gap between rods and assymbly added)						
		run	keff analog	uncertainty	keff implicit	uncertainty	source n's
	Graphite	1	1.01841	0.00048	1.01793	0.00028	20000
	Free Carbon	1	1.03982	0.00036	1.03945	0.00028	20000

0.3	Detailed Model (Rods below)						
		run	keff analog	uncertainty	keff implicit	uncertainty	source n's
	Graphite	1	1.01795	0.00046	1.01808	0.00026	20000
	Free Carbon	1	1.04013	0.00039	1.03998	0.00029	20000

Figure A.15: Effective multiplication factor of models 0.0 through 0.3.

0.4	After the change to 7.6 ppm Boron						
	run	keff analog	uncertainty	keff implicit	uncertainty	source n's	Cycles
	1	1.00355	0.00030	1.00372	0.00019	70000	250
	2	1.00394	0.00051	1.00375	0.00031	15000	500
	3	1.00379	0.00038	1.00405	0.00029	20000	500

1	After the change to 4 U isotopes (234, 235, 236, 238)						
	run	keff analog	uncertainty	keff implicit	uncertainty	source n's	Cycles
	1	1.00176	0.00036	1.00163	0.00035	30000	500
	2	1.00158	0.00030	1.00184	0.00018	70000	300

2	After addition of 2" air gap.						
	run	keff analog	uncertainty	keff implicit	uncertainty	source n's	Cycles
	1	0.99656	0.00036	0.99654	0.00026	30000	500
	2	0.99695	0.00027	0.99678	0.00020	70000	300

3	Changed Zr clad reflectors to similar composition as fuel assy but w/o fuel						
	run	keff analog	uncertainty	keff implicit	uncertainty	source n's	Cycles
	1	0.99156	0.00027	0.99100	0.00025	30000	500
	2	0.99079	0.00027	0.99140	0.00023	70000	300

4	Changed Carbon composition (60% graphite & 40% free gas C)						
	run	keff analog	uncertainty	keff implicit	uncertainty	source n's	Cycles
	1	1.00553	0.00031	1.00533	0.00024	30000	500
	2	1.00584	0.00024	1.00569	0.00018	80000	300

5	Corrected Zircaloy number density. (Had C density in it's place by mistake.)						
	run	keff analog	uncertainty	keff implicit	uncertainty	source n's	Cycles
	1	1.03775	0.00029	1.03767	0.00024	30000	500
	2	1.03789	0.00029	1.03788	0.00019	70000	300

6	Changed Carbon composition (59% graphite & 41% free gas C)						
	run	keff analog	uncertainty	keff implicit	uncertainty	source n's	Cycles
	1	1.03804	0.00032	1.03807	0.00022	30000	500
	2	1.03829	0.00032	1.03829	0.00018	70000	300

7	Added significant impurities from INL TREAT model. Stage 1.						
	run	keff analog	uncertainty	keff implicit	uncertainty	source n's	Cycles
	1	1.03654	0.00033	1.03652	0.00027	30000	500
	2	1.03611	0.00027	1.03599	0.00020	70000	300

d	Added significant impurities from INL TREAT model. Stage 2.						
	run	keff analog	uncertainty	keff implicit	uncertainty	source n's	Cycles
	1	1.02838	0.00034	1.02838	0.00023	30000	500
	2	1.02799	0.00021	1.02854	0.00023	70000	300

e	Cladding between fuel and control rods added.						
	run	keff analog	uncertainty	keff implicit	uncertainty	source n's	Cycles
	1	1.02118	0.00034	1.02107	0.00025	30000	500
	2	1.02150	0.00027	1.02129	0.00020	70000	300

f	Increase B4C density closer to that in INL model.						
	run	keff analog	uncertainty	keff implicit	uncertainty	source n's	Cycles
	1	1.02053	0.00031	1.02119	0.00018	30000	500
	2	1.02155	0.00030	1.02164	0.00021	70000	300

g	Replaced Al Refs with Zr in lattice.						
	run	keff analog	uncertainty	keff implicit	uncertainty	source n's	Cycles
	1	1.02286	0.00029	1.02285	0.00025	30000	500
	2	1.02248	0.00029	1.02263	0.00019	70000	300

h	Replaced Zr Refs with Al in lattice.						
	run	keff analog	uncertainty	keff implicit	uncertainty	source n's	Cycles
	1	1.02054	0.00033	1.02081	0.00023	30000	500
	2	1.02087	0.00031	1.02126	0.00021	70000	300

i	Added out gas tube						
	run	keff analog	uncertainty	keff implicit	uncertainty	source n's	Cycles
	1	1.02117	0.00039	1.02028	0.00024	30000	500
	2	1.02064	0.00032	1.02049	0.00019	70000	300

j	Added air gap between Al and Ref (T&B Reflectors of STD, CTRL and Zr)						
	run	keff analog	uncertainty	keff implicit	uncertainty	source n's	Cycles
	1	1.01016	0.00031	1.01035	0.00028	30000	500
	2	1.01055	0.00032	1.01032	0.00023	70000	300

k	Added air gap between Al and Ref (Al Dummy Reflectors)						
	run	keff analog	uncertainty	keff implicit	uncertainty	source n's	Cycles
	1	1.00700	0.00039	1.00661	0.00022	30000	500
	2	1.00671	0.00028	1.00706	0.00021	70000	300

Figure A.16: Effective multiplication factor of models 0.4 through k.

m	Added Al end caps on Al Dummy Reflectors						
	run	keff analog	uncertainty	keff implicit	uncertainty	source n's	Cycles
	1	1.00702	0.00034	1.00659	0.00023	30000	500
	2	1.00717	0.00032	1.00712	0.00023	70000	300

n	Homogenized Core Assemblies						
	run	keff analog	uncertainty	keff implicit	uncertainty	source n's	Cycles
	1	0.97200	0.00023	0.97193	0.00022	30000	500
	2	0.97156	0.00027	0.97161	0.00015	70000	300

n	Fixed Lattice, removed repeated titanium in #density (al&ref)						
	run	keff analog	uncertainty	keff implicit	uncertainty	source n's	Cycles
	1	1.00635	0.00031	1.00646	0.00027	30000	500
	2	1.00601	0.00024	1.00636	0.00018	70000	300

n	Unhomogenized fuel (std assy and ctrl assy)						
	run	keff analog	uncertainty	keff implicit	uncertainty	source n's	Cycles
	1	1.01429	0.00031	1.01422	0.00019	30000	500
	2	1.01385	0.00030	1.01387	0.00023	70000	300

n	Put rods to 60" instead of 60.34375"						
	run	keff analog	uncertainty	keff implicit	uncertainty	source n's	Cycles
	1	1.00617	0.00039	1.00635	0.00022	30000	500
	2	1.00571	0.00024	1.00577	0.00016	70000	300

o	Rods moved above core.						
	run	keff analog	uncertainty	keff implicit	uncertainty	source n's	Cycles
	1	1.00721	0.00036	1.00722	0.00023	30000	500
	2	1.00651	0.00027	1.00657	0.00013	70000	300

p	Returned number densities to rev 6 values.						
	run	keff analog	uncertainty	keff implicit	uncertainty	source n's	Cycles
	1	1.01663	0.00034	1.01668	0.00021	30000	500
	2					70000	300

Figure A.17: Effective multiplication factor of models m through p.

A.7 Thermal Expansion

My thermal expansion calculations only account for axial expansion because the effects of radial expansion are expected to be very limited due to the void between the graphite and the cladding. This simplifies the problem greatly so that only the linear expansion coefficient is required. Since I have been specifically comparing isothermal temperature coefficients of reactivity I expanded all core and reflector assemblies in equal amounts. I did not account for expansion of any other material besides the graphite. The linear expansion coefficient I used was the largest I found and thus would have the greatest effect. The idea being that if I did not see a significant change with this expansion coefficient and then the change should be even less for a smaller expansion coefficient and thus probably not worth calculating.

	Inches	cm
Height of fuel	24	60.96
(From Center)		
Height of Reflector	24	60.96
(From Center)		
Total	48	121.92

T (K)	ΔT (K)	ΔPZ	
400	104	0.038039	cm
500	204	0.074615	cm
600	304	0.111191	cm
700	404	0.147767	cm
800	504	0.184343	cm
1000	704	0.257495	cm
1200	904	0.330647	cm
1600	1304	0.476951	cm
1999	1703	0.622889	cm

Planes	±	Position	400	500	600	700	800	1000	1200	1600	1999
PZ-5 & 6	±	60.96	60.99804	61.03462	61.07119	61.10777	61.14434	61.2175	61.29065	61.43695	61.58289
PZ-7 & 8	±	61.595	6.16E+01	61.66962	61.70619	61.74277	61.77934	61.8525	61.92565	62.07195	62.21789
PZ-9 & 10	±	61.833125	61.87116	61.90774	61.94432	61.98089	62.01747	62.09062	62.16377	62.31008	62.45601
PZ-11 & 12	±	61.960125	61.99816	62.03474	62.07132	62.10789	62.14447	62.21762	62.29077	62.43708	62.58301
		Double the Change because these regions are beyond the reflector graphite									
PZ-13 & 14	±	122.92013	122.9962	123.0694	123.1425	123.2157	123.2888	123.4351	123.5814	123.874	124.1659
PZ-15 & 16	±	123.04713	123.1232	123.1964	123.2695	123.3427	123.4158	123.5621	123.7084	124.001	124.2929

T (K)	400	500	600	700	800	1000	1200	1600	1999
ΔT (K)	104	204	304	404	504	704	904	1304	1703
ΔPZ	3.80E-02	0.074615	0.111191	0.147767	0.184343	0.257495	0.330647	0.476951	0.622889

Figure A.18: Change in planes perpendicular to z by thermal expansion.

	To simplify the calc I converted V to XS area by dividing by height then multipled that by the new heights.										
	V (cc)	400	500	600	700	800	1000	1200	1600	1999	
Fuel	11112.65	11119.58612	11126.25372	11132.92131	11139.5889	11146.25649	11159.59167	11172.92685	11199.59722	11226.20091	
Reflectors	11451.83	11458.97894	11465.85004	11472.72114	11479.59224	11486.46334	11500.20554	11513.94774	11541.43214	11568.84783	
	XSA (cm^2)										
Fuel	91.14708										
Reflector	93.92908										
New number densities to account for the change in volume with the same total number of atoms.											
		296 N[(b*cm)$^{-1}$]	400	500	600	700	800	1000	1200	1600	1999
Fuel	U-234	9.33150000E-08	9.32568078E-08	9.32009221E-08	9.31451033E-08	9.30893514E-08	9.30336662E-08	9.29224954E-08	9.28115899E-08	9.25905714E-08	9.23711516E-08
	U-235	8.64137000E-06	8.63598115E-06	8.63080589E-06	8.62563684E-06	8.62047397E-06	8.61531728E-06	8.60502239E-06	8.59475206E-06	8.57428480E-06	8.55396558E-06
	U-236	1.85836000E-08	1.85720111E-08	1.85608815E-08	1.85497652E-08	1.85386623E-08	1.85275726E-08	1.85054331E-08	1.84833463E-08	1.84393307E-08	1.83956334E-08
	U-238	5.32131000E-07	5.31799157E-07	5.31480468E-07	5.31162160E-07	5.30844234E-07	5.30526687E-07	5.29892733E-07	5.29260292E-07	5.27999929E-07	5.26748682E-07
	Graphite	5.17435180E-02	5.17112502E-02	5.16802614E-02	5.16493097E-02	5.16183950E-02	5.15875173E-02	5.15258727E-02	5.14643752E-02	5.13418196E-02	5.12201505E-02
	Free C	3.44956780E-02	3.44741661E-02	3.44535069E-02	3.44328724E-02	3.44122627E-02	3.43916776E-02	3.43505811E-02	3.43095828E-02	3.42278791E-02	3.41467663E-02
	Boron-10	1.45913000E-07	1.45822007E-07	1.45734621E-07	1.45647339E-07	1.45560162E-07	1.45473089E-07	1.45299256E-07	1.45125837E-07	1.44780239E-07	1.44437141E-07
	Boron-11	5.83652000E-07	5.83288028E-07	5.82938483E-07	5.82589357E-07	5.82240649E-07	5.81892358E-07	5.81197024E-07	5.80503350E-07	5.79120958E-07	5.77748565E-07
	Iron	1.85516144E-05	1.85400454E-05	1.85289350E-05	1.85178379E-05	1.85067540E-05	1.84956835E-05	1.84735820E-05	1.84515333E-05	1.84075934E-05	1.83639713E-05
Reflector	Carbon	8.37490700E-02	8.36968432E-02	8.36466865E-02	8.35965898E-02	8.35465532E-02	8.34965764E-02	8.33968019E-02	8.32972656E-02	8.30989042E-02	8.29019776E-02
	Boron-10	3.71059680E-08	3.70828283E-08	3.70606058E-08	3.70384099E-08	3.70162406E-08	3.69940978E-08	3.69498917E-08	3.69057910E-08	3.68179047E-08	3.67306542E-08
	Boron-11	1.48423872E-07	1.48331313E-07	1.48242423E-07	1.48153640E-07	1.48064963E-07	1.47976391E-07	1.47799567E-07	1.47623164E-07	1.47271619E-07	1.46922617E-07
	Iron	1.80174500E-05	1.80062141E-05	1.79954236E-05	1.79846460E-05	1.79738813E-05	1.79631295E-05	1.79416644E-05	1.79202506E-05	1.78775758E-05	1.78352098E-05

Figure A.19: Change in density by thermal expansion.

The thermal expansion will cause a change in volume as the height of the assemblies increase however there is no change in mass so the densities must decrease. To calculate the change in volume first the cross sectional area of the assemblies was determined. As I was not accounting for radial expansion the cross sectional area remained constant, thus volumes could be calculated based solely on the change in height. With the initial volume and the calculations made for the volumes at each temperature number density

calculations were made by multiplying the reference number densities (at 296 K) by the ratio of the initial volume to the volume at the elevated temperature. With the new values for the planes perpendicular to z and the new number densities these values were put into their corresponding Serpent codes and effective multiplication calculations were ran, with the following results.

	Rev 4	Rev 4	Temp.	Isothermal αT		ANL-6173	
	Graph/FreeC	Therm Expan	Range	Over Temp. Range		$1.8x10^{-4}$	
C	Δ K-eff		(K)	NO Ther.	Ther. Exp.	22	0
22.85	0	0				37.5	-0.00279
126.85	-0.01558	-0.01549	296-400	-1.50E-04	-1.49E-04	1725.85	-0.30669
226.85	-0.02882	-0.02968	296-500	-1.41E-04	-1.45E-04		
326.85	-0.04214	-0.04309	296-600	-1.39E-04	-1.42E-04		
426.85	-0.05396	-0.05394					
526.85	-0.06462	-0.06582	296-800	-1.28E-04	-1.31E-04		
726.85	-0.08339	-0.08603					
926.85	-0.10074	-0.10344	296-1200	-1.11E-04	-1.14E-04		
1326.85	-0.13145	-0.13538					
1725.85	-0.16004	-0.16578	296-1999	-9.40E-05	-9.73E-05		

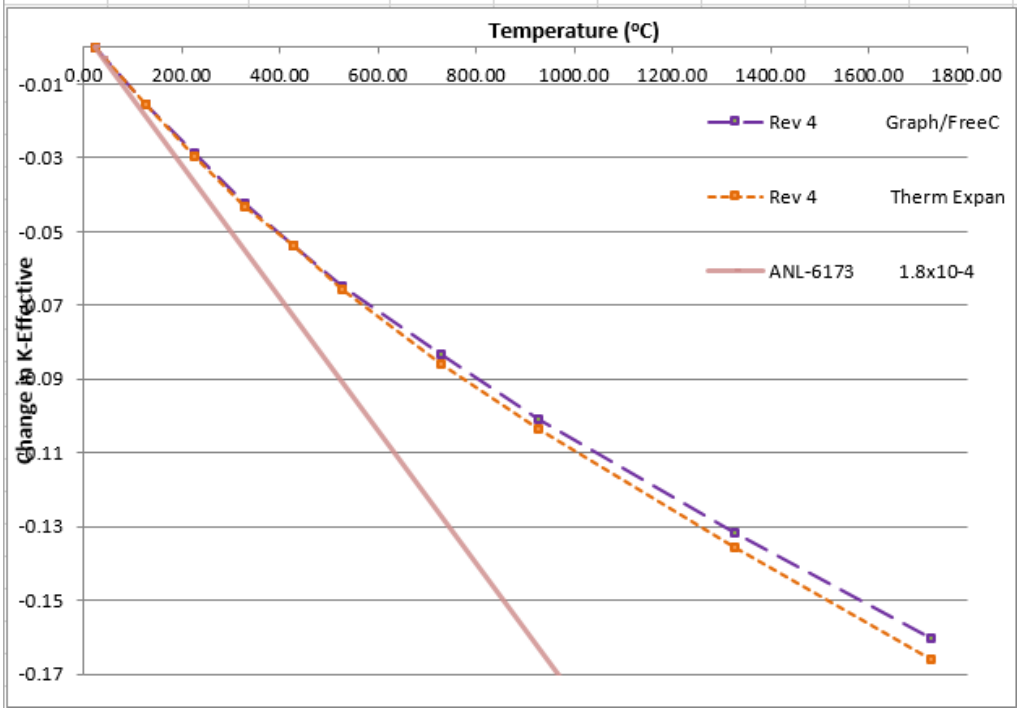


Figure A.20: Temperature coefficient comparison with thermal expansion.

Considering how small the effect of thermal expansion it does not seem worth the effort required.

A.8 Homogenization

In order to homogenize the assemblies a key parameter to obtain is the volume fractions of the materials. Although Serpent is capable of performing this action using the "checkvolume" command I calculated these volume fractions by hand and then compared my results with outputs from Serpent. Although I will not go into all of the details of performing these calculations in short it involved calculating the cross sectional areas of the square and octagonal cylinders then multiplying them by the heights. In order to calculate the cross sectional area of the octagonal surfaces I calculated the area of a square and subtracted away the four corners (triangles). I eventually developed this technique into a quick and repeatable formula based off of the two input parameters for serpent: the radius of the square (r1) and the radius of the diagonal (r2) as shown in figure A.20.

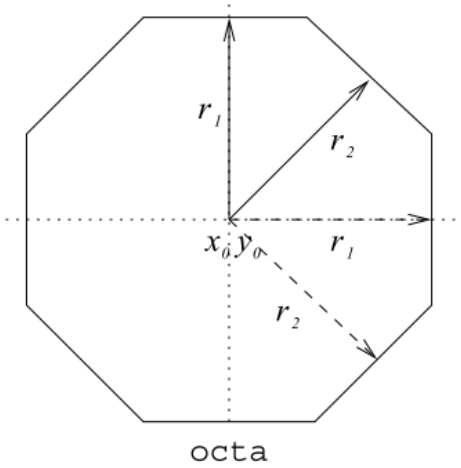


Figure A.21: Octagonal cylinder input.

$$Area = (2r_1)^2 - 4\left[r_2 - 1/2\sqrt{(2r_1)^2 + (2r_1)^2}\right]^2 \quad \textbf{(A.5)}$$

I eventually found that determining the central materials first, such as fuel and reflector, made the process easier. Once those were determined the void around them could be calculated by determining the volume of the void as if there were no fuel/reflector and then subtracting away the fuel/reflector volume. Inconsistencies such as the zirconium spacer, voids for the outgas tubes and the rivets that hold the reflector cans to the fuel cans added some difficulty in performing the calculations. The control rod assemblies proved to be especially difficult. In the end however I was able to perform all

the calculations and get results that compared almost exactly with the output from Serpent, thus giving me confidence that the geometry of my model was as I intended it to be.

(a)

Al Ref Vol				Coolant Volume			Al Volume			Air Volume	
	inches	cm		1125.72	cc		1185.959	cc		1009.7846	cc
l	4	10.16		Fraction	0.044314		Fraction	0.046685		Fraction	0.03975
w	4	10.16					Serpent Output				
h	96.8875	246.094		Reflector Volume			Material coolant	1125.7			
	1550.2	25403.227		22081.76	cc		Material air	1010.0			
		25403.227	cc	Fraction	0.86925		Material aluminium	1185.8			
							Material reflector	22082.0			

(b)

CTRL Fuel Assembly Volume				Coolant Volume			Zr Volume			Void Volume	
	inches	cm		565.69	cc		1076.2	cc		858.285	cc
l	4	10.16		Fraction	0.0551		Fraction	0.1049		Fraction	0.084
w	4	10.16					Serpent Output			Vol*2	
h	48.6875	123.66625		Fuel Volume			Material steel	508.87		507.173	
	779	12765.523		7758.8	cc		Material poison	1410.40		1404.48	
		10259.018	cc	Fraction	0.7563		Material fuel	8641.40		7758.8	
							Material coolant	565.58		565.692	
							Material air	1219.40		858.285	
							Material zircaloy	419.93		1076.24	

(c)

CTRL Top & Bottom Ref Vol				Coolant Volume			Al Volume			Reflector Volume	
	inches	cm		280.01	cc		307.77	cc		4070.81	cc
l	4	10.16		Fraction	0.0551		Fraction	0.0606		Fraction	0.8016
w	4	10.16					Serpent Output			Vol*2	
h	24.1	61.214		Void/Air Volume			Material steel	252.02		252.018	
	385.6	6318.85		419.55	cc		Material poison	698.00		697.896	
		5078.15	cc	Fraction	0.0826		Material coolant	279.99		280.014	
							Material air	290.80		419.547	
							Material aluminium	307.80		307.773	
							Material reflector	4490.25		4070.81	

(d)

Fuel Assembly Volume				Coolant Volume			Zr Volume			Void Volume	
	inches	cm		565.69	cc		455.25	cc		631.931	cc
l	4	10.16		Fraction	0.0443		Fraction	0.0357		Fraction	0.0495
w	4	10.16					Serpent Output				
h	48.6875	123.66625		Fuel Volume			Material fuel	11113.00			
	779	12765.523		11113	cc		Material coolant	565.76			
		12765.523	cc	Fraction	0.8705		Material air	631.95			
							Material zircaloy	455.11			

(e)

Top & Bottom Ref Vol				Coolant Volume			Al Volume			Air Volume	
	inches	cm		280.014	cc		312.7403	cc		450.31533	cc
l	4	10.16		Fraction	0.044314		Fraction	0.049493		Fraction	0.071265
w	4	10.16					Serpent Output			Vol*2	
h	24.1	61.214		Reflector Volume			Material coolant	560.02		560.02799	
	385.6	6318.8519		5275.782	cc		Material air	900.62		900.63066	
		6318.8519	cc	Fraction	0.834927		Material aluminium	625.58		625.48067	
							Material reflector	10552.00		10551.564	
When I calculated outgas tube volume I divided it by two since it is only in the top reflector.											

(f)

Zr Ref Volume				Coolant Volume			Zr Volume			Air Volume	
	inches	cm		1125.7	cc		455.25	cc		1471.03	cc
l	4	10.16		Fraction	0.0443		Fraction	0.0179209		Fraction	0.057907
w	4	10.16							Serpent Output		
h		246.09425		Al Volume			Reflector Volume		Material coolant		1125.70
		25403.227	cc	625.84	cc		21725	cc	Material air		1471.20
		25403.227		Fraction	0.0246		Fraction	0.8552217	Material zircaloy		455.19
									Material aluminium		625.88
									Material reflector		21725.00

Figure A.22: The calculated and serpent output volumes of the materials of: (a) aluminum clad reflector assembly (b) fuel section of the control rod assembly (c) top and bottom reflector section of the control rod assembly (d) fuel section of the standard fuel assembly (e) top and bottom reflector section of the standard fuel assembly (f) zircaloy clad reflector assembly.

For assemblies containing fuel I kept the fuel and reflector sections separate and for all other assemblies I homogenized the entire assembly. I did not homogenize any part of the control rods themselves because of the self-shielding effect.

Once the volume fractions were attained calculating the new number densities was relatively simple. The original number densities were multiplied by the volume fractions of the materials to give me new number densities. Although it was not necessary before putting anything into my code I summed up all repeated number densities. For example Iron in both the fuel graphite and zircaloy in the fuel assemblies so a number density for it shows up twice as you can see in figure A.22 (b).

As previously mentioned the result of full homogenization seems to be poorly representative of TREAT unless the fuel region is left non-homogenized.

(a)

Control Fuel Assy				Control RodUpper (Top) & Lower (Bottom) Reflector				Zircaloy Reflector			
	Fraction	Element	N		Fraction	Element	N		Fraction	Element	N
Coolant	0.13880244			Void	0.082618129			Al6063	0.024636345		
	Nitrogen	7014.03c	6.028673345E-06	Coolant	0.137759094				Iron	26000.03c	1.080361709E-05
	Oxygen	8016.03c	1.415962624E-06		Nitrogen	7014.03c	5.983357206E-06		Aluminum	13027.03c	1.477128446E-03
Zircaloy	0.104907053				Oxygen	8016.03c	1.405319161E-06			22000.03c	4.075795022E-07
	Iron	26000.03c	1.782618730E-05	Al6063	0.060607364					25055.03c	3.625484518E-07
	Tin	50000.03c	8.148551507E-06		Iron	26000.03c	2.657775568E-05			14000.03c	5.673491554E-06
	Zirconium	40000.03c	4.414991463E-03		Aluminum	13027.03c	3.633853238E-03			12000.03c	1.106312314E-05
		7014.03c	1.496604015E-06			22000.03c	1.002677931E-06			24000.03c	3.830609190E-07
		8016.03c	2.371319021E-05			25055.03c	8.918979723E-07				
		1001.03c	9.003333082E-06			14000.03c	1.395723961E-05			27059.03c	1.689856171E-07
		5010.03c	3.796796053E-09			12000.03c	2.721616117E-05	Coolant	0.1022211		
		5011.03c	1.528285945E-08			24000.03c	9.423602698E-07		Nitrogen	7014.03c	4.439817382E-06
		3006.03c	2.255606541E-09						Oxygen	8016.03c	1.042785885E-06
		21045.03c	4.588319766E-07			27059.03c	4.157180329E-07	Zircaloy	0.0179209		
		47000.03c	5.736737273E-07	Reflector	0.801633541				Iron	26000.03c	3.045179978E-06
		49000.03c	2.515094136E-08		B-10	5010.03c	2.974538853E-08		Tin	50000.03c	1.391986154E-06
Void	0.083661474				B-11	5011.03c	1.189815541E-07		Zirconium	40000.03c	7.541962496E-04
Fuel	0.756290507				Iron	26000.03c	1.444339225E-05			7014.03c	2.556591886E-07
	Graph	6012.03c	3.848091226E-02		Carbon II	6012.03c	6.713606667E-02			8016.03c	4.050834361E-06
	Free C	6000.03c	2.674097292E-02			22000.03c	2.021062452E-07			1001.03c	1.538005249E-06
	B-10	5010.03c	1.103526401E-07			23000.03c	1.899069860E-06			5010.03c	6.485922721E-10
	B-11	5011.03c	4.414105604E-07			3006.03c	5.906596260E-09			5011.03c	2.610712925E-09
	Iron	26000.03c	1.403040986E-05			1001.03c	1.789807208E-05			3006.03c	3.853167120E-10
	U-234	92234.03c	7.057328351E-08			8016.03c	8.947031955E-06			21045.03c	7.838052665E-08
	U-235	92235.03c	6.535386365E-06			73181.03c	2.227739612E-07			47000.03c	9.799850742E-08
	U-236	92236.03c	1.405459433E-08							49000.03c	4.296439939E-09
	U-238	92237.03c	4.024456319E-07	1		28000.03c	1.923025876E-08	Void	0.0579070		
		23000.03c	4.640144777E-07					Reflector	0.855221703		
1		8016.03c	1.405944053E-05						B-10	5010.03c	3.173382916E-08
									B-11	5011.03c	1.269353166E-07
									Iron	26000.03c	1.540891428E-05
									Carbon II	6012.03c	7.162402561E-02
										22000.03c	2.156167854E-07
										23000.03c	2.026020215E-06
										3006.03c	6.301444555E-09
										1001.03c	1.909453497E-05
										8016.03c	9.545129432E-06
										73181.03c	2.376661114E-07
								1.0000000		28000.03c	2.051577661E-08

(b)

Fuel Assy				Top and Bottom Reflector				Aluminum Reflector			
	Fraction	Element	N		Fraction	Element	N		Fraction	Element	N
Coolant	0.093816996			Void	0.071265372			Void	0.03975025		
	Nitrogen	7014.03c	4.074798836E-06	Coolant	0.115579435			Coolant	0.084064312		
	Oxygen	8016.03c	9.570534877E-07		Nitrogen	7014.03c	5.020017341E-06		Nitrogen	7014.03c	3.651205819E-06
Zircaloy	0.035662309				Oxygen	8016.03c	1.179058230E-06		Oxygen	8016.03c	8.575636256E-07
	Iron	26000.03c	6.059869066E-06	Al6063	0.049493222			Al6063	0.046685352		
	Tin	50000.03c	2.770034578E-06		Iron	26000.03c	2.170394259E-05		Iron	26000.03c	2.047262578E-05
	Zirconium	40000.03c	1.500840855E-03		Aluminum	13027.03c	2.967479384E-03		Aluminum	13027.03c	2.799127149E-03
		7014.03c	5.087585034E-07			22000.03c	8.188074459E-07			22000.03c	7.723545323E-07
		8016.03c	8.061108377E-06			25055.03c	7.283422505E-07			25055.03c	6.870216448E-07
		1001.03c	3.060610702E-06			14000.03c	1.139776928E-05			14000.03c	1.075114644E-05
		5010.03c	1.290690295E-09			12000.03c	2.222527766E-05			12000.03c	2.096438426E-05
		5011.03c	5.195285208E-09			24000.03c	7.695508018E-07			24000.03c	7.258923360E-07
		3006.03c	7.667753106E-10								
		21045.03c	1.559762419E-07			27059.03c	3.394839063E-07			27059.03c	3.202241686E-07
		47000.03c	1.950157718E-07	Reflector	0.834927344			Reflector	0.869250336		
		49000.03c	8.549860325E-09		B-10	5010.03c	3.098078730E-08		B-10	5010.03c	3.225437514E-08
Void	0.049502933				B-11	5011.03c	1.239231492E-07		B-11	5011.03c	1.290175006E-07
Fuel	0.870520695				Iron	26000.03c	1.504326167E-05		Iron	26000.03c	1.566167446E-05
	Graph	6012.03c	4.429307279E-02		Carbon II	6012.03c	6.992439178E-02		Carbon II	6012.03c	7.279891057E-02
	Free C	6000.03c	3.077993194E-02			22000.03c	2.105002121E-07			22000.03c	2.191536561E-07
	B-10	5010.03c	1.270203130E-07			23000.03c	1.977942877E-06			23000.03c	2.059254045E-06
	B-11	5011.03c	5.080812521E-07			3006.03c	6.151911654E-09			3006.03c	6.404810323E-09
	Iron	26000.03c	1.614956426E-05			1001.03c	1.864142280E-05			1001.03c	1.940775224E-05
	U-234	92234.03c	8.123267876E-08			8016.03c	9.318624084E-06			8016.03c	9.701702996E-06
	U-235	92235.03c	7.522491724E-06			73181.03c	2.320263088E-07			73181.03c	2.415646683E-07
	U-236	92236.03c	1.617740156E-08								
	U-238	92237.03c	4.632310572E-07	1		28000.03c	2.002893846E-08	1		28000.03c	2.085230722E-08
		23000.03c	5.340992672E-07								
1		8016.03c	1.618297972E-05								

Figure A.23: Number densities of all homogenized assemblies and assembly sections.

APPENDIX B: DIAGRAMS AND DRAWINGS

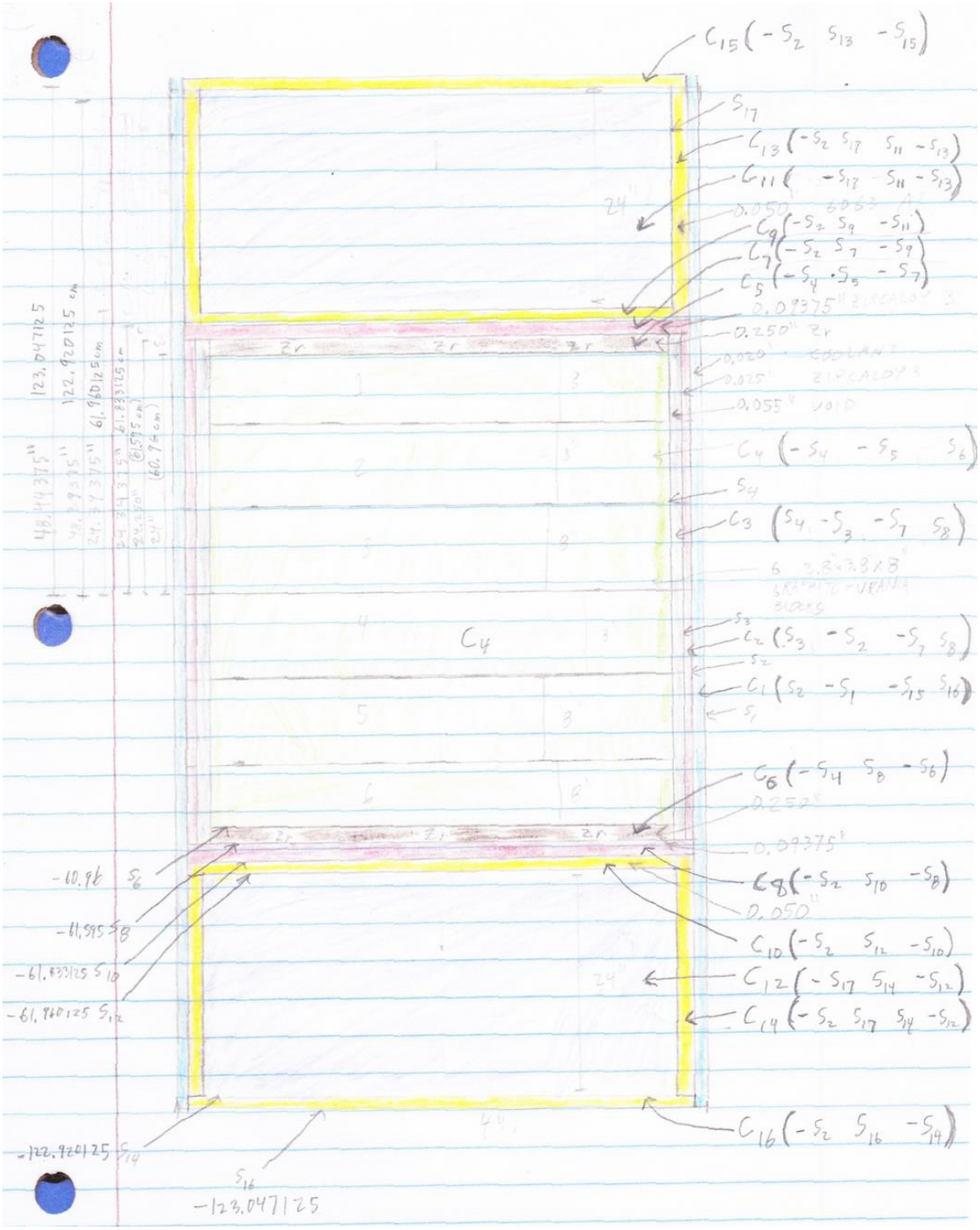


Figure B.1: Drawing of standard fuel assembly for revision 0.0 TREAT model.



Figure B.2: Radii for the octagonal cylinder surface input cards.

APPENDIX C: APPENDIX C: CODES

In this appendix I originally intend to list all of the input decks for all of the revisions I have made to my model, however I realized this would be far too many pages. I will only list revisions with major changes where I calculated all the physics comparisons. I will provide various temperatures and rod heights as examples of these changes. I will list the revisions in the order in which they were created and provide a brief description of the changes made to the model in between revisions. These are the same input codes ran by Serpent in my calculations except for some changes to the tabulation in order to make the text documents fit better in word and in some cases I added some more comments.

C.1 Spherical Model

The first revision is based off of the spherical model described in ANL-6174. The cross section data temperature is for 296 K. Free carbon thermal neutron cross sections are used for the fuel while graphite thermal neutron cross sections are used for the reflector.

```
% --- TREAT Spherical Approximation --- %

% --- Surface Input --- %
surf 1 sph 0 0 0 71
surf 2 sph 0 0 0 166.7

% --- Cell Input --- %
cell 1 0 fuel -1
cell 2 0 reflector 1 -2
cell 3 0 outside 2

% --- Material Input --- %

therm gre gre6.00t                          %Graphite thermal XS at 296 K.

mat fuel sum
92235.03c 7.5742e-6                         %U-235
92238.03c 5.5431e-7                         %U-238
40000.03c 1.1903e-3                         %Zirconium
5010.03c 1.0044e-7                          %Boron-10
5011.03c 4.0426e-7                          %Boron-11
26000.03c 3.3435e-5                         %Iron
6012.03c 0.0760275                          %Carbon-12 Free gas therm. XS.
```

```
mat reflector sum  moder gre 6012          %Graphite thermal XS only used for reflector.
40000.03c 1.9533e-4                        %Zirconium
5010.03c 3.1762e-8                         %Boron-10
5011.03c 1.2785e-7                         %Boron-11
26000.03c 7.8934e-5                        %Iron
13027.03c 2.605e-3                         %Aluminium
6012.03c 0.072216                          %Carbon-12

% --- Library File Path --- %
set acelib "/home/SERPENT_XSDATA/XSData/endfb7/endfb7.xs"
set declib "/home/SERPENT_XSDATA/XSData/endfb7/sss_endfb7.dec"
set nfylib "/home/SERPENT_XSDATA/XSData/endfb7/sss_endfb7.nfy"

%--- Mesh Generation --- %
%mesh 3 1000 1000
plot 3 2000 2000

% --- Calculation Input --- %
set pop 2000 500 50 1.0 10

% --- Multigroup Cross Section Generation --- %
set gcu 0
set nfg 3 0.4e-6 1.44e-6
```

C.2 Revision 0.0

This revision is the very first detailed model I created. Although you will see control rod assemblies there are not actually any control rods that run through it, instead there is a void in this region. The cross section data is for 400 K and thus “tmp 400” is used to correct the Doppler-broadening and “gre6.04t” is used to ensure the graphite thermal neutron cross section data is that at 400 K. This is with the minimum core loading of 133 fuel assemblies.

```
% --- Treat Rev. 0.0 --- %   %temperature set to 400K (126.85C)%


% --- Library File Path --- %
set acelib "/home/SERPENT_XSDATA/XSData/endfb7/endfb7.xs"
set declib "/home/SERPENT_XSDATA/XSData/endfb7/sss_endfb7.dec"
set nfylib "/home/SERPENT_XSDATA/XSData/endfb7/sss_endfb7.nfy"


% --- Surface Card --- %

surf 1 sqc 0 0 5.08                  %Assembly including coolant gaps.
surf 2 octa 0 0 5.0292 6.318613      %Surface at the outside edge of the Zr.
surf 3 octa 0 0 4.9657 6.255113      %Surface at the outside edge of the void.
surf 4 octa 0 0 4.826 6.115413       %Surface at the outside edge of the fuel.
surf 5 pz 60.96                      %The top of the fuel.
surf 6 pz -60.96                     %The bottom of the fuel.
surf 7 pz 61.595                     %The top of the top Zr spacer.
surf 8 pz -61.595                    %The bottom of the bottom Zr spacer.
surf 9 pz 61.833125                  %The top surface between the zircaloy 3 cladding and Al 6063 cladding.
surf 10 pz -61.833125                %The bottom surface between the zircaloy 3 cladding and Al 6063 cladding.
surf 11 pz 61.960125                 %The top inside surface between the Al 6063 cladding and graphite reflector.
surf 12 pz -61.960125                %The bottom inside surface between the Al 6063 cladding and graphite reflector.
```

```
surf 13 pz 122.920125                %The top outside surface between the Al 6063 cladding and graphite reflector.
surf 14 pz -122.920125          %The bottom outside surface between the Al 6063 cladding and graphite reflector.
surf 15 pz 123.047125                %The top surface of the Al 6063 cladding (top of core).
surf 16 pz -123.047125               %The bottom surface of the Al 6063 cladding (bottom of core).
surf 17 octa 0 0 4.9022 6.191613     %Surface at the outside edge of the reflector.
surf 18 sqc 0 0 96.52                %Outer edge of the core.
%surf 19 sqc 0 0 101.6               %Inner edge of the reflector. (will be used if there is an air gap)
surf 20 sqc 0 0 157.48               %Outer edge of the reflector. (162.56 instead of 157.48 if there is an air gap)
surf 21 cyl 0 0 2.2225               %Control rod.


% --- Cell Card --- %

% Standard Fuel Assembly %
cell 1 1 coolant 2 -1 -15 16                %Coolant channel around assembly.
cell 2 1 zircaloy 3 -2 -7 8                 %Zircaloy 3 casing of assembly (25 mils).
cell 3 1 void 4 -3 -7 8                     %Void within assembly (55 mils).
cell 4 1 fuel -4 -5 6                       %Fuel within assembly (six 3.9"x3.9"x8" blocks stacked 48" high).
cell 5 1 zircaloy -4 5 -7                   %Top Zr spacer (1/4").
cell 6 1 zircaloy -4 8 -6                   %Bottom Zr spacer (1/4").
cell 7 1 zircaloy -2 7 -9                   %Top Zircaloy 3 fuel end-cap (3/32").
cell 8 1 zircaloy -2 10 -8                  %Bottom Zircaloy 3 fuel end-cap (3/32").
cell 9 1 aluminium -2 9 -11                 %Top Al 6063 reflector cladding bottom end-cap(50 mils).
cell 10 1 aluminium -2 12 -10               %Bottom Al 6063 reflector cladding top end-cap(50 mils).
cell 11 1 reflector -17 11 -13              %Top assembly reflector (24").
cell 12 1 reflector -17 14 -12              %Bottom assembly reflector (24").
cell 13 1 aluminium -2 17 11 -13            %Top Reflector Al 6063 cladding (50 mils).
cell 14 1 aluminium -2 17 14 -12            %Bottom Reflector Al 6063 cladding (50 mils).
cell 15 1 aluminium -2 13 -15               %Top Al 6063 reflector cladding top end-cap(50 mils).
cell 16 1 aluminium -2 16 -14               %Bottom Al 6063 reflector cladding bottom end-cap(50 mils).

% Control Rod Fuel Assembly %
cell 41 2 coolant 2 -1 -15 16               %Coolant channel around assembly.
cell 42 2 zircaloy 3 -2 -7 8                %Zircaloy 3 casing of assembly (25 mils).
cell 43 2 void 4 -3 -7 8                    %Void within assembly (55 mils).
cell 44 2 fuel 21 -4 -5 6                   %Fuel within assembly (six 3.9"x3.9"x8" blocks stacked 48" high).
cell 45 2 zircaloy 21 -4 5 -7               %Top Zr spacer (1/4").
cell 46 2 zircaloy 21 -4 8 -6               %Bottom Zr spacer (1/4").
cell 47 2 zircaloy 21 -2 7 -9               %Top Zircaloy 3 fuel end-cap (3/32").
cell 48 2 zircaloy 21 -2 10 -8              %Bottom Zircaloy 3 fuel end-cap (3/32").
cell 49 2 aluminium 21 -2 9 -11             %Top Al 6063 reflector cladding bottom end-cap(50 mils).
cell 50 2 aluminium 21 -2 12 -10            %Bottom Al 6063 reflector cladding top end-cap(50 mils).
cell 51 2 reflector 21 -17 11 -13           %Top assembly reflector (24").
cell 52 2 reflector 21 -17 14 -12           %Bottom assembly reflector (24").
cell 53 2 aluminium -2 17 11 -13            %Top Reflector Al 6063 cladding (50 mils).
cell 54 2 aluminium -2 17 14 -12            %Bottom Reflector Al 6063 cladding (50 mils).
cell 55 2 aluminium 21 -2 13 -15            %Top Al 6063 reflector cladding top end-cap(50 mils).
cell 56 2 aluminium 21 -2 16 -14            %Bottom Al 6063 reflector cladding bottom end-cap(50 mils).
cell 57 2 void -21 -15 16                   %Void where the control rod would go through.

% Aluminium Can Dummy Fuel Assembly %
cell 61 3 coolant 2 -1 -15 16               %Coolant channel around assembly.
cell 63 3 aluminium -2 17 -15 16            %Reflector Al 6063 cladding (50 mils).
cell 64 3 reflector -17 -15 16              %Reflector.

% Zircaloy Can Dummy Fuel Assembly %
cell 81 4 coolant 2 -1 -15 16               %Coolant channel around assembly.
cell 82 4 zircaloy 3 -2 -15 16              %Zircaloy 3 casing of assembly (25 mils).
cell 83 4 reflector -3 -15 16               %Reflector.

% Access Hole Fuel Assembly %

% Access Hole Dummy Fuel Assembly %

% Shielding Assembly %

% Thermocouple Fuel Assembly %

% Core %
cell 17 0 outside -16                       %Brings flux to zero outside of the core (sets boundary conditions).
```

```
cell 18 0 outside 15                    %Brings flux to zero outside of the core (sets boundary conditions).
cell 19 0 outside 20 -15 16             %Brings flux to zero outside of the core (sets boundary conditions).
cell 20 0 fill 10 -18 -15 16            %Fuel assembly.
%cell 21 0 air 18 -19 -15 -16           %Air gap between core and reflector. (not sure if there is a air gap)
cell 22 0 reflector 18 -20 -15 16       %Outside reflector.


% --- Lattice --- %
lat 10 1 0 0 19 19 10.16

3 3 3 3 3 3 3 3 3 3 3 3 3 3 3 3 3 3 3
3 3 3 3 3 3 3 3 3 3 3 3 3 3 3 3 3 3 3
3 3 3 3 3 3 4 4 4 4 4 4 4 3 3 3 3 3 3
3 3 3 3 3 4 1 1 1 4 1 1 1 4 3 3 3 3 3
3 3 3 3 4 1 1 1 1 1 1 1 1 4 3 3 3 3 3
3 3 3 4 1 1 1 2 1 1 1 2 1 1 1 4 3 3 3
3 3 4 1 1 1 1 1 1 1 1 1 1 1 1 1 4 3 3
3 3 4 1 1 2 1 1 1 1 1 1 2 1 1 4 3 3 3
3 3 4 1 1 1 1 1 1 1 1 1 1 1 1 1 4 3 3
3 3 4 4 1 1 1 1 1 1 1 1 1 1 1 4 4 3 3
3 3 4 1 1 1 1 1 1 1 1 1 1 1 1 1 4 3 3
3 3 4 1 1 2 1 1 1 1 1 1 2 1 1 4 3 3 3
3 3 4 1 1 1 1 1 1 1 1 1 1 1 1 1 4 3 3
3 3 3 4 1 1 1 2 1 1 1 2 1 1 1 4 3 3 3
3 3 3 3 4 1 1 1 1 1 1 1 1 1 4 3 3 3 3
3 3 3 3 3 4 1 1 1 4 1 1 1 4 3 3 3 3 3
3 3 3 3 3 3 4 4 4 4 4 4 4 3 3 3 3 3 3
3 3 3 3 3 3 3 3 3 3 3 3 3 3 3 3 3 3 3
3 3 3 3 3 3 3 3 3 3 3 3 3 3 3 3 3 3 3


% --- Material Card --- %

therm gre gre6.04t

mat fuel sum moder gre 6012 tmp 400     %Fuel
92235.03c 8.6516144e-6                  %U-235
92238.03c 6.313164e-7                   %U-238
%8016.03c 8.265813e-1                   %Oxygen
6012.03c 0.0862391959                   %Carbon
5010.03c 1.14864798e-7                  %Boron-10
5011.03c 4.59459192e-7                  %Boron-11
26000.03c 1.85516144e-5                 %Iron

mat coolant -0.001294 tmp 400           %Coolant
7014.03c 4.3433e-5                      %Nitrogen
%6000.03c 5.3107e-9                     %Carbon
8016.03c 1.0212e-5                      %Oxygen
%1001.03c 3.8648e-10                    %Hydrogen
%18040.03c 1.8195e-7                    %Argon
%code 6.9491e-10                        %Neon
%2000.03c 9.7320e-10                    %Helium
%36084.03c 9.2970e-12                   %Krypton
%54131.03c 5.3405e-13                   %Xenon

%mat air -0.001294 tmp 400              %Air Gap
%7014.03c 4.3433e-5                     %Nitrogen
%6012.03c 5.3107e-9                     %Carbon
%8016.03c 1.0212e-5                     %Oxygen

Mat zircaloy sum tmp 400                %Zircaloy
%24000.03c 7.5977e-4                    %Chromium
26000.03c 0.0001699236                  %Iron
50000.03c 0.000077674                   %Tin
40000.03c 0.08374907                    %Zirconium

%Mat zirconium -5.68 tmp 400            %Zirconium spacer
%40000.03c -1.0                         %Zirconium

Mat aluminium sum tmp 400               %Al 6063
```

```
13027.03c 0.0599572887                    %Aluminium
%24000.03c .001                           %Chromium
26000.03c .0004385235                     %Iron
%30000.03c .001                           %Zinc
%12000.03c .00675                         %Magnesium
%25055.03c .001                           %Manganese
%14000.03c .005                           %Silicon
%22000.03c .001                           %Titanium
%29000.03c .001                           %Copper

Mat reflector sum moder gre 6012 tmp 400  %Graphite
6012.03c 0.08374907                       %Carbon
5010.03c 3.7105968e-8                     %Boron-10
5011.03c 1.48423872e-7                    %Boron-11
26000.03c 1.801745e-5                     %Iron

%--- Mesh Generation --- %
%mesh 3 2000 2000
%plot 3 5000 5000
%plot 2 6300 4920
%mesh 2 3150 2460

% --- Calculation Input --- %
set pop 2000 500 50 1.0 10
```

C.3 Revision 0.4

In this revision, 0.4, I have added control rods which rise up from below the core, which is incorrect. Additionally with the rods withdrawn a void runs through the core, which is incorrect as well. These issues were corrected in revision o and can be seen in revision p below. Control rod 1 is fully withdrawn in this example and could be adjusted by changing surfaces 23 and 24. This is the first revision in which the boron impurity in the fuel was increased from 6 ppm to 7.6 ppm.

```
% --- Treat Rev. 0.4 --- %                    %133 fuel elements.

% --- Library File Path --- %
set acelib "/home/SERPENT_XSDATA/XSData/endfb7/endfb7.xs"
set declib "/home/SERPENT_XSDATA/XSData/endfb7/sss_endfb7.dec"
set nfylib "/home/SERPENT_XSDATA/XSData/endfb7/sss_endfb7.nfy"

% --- Surface Card --- %

surf 1 sqc 0 0 5.08                       %Assembly including coolant gaps.
surf 2 octa 0 0 5.0292 6.318613           %Surface at the outside edge of the Zr.
surf 3 octa 0 0 4.9657 6.255113           %Surface at the outside edge of the void.
surf 4 octa 0 0 4.826 6.115413            %Surface at the outside edge of the fuel.
surf 5 pz 60.96                           %The top of the fuel.
surf 6 pz -60.96                          %The bottom of the fuel.
surf 7 pz 61.595                          %The top of the top Zr spacer.
surf 8 pz -61.595                         %The bottom of the bottom Zr spacer.
surf 9 pz 61.833125                       %The top surface between the zircaloy 3 cladding and Al 6063 cladding.
surf 10 pz -61.833125                     %The bottom surface between the zircaloy 3 cladding and Al 6063 cladding.
surf 11 pz 61.960125                      %The top inside surface between the Al 6063 cladding and graphite reflector.
surf 12 pz -61.960125                     %The bottom inside surface between the Al 6063 cladding and graphite reflector.
```

```
surf 13 pz 122.920125                %The top outside surface between the Al 6063 cladding and graphite reflector.
surf 14 pz -122.920125          %The bottom outside surface between the Al 6063 cladding and graphite reflector.
surf 15 pz 123.047125                %The top surface of the Al 6063 cladding (top of core).
surf 16 pz -123.047125               %The bottom surface of the Al 6063 cladding (bottom of core).
surf 17 octa 0 0 4.9022 6.191613     %Surface at the outside edge of the reflector.
surf 18 sqc 0 0 96.52                %Outer edge of the core.
%surf 19 sqc 0 0 101.6               %Inner edge of the reflector. (will be used if there is an air gap)
surf 20 sqc 0 0 157.48          %Outer edge of the reflector. (162.56 instead of 157.48 if there is an air gap)
surf 21 cyl 0 0 2.2225               %Control rod steel tube OD.
surf 22 cyl 0 0 1.905                %Control rod steel tube ID.
surf 23 pz -77.073125                %Bottom of the control rod 1.
surf 24 pz -229.473125               %Surface between poison and zircaloy follower of control rod 1.
%surf 25 pz -381.873125              %Top of the control rod 1.
surf 26 pz -77.073125                %Bottom of the control rod 2.
surf 27 pz -229.473125               %Surface between poison and zircaloy follower of control rod 2.
%surf 28 pz -381.873125%             Top of the control rod 2.
surf 29 pz -77.073125                %Bottom of SD control rod.
surf 30 pz -229.473125               %Surface between poison and zircaloy follower of SD control rod.
%surf 31 pz -381.873125               %Top of SD control rod.
surf 32 pz -381.873125               %Top of control rods.
surf 33 cyl 0 0 2.54                 %Control rod assembly hole ANL-6173 pg 12.


% --- Cell Card --- %

% Control Rod 1 %
cell 141 5 coolant 2 -1 -15 16       %Coolant channel around assembly.
cell 142 5 zircaloy 3 -2 -7 8        %Zircaloy 3 casing of assembly (25 mils).
cell 143 5 air 4 -3 -7 8             %Void within assembly (55 mils).
cell 144 5 fuel 33 -4 -5 6           %Fuel within assembly (six 3.9"x3.9"x8" blocks stacked 48" high).
cell 145 5 zircaloy 33 -4 5 -7       %Top Zr spacer (1/4").
cell 146 5 zircaloy 33 -4 8 -6       %Bottom Zr spacer (1/4").
cell 147 5 zircaloy 33 -2 7 -9       %Top Zircaloy 3 fuel end-cap (3/32").
cell 148 5 zircaloy 33 -2 10 -8      %Bottom Zircaloy 3 fuel end-cap (3/32").
cell 149 5 aluminium 33 -2 9 -11     %Top Al 6063 reflector cladding bottom end-cap(50 mils).
cell 150 5 aluminium 33 -2 12 -10    %Bottom Al 6063 reflector cladding top end-cap(50 mils).
cell 151 5 reflector 33 -17 11 -13   %Top assembly reflector (24").
cell 152 5 reflector 33 -17 14 -12   %Bottom assembly reflector (24").
cell 153 5 aluminium -2 17 11 -13    %Top Reflector Al 6063 cladding (50 mils).
cell 154 5 aluminium -2 17 14 -12    %Bottom Reflector Al 6063 cladding (50 mils).
cell 155 5 aluminium 33 -2 13 -15    %Top Al 6063 reflector cladding top end-cap(50 mils).
cell 156 5 aluminium 33 -2 16 -14    %Bottom Al 6063 reflector cladding bottom end-cap(50 mils).
cell 157 5 air -21 23 -15            %Void where the control rod would go through.
cell 158 5 steel -21 22 -23 24       %Control rod poison carbon steel housing.
cell 159 5 poison -22 -23 24         %Control rod poison.
cell 160 5 zircaloy -21 22 -24 32    %Control rod zircaloy follower housing.
cell 161 5 reflector -22 -24 32      %Control rod zircaloy follower.
cell 162 5 outside 21 -16 32 -1      %Brings flux to zero outside of the core (sets boundary conditions).
cell 163 5 air -33 21 -15 16         %Control rod assembly hole.

% Control Rod 2 %
cell 241 6 coolant 2 -1 -15 16       %Coolant channel around assembly.
cell 242 6 zircaloy 3 -2 -7 8        %Zircaloy 3 casing of assembly (25 mils).
cell 243 6 air 4 -3 -7 8             %Void within assembly (55 mils).
cell 244 6 fuel 33 -4 -5 6           %Fuel within assembly (six 3.9"x3.9"x8" blocks stacked 48" high).
cell 245 6 zircaloy 33 -4 5 -7       %Top Zr spacer (1/4").
cell 246 6 zircaloy 33 -4 8 -6       %Bottom Zr spacer (1/4").
cell 247 6 zircaloy 33 -2 7 -9       %Top Zircaloy 3 fuel end-cap (3/32").
cell 248 6 zircaloy 33 -2 10 -8      %Bottom Zircaloy 3 fuel end-cap (3/32").
cell 249 6 aluminium 33 -2 9 -11     %Top Al 6063 reflector cladding bottom end-cap(50 mils).
cell 250 6 aluminium 33 -2 12 -10    %Bottom Al 6063 reflector cladding top end-cap(50 mils).
cell 251 6 reflector 33 -17 11 -13   %Top assembly reflector (24").
cell 252 6 reflector 33 -17 14 -12   %Bottom assembly reflector (24").
cell 253 6 aluminium -2 17 11 -13    %Top Reflector Al 6063 cladding (50 mils).
cell 254 6 aluminium -2 17 14 -12    %Bottom Reflector Al 6063 cladding (50 mils).
cell 255 6 aluminium 33 -2 13 -15    %Top Al 6063 reflector cladding top end-cap(50 mils).
cell 256 6 aluminium 33 -2 16 -14    %Bottom Al 6063 reflector cladding bottom end-cap(50 mils).
cell 257 6 air -21 26 -15            %Void where the control rod would go through.
cell 258 6 steel -21 22 -26 27       %Control rod poison carbon steel housing.
cell 259 6 poison -22 -26 27         %Control rod poison.
```

```
cell 260 6 zircaloy -21 22 -27 32          %Control rod zircaloy follower housing.
cell 261 6 reflector -22 -27 32            %Control rod zircaloy follower.
cell 262 6 outside 21 -16 32 -1            %Brings flux to zero outside of the core (sets boundary conditions).
cell 263 6 air -33 21 -15 16               %Control rod assembly hole.

% Shutdown Control Rod Fuel Assembly %
cell 41 2 coolant 2 -1 -15 16              %Coolant channel around assembly.
cell 42 2 zircaloy 3 -2 -7 8               %Zircaloy 3 casing of assembly (25 mils).
cell 43 2 air 4 -3 -7 8                    %Void within assembly (55 mils).
cell 44 2 fuel 33 -4 -5 6                  %Fuel within assembly (six 3.9"x3.9"x8" blocks stacked 48" high).
cell 45 2 zircaloy 33 -4 5 -7              %Top Zr spacer (1/4").
cell 46 2 zircaloy 33 -4 8 -6              %Bottom Zr spacer (1/4").
cell 47 2 zircaloy 33 -2 7 -9              %Top Zircaloy 3 fuel end-cap (3/32").
cell 48 2 zircaloy 33 -2 10 -8             %Bottom Zircaloy 3 fuel end-cap (3/32").
cell 49 2 aluminium 33 -2 9 -11            %Top Al 6063 reflector cladding bottom end-cap(50 mils).
cell 50 2 aluminium 33 -2 12 -10           %Bottom Al 6063 reflector cladding top end-cap(50 mils).
cell 51 2 reflector 33 -17 11 -13          %Top assembly reflector (24").
cell 52 2 reflector 33 -17 14 -12          %Bottom assembly reflector (24").
cell 53 2 aluminium -2 17 11 -13           %Top Reflector Al 6063 cladding (50 mils).
cell 54 2 aluminium -2 17 14 -12           %Bottom Reflector Al 6063 cladding (50 mils).
cell 55 2 aluminium 33 -2 13 -15           %Top Al 6063 reflector cladding top end-cap(50 mils).
cell 56 2 aluminium 33 -2 16 -14           %Bottom Al 6063 reflector cladding bottom end-cap(50 mils).
cell 57 2 air -21 29 -15                   %Void where the control rod would go through.
cell 58 2 steel -21 22 -29 30              %Carbon steel tube.
cell 59 2 poison -22 -29 30                %Boron-carbide powder compacted to 1.6g/cc.
cell 60 2 zircaloy -21 22 -30 32           %Zircaloy follower housing.
cell 61 2 reflector    -22          -30 32 %Zircaloy follower.
cell 62 2 outside 21 -16 32 -1             %Brings flux to zero outside of the core (sets boundary conditions).
cell 63 2 air -33 21 -15 16                %Control rod assembly hole.

% Standard Fuel Assembly %
cell 1 1 coolant 2 -1 -15 16               %Coolant channel around assembly.
cell 2 1 zircaloy 3 -2 -7 8                %Zircaloy 3 casing of assembly (25 mils).
cell 3 1 air 4 -3 -7 8                     %Void within assembly (55 mils).
cell 4 1 fuel -4 -5 6                      %Fuel within assembly (six 3.9"x3.9"x8" blocks stacked 48" high).
cell 5 1 zircaloy -4 5 -7                  %Top Zr spacer (1/4").
cell 6 1 zircaloy -4 8 -6                  %Bottom Zr spacer (1/4").
cell 7 1 zircaloy -2 7 -9                  %Top Zircaloy 3 fuel end-cap (3/32").
cell 8 1 zircaloy -2 10 -8                 %Bottom Zircaloy 3 fuel end-cap (3/32").
cell 9 1 aluminium -2 9 -11                %Top Al 6063 reflector cladding bottom end-cap(50 mils).
cell 10 1 aluminium -2 12 -10              %Bottom Al 6063 reflector cladding top end-cap(50 mils).
cell 11 1 reflector -17 11 -13             %Top assembly reflector (24").
cell 12 1 reflector -17 14 -12             %Bottom assembly reflector (24").
cell 13 1 aluminium -2 17 11 -13           %Top Reflector Al 6063 cladding (50 mils).
cell 14 1 aluminium -2 17 14 -12           %Bottom Reflector Al 6063 cladding (50 mils).
cell 15 1 aluminium -2 13 -15              %Top Al 6063 reflector cladding top end-cap(50 mils).
cell 16 1 aluminium -2 16 -14              %Bottom Al 6063 reflector cladding bottom end-cap(50 mils).
cell 17 1 outside -16 32 -1                %Brings flux to zero outside of the core (sets boundary conditions).

% Aluminium Can Dummy Fuel Assembly %
cell 71 3 coolant 2 -1 -15 16              %Coolant channel around assembly.
cell 72 3 aluminium -2 17 -15 16           %Reflector Al 6063 cladding (50 mils).
cell 73 3 reflector -17 -15 16             %Reflector.
cell 74 3 outside -16 32 -1                %Brings flux to zero outside of the core (sets boundary conditions).

% Zircaloy Can Dummy Fuel Assembly %
cell 81 4 coolant 2 -1 -15 16              %Coolant channel around assembly.
cell 82 4 zircaloy 3 -2 -15 16             %Zircaloy 3 casing of assembly (25 mils).
cell 83 4 reflector -3 -15 16              %Reflector.
cell 84 4 outside -16 32 -1                %Brings flux to zero outside of the core (sets boundary conditions).

% Access Hole Fuel Assembly %

% Access Hole Dummy Fuel Assembly %

% Shielding Assembly %

% Thermocouple Fuel Assembly %

% Core %
```

```
cell 20 0 outside 15                    %Brings flux to zero outside of the core (sets boundary conditions).
cell 21 0 outside -32                   %Brings flux to zero outside of the core (sets boundary conditions).
cell 22 0 outside 20 -15 16             %Brings flux to zero outside of the core (sets boundary conditions).
cell 23 0 outside -16 32 18             %Brings flux to zero outside of the core (sets boundary conditions).
cell 24 0 fill 10 -18 32 -15            %Core.
%cell 25 0 air 18 -19 -15 -16           %Air gap between core and reflector. (not sure if there is a air gap)
cell 26 0 reflector 18 -20 -15 16       %Outside reflector.


% --- Lattice --- %
lat 10 1 0 0 19 19 10.16

3 3 3 3 3 3 3 3 3 3 3 3 3 3 3 3 3 3 3
3 3 3 3 3 3 3 3 3 3 3 3 3 3 3 3 3 3 3
3 3 3 3 3 3 4 4 4 4 4 4 4 3 3 3 3 3 3
3 3 3 3 3 4 1 1 1 4 1 1 1 4 3 3 3 3 3
3 3 3 3 4 1 1 1 1 1 1 1 1 1 4 3 3 3 3
3 3 3 4 1 1 1 2 1 1 1 5 1 1 1 4 3 3 3
3 3 4 1 1 1 1 1 1 1 1 1 1 1 1 1 4 3 3
3 3 4 1 1 2 1 1 1 1 1 1 1 2 1 1 4 3 3
3 3 4 1 1 1 1 1 1 1 1 1 1 1 1 1 4 3 3
3 3 4 4 1 1 1 1 1 1 1 1 1 1 1 4 4 3 3
3 3 4 1 1 1 1 1 1 1 1 1 1 1 1 1 4 3 3
3 3 4 1 1 2 1 1 1 1 1 1 1 2 1 1 4 3 3
3 3 4 1 1 1 1 1 1 1 1 1 1 1 1 1 4 3 3
3 3 3 4 1 1 1 2 1 1 1 2 1 1 1 4 3 3 3
3 3 3 3 4 1 1 1 1 1 1 1 1 1 1 4 3 3 3 3
3 3 3 3 3 4 1 1 1 4 1 1 1 4 3 3 3 3 3
3 3 3 3 3 3 4 4 4 4 4 4 4 3 3 3 3 3 3
3 3 3 3 3 3 3 3 3 3 3 3 3 3 3 3 3 3 3
3 3 3 3 3 3 3 3 3 3 3 3 3 3 3 3 3 3 3

%1=regular fuel assembly
%2=control rod fuel assembly
%3=zircaloy clad reflector assembly
%4=Al clad reflector assembly
%5=CR#1
%6=CR#2
%135 regular fuel elements
%+ 8 control rod elements
%= approximately 142 regular fuel elements


% --- Material Card --- %

therm gre gre6.00t

mat steel sum
26000.03c 8.51888875e-2                 %Iron
25055.03c 8.46518204e-4                 %Manganese

mat poison sum
5010.03c 1.39515714e-2                  %Boron-10
5011.03c 5.58062855e-2                  %Boron-11
6012.03c 1.74394642e-2                  %Carbon

mat fuel sum moder gre 6012             %Fuel
92235.03c 8.6516144e-6                  %U-235
92238.03c 6.313164e-7                   %U-238
6012.03c 0.0862391959                   %Carbon
5010.03c 1.45913E-07                    %Boron-10
5011.03c 5.83652E-07                    %Boron-11
26000.03c 1.85516144e-5                 %Iron

mat coolant sum                         %Coolant
7014.03c 4.3433e-5                      %Nitrogen
8016.03c 1.0212e-5                      %Oxygen

mat air sum                             %Air Gap
7014.03c 4.3433e-5                      %Nitrogen
```

```
8016.03c 1.0212e-5                                  %Oxygen

Mat zircaloy sum                                    %Zircaloy
26000.03c 0.0001699236                              %Iron
50000.03c 0.000077674                               %Tin
40000.03c 0.08374907                                %Zirconium

Mat aluminium sum                                   %Al 6063
13027.03c 0.0599572887                              %Aluminium
26000.03c .0004385235                               %Iron

Mat reflector sum moder gre 6012                    %Graphite
6012.03c 0.08374907                                 %Carbon
5010.03c 3.7105968e-8                               %Boron-10
5011.03c 1.48423872e-7                              %Boron-11
26000.03c 1.801745e-5                               %Iron


%--- Mesh Generation --- %
%mesh 3 2000 2000 [0]
%plot 3 5000 5000 [130.823]
%plot 3 5000 5000 [80.823]
%plot 3 5000 5000 [0]
%plot 3 5000 5000 [-80.823]
plot 3 2000 2000 [-54.97]
%plot 2 8300 3920 [-40.64]
plot 2 2000 2000 [-42.818]
%mesh 2 3150 2460


% --- Calculation Input --- %
set pop 70000 250 50 1.0 10
```

C.4 Revision 4

Revision 4 was the first to have a graphite to free carbon ratio, although it was 60/40 instead of the proper 59/41. I had also added a two inch air gap between the assemblies and the permanent reflector. The uranium number densities were changed to include U-234 and U-236 and the zircaloy clad reflectors were changed to be like standard fuel assemblies with reflector in place of fuel. In this example I had used 135 fuel assemblies instead of the minimum 133. The two additional fuel assemblies were reportedly used in ANL-6173 in their flux distribution measurements. I have also put control rod 1 to 48.5 in. as described in ANL-6173.These flux calculations using the detectors here were made later, as initially I had some issues setting up my detector orientation and the results for my initial calculations were incorrect.

```
% --- Treat Rev. 4 --- %                          %135 fuel elements for symmetry for flux measurements.
```

```
% --- Library File Path --- %
set acelib "/Users/serpent//SERPENT2/XSData/sss_endfb7u.xsdata"
set declib "/Users/serpent/SERPENT2/XSData/sss_endfb7.dec"
set nfylib "/Users/serpent/SERPENT2/XSData/sss_endfb7.nfy"


% --- Surface Card --- %

surf 1 sqc 0 0 5.08                         %Assembly including coolant gaps.
surf 2 octa 0 0 5.0292 6.318613             %Surface at the outside edge of the Zr.
surf 3 octa 0 0 4.9657 6.255113             %Surface at the outside edge of the void.
surf 4 octa 0 0 4.826 6.115413              %Surface at the outside edge of the fuel.
surf 5 pz 60.96                             %The top of the fuel.
surf 6 pz -60.96                            %The bottom of the fuel.
surf 7 pz 61.595                            %The top of the top Zr spacer.
surf 8 pz -61.595                           %The bottom of the bottom Zr spacer.
surf 9 pz 61.833125                 %The top surface between the zircaloy 3 cladding and Al 6063 cladding.
surf 10 pz -61.833125               %The bottom surface between the zircaloy 3 cladding and Al 6063 cladding.
surf 11 pz 61.960125                %The top inside surface between the Al 6063 cladding and graphite reflector.
surf 12 pz -61.960125               %The bottom inside surface between the Al 6063 cladding and graphite reflector.
surf 13 pz 122.920125               %The top outside surface between the Al 6063 cladding and graphite reflector.
surf 14 pz -122.920125      %The bottom outside surface between the Al 6063 cladding and graphite reflector.
surf 15 pz 123.047125                       %The top surface of the Al 6063 cladding (top of core).
surf 16 pz -123.047125                      %The bottom surface of the Al 6063 cladding (bottom of core).
surf 17 octa 0 0 4.9022 6.191613            %Surface at the outside edge of the reflector.
surf 18 sqc 0 0 96.52                       %Outer edge of the core.
surf 19 sqc 0 0 101.6                       %Inner edge of the reflector. Outside the 2" air gap.
surf 20 sqc 0 0 162.56                      %Outer edge of the reflector.
surf 21 cyl 0 0 2.2225                      %Control rod steel tube OD.
surf 22 cyl 0 0 1.905                       %Control rod steel tube ID.
surf 23 pz -46.99                           %Bottom of the control rod 1.
surf 24 pz -199.39                          %Surface between poison and zircaloy follower of control rod 1.
%surf 25 pz -381.873125                     %Top of the control rod 1.
surf 26 pz -77.073125                       %Bottom of the control rod 2.
surf 27 pz -229.473125                      %Surface between poison and zircaloy follower of control rod 2.
%surf 28 pz -381.873125                     %Top of the control rod 2.
surf 29 pz -77.073125                       %Bottom of SD control rod.
surf 30 pz -229.473125                      %Surface between poison and zircaloy follower of SD control rod.
%surf 31 pz -381.873125             %Top of SD control rod.
surf 32 pz -381.873125  %Top of control rods. (To simplify outside boundary conditions all control rods will extend here.)
surf 33 cyl 0 0 2.54                        %Control rod assembly hole ANL-6173 pg 12.


% --- Cell Card --- %

% Control Rod 1 %
cell 141 5 coolant 2 -1 -15 16              %Coolant channel around assembly.
cell 142 5 zircaloy 3 -2 -7 8               %Zircaloy 3 casing of assembly (25 mils).
cell 143 5 air 4 -3 -7 8                    %Void within assembly (55 mils).
cell 144 5 fuel 33 -4 -5 6                  %Fuel within assembly (six 3.9"x3.9"x8" blocks stacked 48" high).
cell 145 5 zircaloy 33 -4 5 -7              %Top Zr spacer (1/4").
cell 146 5 zircaloy 33 -4 8 -6              %Bottom Zr spacer (1/4").
cell 147 5 zircaloy 33 -2 7 -9              %Top Zircaloy 3 fuel end-cap (3/32").
cell 148 5 zircaloy 33 -2 10 -8             %Bottom Zircaloy 3 fuel end-cap (3/32").
cell 149 5 aluminium 33 -2 9 -11            %Top Al 6063 reflector cladding bottom end-cap(50 mils).
cell 150 5 aluminium 33 -2 12 -10           %Bottom Al 6063 reflector cladding top end-cap(50 mils).
cell 151 5 reflector 33 -17 11 -13          %Top assembly reflector (24").
cell 152 5 reflector 33 -17 14 -12          %Bottom assembly reflector (24").
cell 153 5 aluminium -2 17 11 -13           %Top Reflector Al 6063 cladding (50 mils).
cell 154 5 aluminium -2 17 14 -12           %Bottom Reflector Al 6063 cladding (50 mils).
cell 155 5 aluminium 33 -2 13 -15           %Top Al 6063 reflector cladding top end-cap(50 mils).
cell 156 5 aluminium 33 -2 16 -14           %Bottom Al 6063 reflector cladding bottom end-cap(50 mils).
cell 157 5 air -21 23 -15                   %Void where the control rod would go through.
cell 158 5 steel -21 22 -23 24              %Control rod poison carbon steel housing.
cell 159 5 poison -22 -23 24                %Control rod poison.
cell 160 5 zircaloy -21 22 -24 32           %Control rod zircaloy follower housing.
cell 161 5 reflector -22 -24 32             %Control rod zircaloy follower.
cell 162 5 outside 21 -16 32 -1             %Brings flux to zero outside of the core (sets boundary conditions).
cell 163 5 air -33 21 -15 16                %Control rod assembly hole.
```

```
% Control Rod 2 %
cell 241 6 coolant 2 -1 -15 16          %Coolant channel around assembly.
cell 242 6 zircaloy 3 -2 -7 8           %Zircaloy 3 casing of assembly (25 mils).
cell 243 6 air 4 -3 -7 8                %Void within assembly (55 mils).
cell 244 6 fuel 33 -4 -5 6              %Fuel within assembly (six 3.9"x3.9"x8" blocks stacked 48" high).
cell 245 6 zircaloy 33 -4 5 -7          %Top Zr spacer (1/4").
cell 246 6 zircaloy 33 -4 8 -6          %Bottom Zr spacer (1/4").
cell 247 6 zircaloy 33 -2 7 -9          %Top Zircaloy 3 fuel end-cap (3/32").
cell 248 6 zircaloy 33 -2 10 -8         %Bottom Zircaloy 3 fuel end-cap (3/32").
cell 249 6 aluminium 33 -2 9 -11        %Top Al 6063 reflector cladding bottom end-cap(50 mils).
cell 250 6 aluminium 33 -2 12 -10       %Bottom Al 6063 reflector cladding top end-cap(50 mils).
cell 251 6 reflector 33 -17 11 -13      %Top assembly reflector (24").
cell 252 6 reflector 33 -17 14 -12      %Bottom assembly reflector (24").
cell 253 6 aluminium -2 17 11 -13       %Top Reflector Al 6063 cladding (50 mils).
cell 254 6 aluminium -2 17 14 -12       %Bottom Reflector Al 6063 cladding (50 mils).
cell 255 6 aluminium 33 -2 13 -15       %Top Al 6063 reflector cladding top end-cap(50 mils).
cell 256 6 aluminium 33 -2 16 -14       %Bottom Al 6063 reflector cladding bottom end-cap(50 mils).
cell 257 6 air -21 26 -15               %Void where the control rod would go through.
cell 258 6 steel -21 22 -26 27          %Control rod poison carbon steel housing.
cell 259 6 poison -22 -26 27            %Control rod poison.
cell 260 6 zircaloy -21 22 -27 32       %Control rod zircaloy follower housing.
cell 261 6 reflector -22 -27 32         %Control rod zircaloy follower.
cell 262 6 outside 21 -16 32 -1         %Brings flux to zero outside of the core (sets boundary conditions).
cell 263 6 air -33 21 -15 16            %Control rod assembly hole.

% Shutdown Control Rod Fuel Assembly %
cell 41 2 coolant 2 -1 -15 16           %Coolant channel around assembly.
cell 42 2 zircaloy 3 -2 -7 8            %Zircaloy 3 casing of assembly (25 mils).
cell 43 2 air 4 -3 -7 8                 %Void within assembly (55 mils).
cell 44 2 fuel 33 -4 -5 6               %Fuel within assembly (six 3.9"x3.9"x8" blocks stacked 48" high).
cell 45 2 zircaloy 33 -4 5 -7           %Top Zr spacer (1/4").
cell 46 2 zircaloy 33 -4 8 -6           %Bottom Zr spacer (1/4").
cell 47 2 zircaloy 33 -2 7 -9           %Top Zircaloy 3 fuel end-cap (3/32").
cell 48 2 zircaloy 33 -2 10 -8          %Bottom Zircaloy 3 fuel end-cap (3/32").
cell 49 2 aluminium 33 -2 9 -11         %Top Al 6063 reflector cladding bottom end-cap(50 mils).
cell 50 2 aluminium 33 -2 12 -10        %Bottom Al 6063 reflector cladding top end-cap(50 mils).
cell 51 2 reflector 33 -17 11 -13       %Top assembly reflector (24").
cell 52 2 reflector 33 -17 14 -12       %Bottom assembly reflector (24").
cell 53 2 aluminium -2 17 11 -13        %Top Reflector Al 6063 cladding (50 mils).
cell 54 2 aluminium -2 17 14 -12        %Bottom Reflector Al 6063 cladding (50 mils).
cell 55 2 aluminium 33 -2 13 -15        %Top Al 6063 reflector cladding top end-cap(50 mils).
cell 56 2 aluminium 33 -2 16 -14        %Bottom Al 6063 reflector cladding bottom end-cap(50 mils).
cell 57 2 air -21 29 -15                %Void where the control rod would go through.
cell 58 2 steel -21 22 -29 30           %Carbon steel tube.
cell 59 2 poison -22 -29 30             %Boron-carbide powder compacted to 1.6g/cc.
cell 60 2 zircaloy -21 22 -30 32        %Zircaloy follower housing.
cell 61 2 reflector     -22         -30 32  %Zircaloy follower.
cell 62 2 outside 21 -16 32 -1          %Brings flux to zero outside of the core (sets boundary conditions).
cell 63 2 air -33 21 -15 16             %Control rod assembly hole.

% Standard Fuel Assembly %
cell 1 1 coolant 2 -1 -15 16            %Coolant channel around assembly.
cell 2 1 zircaloy 3 -2 -7 8             %Zircaloy 3 casing of assembly (25 mils).
cell 3 1 air 4 -3 -7 8                  %Void within assembly (55 mils).
cell 4 1 fuel -4 -5 6                   %Fuel within assembly (six 3.9"x3.9"x8" blocks stacked 48" high).
cell 5 1 zircaloy -4 5 -7               %Top Zr spacer (1/4").
cell 6 1 zircaloy -4 8 -6               %Bottom Zr spacer (1/4").
cell 7 1 zircaloy -2 7 -9               %Top Zircaloy 3 fuel end-cap (3/32").
cell 8 1 zircaloy -2 10 -8              %Bottom Zircaloy 3 fuel end-cap (3/32").
cell 9 1 aluminium -2 9 -11             %Top Al 6063 reflector cladding bottom end-cap(50 mils).
cell 10 1 aluminium -2 12 -10           %Bottom Al 6063 reflector cladding top end-cap(50 mils).
cell 11 1 reflector -17 11 -13          %Top assembly reflector (24").
cell 12 1 reflector -17 14 -12          %Bottom assembly reflector (24").
cell 13 1 aluminium -2 17 11 -13        %Top Reflector Al 6063 cladding (50 mils).
cell 14 1 aluminium -2 17 14 -12        %Bottom Reflector Al 6063 cladding (50 mils).
cell 15 1 aluminium -2 13 -15           %Top Al 6063 reflector cladding top end-cap(50 mils).
cell 16 1 aluminium -2 16 -14           %Bottom Al 6063 reflector cladding bottom end-cap(50 mils).
cell 17 1 outside -16 32 -1             %Brings flux to zero outside of the core (sets boundary conditions).

% Aluminium Can Dummy Fuel Assembly %
```

```
cell 71 3 coolant 2 -1 -15 16          %Coolant channel around assembly.
cell 72 3 aluminium -2 17 -15 16       %Reflector Al 6063 cladding (50 mils).
cell 73 3 reflector -17 -15 16         %Reflector.
cell 74 3 outside -16 32 -1            %Brings flux to zero outside of the core (sets boundary conditions).

% Zircaloy Can Dummy Fuel Assembly %
cell 81 4 coolant 2 -1 -15 16          %Coolant channel around assembly.
cell 82 4 zircaloy 3 -2 -7 8           %Zircaloy 3 casing of assembly (25 mils).
cell 83 4 air 4 -3 -7 8                %Void within assembly (55 mils).
cell 84 4 reflector -4 -5 6            %Fuel within assembly (six 3.9"x3.9"x8" blocks stacked 48" high).
cell 85 4 zircaloy -4 5 -7             %Top Zr spacer (1/4").
cell 86 4 zircaloy -4 8 -6             %Bottom Zr spacer (1/4").
cell 87 4 zircaloy -2 7 -9             %Top Zircaloy 3 fuel end-cap (3/32").
cell 88 4 zircaloy -2 10 -8            %Bottom Zircaloy 3 fuel end-cap (3/32").
cell 89 4 aluminium -2 9 -11           %Top Al 6063 reflector cladding bottom end-cap(50 mils).
cell 90 4 aluminium -2 12 -10          %Bottom Al 6063 reflector cladding top end-cap(50 mils).
cell 91 4 reflector -17 11 -13         %Top assembly reflector (24").
cell 92 4 reflector -17 14 -12         %Bottom assembly reflector (24").
cell 93 4 aluminium -2 17 11 -13       %Top Reflector Al 6063 cladding (50 mils).
cell 94 4 aluminium -2 17 14 -12       %Bottom Reflector Al 6063 cladding (50 mils).
cell 95 4 aluminium -2 13 -15          %Top Al 6063 reflector cladding top end-cap(50 mils).
cell 96 4 aluminium -2 16 -14          %Bottom Al 6063 reflector cladding bottom end-cap(50 mils).
cell 97 4 outside -16 32 -1            %Brings flux to zero outside of the core (sets boundary conditions).

% Access Hole Fuel Assembly %

% Access Hole Dummy Fuel Assembly %

% Shielding Assembly %

% Thermocouple Fuel Assembly %

% Core %
cell 20 0 outside 15                   %Brings flux to zero outside of the core (sets boundary conditions).
cell 21 0 outside -32                  %Brings flux to zero outside of the core (sets boundary conditions).
cell 22 0 outside 20 -15 16            %Brings flux to zero outside of the core (sets boundary conditions).
cell 23 0 outside -16 32 18            %Brings flux to zero outside of the core (sets boundary conditions).
cell 24 0 fill 10 -18 32 -15           %Core.
cell 25 0 coolant 18 -19 -15 16        %Air gap between core and reflector. (not sure if there is a air gap)
cell 26 0 reflector 19 -20 -15 16      %Outside reflector.


% --- Lattice --- %
lat 10 1 0 0 19 19 10.16

3 3 3 3 3 3 3 3 3 3 3 3 3 3 3 3 3 3 3
3 3 3 3 3 3 3 3 3 3 3 3 3 3 3 3 3 3 3
3 3 3 3 3 3 4 4 4 4 4 4 4 3 3 3 3 3 3
3 3 3 3 3 4 1 1 1 4 1 1 1 4 3 3 3 3 3
3 3 3 3 4 1 1 1 1 1 1 1 1 1 4 3 3 3 3
3 3 3 4 1 1 1 2 1 1 1 5 1 1 1 4 3 3 3
3 3 4 1 1 1 1 1 1 1 1 1 1 1 1 4 3 3
3 3 4 1 1 2 1 1 1 1 1 1 2 1 1 4 3 3
3 3 4 1 1 1 1 1 1 1 1 1 1 1 1 4 3 3
3 3 4 1 1 1 1 1 1 1 1 1 1 1 1 4 3 3
3 3 4 1 1 1 1 1 1 1 1 1 1 1 1 4 3 3
3 3 4 1 1 2 1 1 1 1 1 1 2 1 1 4 3 3
3 3 4 1 1 1 1 1 1 1 1 1 1 1 1 4 3 3
3 3 3 4 1 1 1 2 1 1 1 2 1 1 1 4 3 3 3
3 3 3 3 4 1 1 1 1 1 1 1 1 1 4 3 3 3 3
3 3 3 3 3 4 1 1 1 4 1 1 1 4 3 3 3 3 3
3 3 3 3 3 3 4 4 4 4 4 4 4 3 3 3 3 3 3
3 3 3 3 3 3 3 3 3 3 3 3 3 3 3 3 3 3 3
3 3 3 3 3 3 3 3 3 3 3 3 3 3 3 3 3 3 3

%1=regular fuel assembly
%2=control rod fuel assembly
%3=zircaloy clad reflector assembly
%4=Al clad reflector assembly
%5=CR#1
```

```
%6=CR#2
%135 regular fuel elements
%+ 8 control rod elements
%= approximately 142 regular fuel elements


% --- Material Card --- %

therm gre gre6.00t

mat steel sum rgb <128> <128> <128>                %Steel (Gray)
26000.03c 8.51888875e-2                            %Iron
25055.03c 8.46518204e-4                            %Manganese

mat poison sum rgb <108> <0> <0>                   %BC4 (Dark Red)
5010.03c 1.39515714e-2                             %Boron-10
5011.03c 5.58062855e-2                             %Boron-11
6012.03c 1.74394642e-2                             %Carbon

mat fuel sum moder gre 6012  rgb <187> <138> <23>  %Fuel (Orange)
92234.03c 9.33150E-08                              %U-234
92235.03c 8.64137E-06                              %U-235
92236.03c 1.85836E-08                              %U-236
92238.03c 5.32131E-07                              %U-238
6012.03c 5.1743518E-02                             %Carbon
6000.03c 3.4495678E-02                             %Carbon
5010.03c 1.45913E-07                               %Boron-10
5011.03c 5.83652E-07                               %Boron-11
26000.03c 1.85516144e-5                            %Iron

mat coolant sum      rgb <100> <223> <249>         %Coolant (Light Blue)
7014.03c 4.3433e-5                                 %Nitrogen
8016.03c 1.0212e-5                                 %Oxygen

mat air sum          rgb <230> <251> <255>         %Air Gap (White Blue)
7014.03c 4.3433e-5                                 %Nitrogen
8016.03c 1.0212e-5                                 %Oxygen

Mat zircaloy sum rgb <128> <0> <255>               %Zircaloy (Purple)
26000.03c 0.0001699236                             %Iron
50000.03c 0.000077674                              %Tin
40000.03c 0.08374907                               %Zirconium

Mat aluminium sum rgb <255> <255> <0>              %Al 6063 (Yellow)
13027.03c 0.0599572887                             %Aluminium
26000.03c .0004385235                              %Iron

Mat reflector sum moder gre 6012 rgb <139> <87> <58>  %Graphite (Brown)
6012.03c 0.08374907                                %Carbon
5010.03c 3.7105968e-8                              %Boron-10
5011.03c 1.48423872e-7                             %Boron-11
26000.03c 1.801745e-5                              %Iron

mat u235 18.95                                     %U-235 foils for flux
92235.03c 1                                        %U-235


%--- Mesh Generation --- %
plot 3 2000 2000 [0]
plot 2 2300 1120 [-40.64]
plot 2 2000 2000


% --- Calculation Input --- %
set pop 25000 1000 50 1.0 10

% --- Detector Input --- %                        %Will be used to determine axial and radial flux ratios%

ene 1 1 1E-11 0.625E-6                             %Detector energy grid (single bin).
```

```
det radialthermal                       %Same as detector above but added dz.
de 1                                    %Use energy grid 1. (use de for thermal flux)
dx -96.52 96.52 193                     %193 bins in x-direction.
dy -5.08 5.08 2                         %2 bin in y-direction.

det radialfission                       %Same as detector above but added dz.
dr -6 u235                              %Fission rate. (use dr for fission flux)
dx -96.52 96.52 193                     %193 bins in x-direction.
dy -5.08 5.08 2                         %2 bin in y-direction.

det axialfission                        %One-dimensional mesh (flux distribution).
dr -6 u235                              %Fission rate. (use dr for fission flux)
dx -5.08 -5.08 1                        %1 bins in x-direction. (puts detectors in the channel)
dy 5.08 5.08 1                          %1 bins in y-direction. (puts detectors in the channel)
dz -121.92 121.92 245                   %245 bins in z-direction. (nearly 1 every cm)

det axialthermal                        %One-dimensional mesh (flux distribution).
de 1                                    %Use energy grid 1. (use de for thermal flux)
dx -5.08 -5.08 1                        %1 bins in x-direction. (puts detectors in the channel)
dy 5.08 5.08 1                          %1 bins in y-direction. (puts detectors in the channel)
dz -121.92 121.92 245                   %245 bins in z-direction. (nearly 1 every cm)

det gridfission                         %One-dimensional mesh (flux distribution).
dr -6 fuel                              %Fission rate. (use dr for fission flux)
dx -66.04 66.04 13                      %13 bins in x-direction.
dy -66.04 66.04 13                      %13 bins in x-direction.
dz -60.96 60.96 13                      %13 bins in z-direction.

det gridthermal                         %One-dimensional mesh (flux distribution).
de 1                                    %Use energy grid 1. (use de for thermal flux)
dx -66.04 66.04 13                      %13 bins in x-direction.
dy -66.04 66.04 13                      %13 bins in x-direction.
dz -60.96 60.96 13                      %13 bins in z-direction.cell 1 0 fuel -1
```

C.5 Revision n

From revision 4 to revision n there were many changes. The number densities were changed to more closely match those in INL model of TREAT as well as correcting the zirconium number density in the zircaloy. I had also added a void where the outgas tubes go as well as a void where the rivets attach the fuel cladding to the reflector cladding. I had added cladding and void between the fuel and control rods. My lattice structure was changed to one I believe to be correct. Finally air gaps were added between the aluminum and reflector in the aluminum reflector assemblies. I this example control rod 1 is at 30 in.

```
% --- Treat Rev. n --- %                %133 fuel elements.

% --- Library File Path --- %
set acelib "/Users/serpent//SERPENT2/XSData/sss_endfb7u.xsdata"
set declib "/Users/serpent/SERPENT2/XSData/sss_endfb7.dec"
set nfylib "/Users/serpent/SERPENT2/XSData/sss_endfb7.nfy"
```

```
% --- Surface Card --- %

surf 1 sqc 0 0 5.08                    %Assembly including coolant gaps.
surf 2 octa 0 0 5.0292 6.318613        %Surface at the outside edge of the Zr.
surf 3 octa 0 0 4.9657 6.255113        %Surface at the outside edge of the void.
surf 4 octa 0 0 4.826 6.115413         %Surface at the outside edge of the fuel.
surf 5 pz 60.96                        %The top of the fuel.
surf 6 pz -60.96                       %The bottom of the fuel.
surf 7 pz 61.595                       %The top of the top Zr spacer.
surf 8 pz -61.595                      %The bottom of the bottom Zr spacer.
surf 9 pz 61.833125                    %The top surface between the zircaloy 3 cladding and Al 6063 cladding.
surf 10 pz -61.833125                  %The bottom surface between the zircaloy 3 cladding and Al 6063 cladding.
surf 11 pz 61.960125                   %The top inside surface between the Al 6063 cladding and graphite reflector.
surf 12 pz -61.960125                  %The bottom inside surface between the Al 6063 cladding and graphite reflector.
surf 13 pz 122.920125                  %The top outside surface between the Al 6063 cladding and graphite reflector.
surf 14 pz -122.920125          %The bottom outside surface between the Al 6063 cladding and graphite reflector.
surf 15 pz 123.047125                  %The top surface of the Al 6063 cladding (top of core).
surf 16 pz -123.047125                 %The bottom surface of the Al 6063 cladding (bottom of core).
surf 17 octa 0 0 4.9022 6.191613       %Surface between air gap and Al 6063 cladding of top and bottom reflector.
surf 18 sqc 0 0 96.52                  %Outer edge of the core.
surf 19 sqc 0 0 101.6                  %Inner edge of the reflector. Outside the 2" air gap.
surf 20 sqc 0 0 162.56                 %Outer edge of the reflector.
surf 21 cyl 0 0 2.2225                 %Control rod steel tube OD.
surf 22 cyl 0 0 1.905                  %Control rod steel tube ID.
surf 23 pz 0                           %Bottom of the control rod 1.
surf 24 pz -152.4                      %Surface between poison and zircaloy follower of control rod 1.
%surf 25 pz -381.873125                %Top of the control rod 1
surf 26 pz -77.073125                  %Bottom of the control rod 2.
surf 27 pz -229.473125                 Surface between poison and zircaloy follower of control rod 2.
%surf 28 pz -381.873125                %Top of the control rod 2.
surf 29 pz -77.073125                  %Bottom of SD control rod.
surf 30 pz -229.473125                 %Surface between poison and zircaloy follower of SD control rod.
%surf 31 pz -381.873125                %Top of SD control rod.
surf 32 pz -381.873125                 %Top of control rods. (To simplify outside boundary conditions all control rods
will extend here.)
surf 33 cyl 0 0 2.54                   %Control rod assembly hole ANL-6173 pg 12.
surf 34 cyl 0 0 2.8575                 %ID of control rod fuel cladding. The cladding between the fuel and the control
rod. (From INL model-surf 477)
surf 35 cyl 0 0 2.9591                 %OD of control rod fuel cladding. The cladding between the fuel and the control
rod. (From INL model-surf 472)
surf 36 cyl 0 0 .9525                  %Outgas tube. (INL model-surf 300)
surf 37 pz 83.423125                   %Top of outgas tube. (INL model-surf 301)
surf 38 sqc 0 0 4.1656                 %Square section of top and bottom reflectors. (INL model-surf 200)
surf 39 octa 0 0 4.8006 6.020723628    %Surface between reflector and air gap of top and bottom reflector. (INL model-
surf 201)
%surf 40
surf 41 pz 70.246875                   %Top reflector transition from octahedral to cuboid. (INL model-surf 250)
surf 42 pz -70.246875                  %Bottom reflector transition from octahedral to cuboid. (INL model-surf 250)


% --- Cell Card --- %

% Control Rod 1 %
cell 141 5 coolant 2 -1 -15 16         %Coolant channel around assembly.
cell 142 5 zircaloy 3 -2 -7 8          %Zircaloy 3 casing of assembly (25 mils).
cell 143 5 air 4 -3 -7 8               %Void within assembly (55 mils).
cell 144 5 fuel 35 -4 -5 6             %Fuel within assembly (six 3.9"x3.9"x8" blocks stacked 48" high).
cell 145 5 zircaloy 33 -4 5 -7         %Top Zr spacer (1/4").
cell 146 5 zircaloy 33 -4 8 -6         %Bottom Zr spacer (1/4").
cell 147 5 zircaloy 33 -2 7 -9         %Top Zircaloy 3 fuel end-cap (3/32").
cell 148 5 zircaloy 33 -2 10 -8        %Bottom Zircaloy 3 fuel end-cap (3/32").
cell 149 5 aluminium 33 -2 9 -11       %Top Al 6063 reflector cladding bottom end-cap(50 mils).
cell 150 5 aluminium 33 -2 12 -10      %Bottom Al 6063 reflector cladding top end-cap(50 mils).
cell 151 5 reflector 33 -39 41 -13     %Top assembly reflector (24").
cell 152 5 reflector 33 -39 14 -42     %Bottom assembly reflector (24").
cell 153 5 aluminium -2 17 11 -13      %Top Reflector Al 6063 cladding (50 mils).
cell 154 5 aluminium -2 17 14 -12      %Bottom Reflector Al 6063 cladding (50 mils).
cell 155 5 aluminium 33 -2 13 -15      %Top Al 6063 reflector cladding top end-cap(50 mils).
```

```
cell 156 5 aluminium 33 -2 16 -14      %Bottom Al 6063 reflector cladding bottom end-cap(50 mils).
cell 157 5 air -21 23 -15              %Void where the control rod would go through.
cell 158 5 steel -21 22 -23 24         %Control rod poison carbon steel housing.
cell 159 5 poison -22 -23 24           %Control rod poison.
cell 160 5 zircaloy -21 22 -24 32      %Control rod zircaloy follower housing.
cell 161 5 reflector -22 -24 32        %Control rod zircaloy follower.
cell 162 5 outside 21 -16 32 -1        %Brings flux to zero outside of the core (sets boundary conditions).
cell 163 5 air -33 21 -15 16           %Control rod assembly hole.
cell 164 5 air -35 34 -5 6             %Void between fuel and cladding (wraps around control rod).
cell 165 5 zircaloy -34 33 -5 6        %Fuel cladding (wraps around control rod).
cell 166 5 air 39 -17 11 -13           %Top reflector air gap between reflector and Al.
cell 167 5 air 39 -17 -12 14           %Bottom reflector air gap between reflector and Al.
cell 168 5 reflector 33 -38 11 -41     %Top reflector square portion.
cell 169 5 air 38 -39 11 -41           %Top reflector air gap between reflector and Al in the square portion.
cell 170 5 reflector 33 -38 -12 42     %Bottom reflector square portion.
cell 171 5 air 38 -39 -12 42           %Bottom reflector air gap between reflector and Al in the square portion.

% Control Rod 2 %
cell 241 6 coolant 2 -1 -15 16         %Coolant channel around assembly.
cell 242 6 zircaloy 3 -2 -7 8          %Zircaloy 3 casing of assembly (25 mils).
cell 243 6 air 4 -3 -7 8               %Void within assembly (55 mils).
cell 244 6 fuel 35 -4 -5 6             %Fuel within assembly (six 3.9"x3.9"x8" blocks stacked 48" high).
cell 245 6 zircaloy 33 -4 5 -7         %Top Zr spacer (1/4").
cell 246 6 zircaloy 33 -4 8 -6         %Bottom Zr spacer (1/4").
cell 247 6 zircaloy 33 -2 7 -9         %Top Zircaloy 3 fuel end-cap (3/32").
cell 248 6 zircaloy 33 -2 10 -8        %Bottom Zircaloy 3 fuel end-cap (3/32").
cell 249 6 aluminium 33 -2 9 -11       %Top Al 6063 reflector cladding bottom end-cap(50 mils).
cell 250 6 aluminium 33 -2 12 -10      %Bottom Al 6063 reflector cladding top end-cap(50 mils).
cell 251 6 reflector 33 -39 41 -13     %Top assembly reflector (24").
cell 252 6 reflector 33 -39 14 -42     %Bottom assembly reflector (24").
cell 253 6 aluminium -2 17 11 -13      %Top Reflector Al 6063 cladding (50 mils).
cell 254 6 aluminium -2 17 14 -12      %Bottom Reflector Al 6063 cladding (50 mils).
cell 255 6 aluminium 33 -2 13 -15      %Top Al 6063 reflector cladding top end-cap(50 mils).
cell 256 6 aluminium 33 -2 16 -14      %Bottom Al 6063 reflector cladding bottom end-cap(50 mils).
cell 257 6 air -21 26 -15              %Void where the control rod would go through.
cell 258 6 steel -21 22 -26 27         %Control rod poison carbon steel housing.
cell 259 6 poison -22 -26 27           %Control rod poison.
cell 260 6 zircaloy -21 22 -27 32      %Control rod zircaloy follower housing.
cell 261 6 reflector -22 -27 32        %Control rod zircaloy follower.
cell 262 6 outside 21 -16 32 -1        %Brings flux to zero outside of the core (sets boundary conditions).
cell 263 6 air -33 21 -15 16           %Control rod assembly hole.
cell 264 6 air -35 34 -5 6             %Void between fuel and cladding (wraps around control rod).
cell 265 6 zircaloy -34 33 -5 6        %Fuel cladding (wraps around control rod).
cell 266 6 air 39 -17 11 -13           %Top reflector air gap between reflector and Al.
cell 267 6 air 39 -17 -12 14           %Bottom reflector air gap between reflector and Al.
cell 268 6 reflector 33 -38 11 -41     %Top reflector square portion.
cell 269 6 air 38 -39 11 -41           %Top reflector air gap between reflector and Al in the square portion.
cell 270 6 reflector 33 -38 -12 42     %Bottom reflector square portion.
cell 271 6 air 38 -39 -12 42           %Bottom reflector air gap between reflector and Al in the square portion.

% Shutdown Control Rod Fuel Assembly %
cell 41 2 coolant 2 -1 -15 16          %Coolant channel around assembly.
cell 42 2 zircaloy 3 -2 -7 8           %Zircaloy 3 casing of assembly (25 mils).
cell 43 2 air 4 -3 -7 8                %Void within assembly (55 mils).
cell 44 2 fuel 35 -4 -5 6              %Fuel within assembly (six 3.9"x3.9"x8" blocks stacked 48" high).
cell 45 2 zircaloy 33 -4 5 -7          %Top Zr spacer (1/4").
cell 46 2 zircaloy 33 -4 8 -6          %Bottom Zr spacer (1/4").
cell 47 2 zircaloy 33 -2 7 -9          %Top Zircaloy 3 fuel end-cap (3/32").
cell 48 2 zircaloy 33 -2 10 -8         %Bottom Zircaloy 3 fuel end-cap (3/32").
cell 49 2 aluminium 33 -2 9 -11        %Top Al 6063 reflector cladding bottom end-cap(50 mils).
cell 50 2 aluminium 33 -2 12 -10       %Bottom Al 6063 reflector cladding top end-cap(50 mils).
cell 51 2 reflector 33 -39 41 -13      %Top assembly reflector (24").
cell 52 2 reflector 33 -39 14 -42      %Bottom assembly reflector (24").
cell 53 2 aluminium -2 17 11 -13       %Top Reflector Al 6063 cladding (50 mils).
cell 54 2 aluminium -2 17 14 -12       %Bottom Reflector Al 6063 cladding (50 mils).
cell 55 2 aluminium 33 -2 13 -15       %Top Al 6063 reflector cladding top end-cap(50 mils).
cell 56 2 aluminium 33 -2 16 -14       %Bottom Al 6063 reflector cladding bottom end-cap(50 mils).
cell 57 2 air -21 29 -15               %Void where the control rod would go through.
cell 58 2 steel -21 22 -29 30          %Carbon steel tube.
cell 59 2 poison -22 -29 30            %Boron-carbide powder compacted to 1.6g/cc.
```

```
cell 60 2 zircaloy -21 22 -30 32        %Zircaloy follower housing.
cell 61 2 reflector -22 -30 32          %Zircaloy follower.
cell 62 2 outside 21 -16 32 -1          %Brings flux to zero outside of the core (sets boundary conditions).
cell 63 2 air -33 21 -15 16             %Control rod assembly hole.
cell 64 2 air -35 34 -5 6               %Void between fuel and cladding (wraps around control rod).
cell 65 2 zircaloy -34 33 -5 6          %Fuel cladding (wraps around control rod).
cell 66 2 air 39 -17 11 -13             %Top reflector air gap between reflector and Al.
cell 67 2 air 39 -17 -12 14             %Bottom reflector air gap between reflector and Al.
cell 68 2 reflector 33 -38 11 -41       %Top reflector square portion.
cell 69 2 air 38 -39 11 -41             %Top reflector air gap between reflector and Al in the square portion.
cell 70 2 reflector 33 -38 -12 42       %Bottom reflector square portion.
cell 71 2 air 38 -39 -12 42             %Bottom reflector air gap between reflector and Al in the square portion.

% Standard Fuel Assembly %
cell 1 1 coolant 2 -1 -15 16            %Coolant channel around assembly.
cell 2 1 zircaloy 3 -2 -7 8             %Zircaloy 3 casing of assembly (25 mils).
cell 3 1 air 4 -3 -7 8                  %Void within assembly (55 mils).
cell 4 1 fuel -4 -5 6                   %Fuel within assembly (six 3.9"x3.9"x8" blocks stacked 48" high).
cell 5 1 zircaloy -4 5 -7               %Top Zr spacer (1/4").
cell 6 1 zircaloy -4 8 -6               %Bottom Zr spacer (1/4").
cell 7 1 zircaloy -2 7 -9               %Top Zircaloy 3 fuel end-cap (3/32").
cell 8 1 zircaloy -2 10 -8              %Bottom Zircaloy 3 fuel end-cap (3/32").
cell 9 1 aluminium -2 36 9 -11          %Top Al 6063 reflector cladding bottom end-cap(50 mils).
cell 10 1 aluminium -2 12 -10           %Bottom Al 6063 reflector cladding top end-cap(50 mils).
cell 11 1 reflector -39 37 -13          %Top assembly reflector (24").
cell 12 1 reflector -39 14 -42          %Bottom assembly reflector (24").
cell 13 1 aluminium -2 17 11 -13        %Top Reflector Al 6063 cladding (50 mils).
cell 14 1 aluminium -2 17 14 -12        %Bottom Reflector Al 6063 cladding (50 mils).
cell 15 1 aluminium -2 13 -15           %Top Al 6063 reflector cladding top end-cap(50 mils).
cell 16 1 aluminium -2 16 -14           %Bottom Al 6063 reflector cladding bottom end-cap(50 mils).
cell 17 1 outside -16 32 -1             %Brings flux to zero outside of the core (sets boundary conditions).
cell 18 1 air -36 9 -37                 %Outgas Tube.
cell 19 1 air 39 -17 11 -13             %Top reflector air gap between reflector and Al.
cell 20 1 air 39 -17 -12 14             %Bottom reflector air gap between reflector and Al.
cell 21 1 reflector -39 36 41 -37       %Top reflector octahedral portion with outgas tube.
cell 22 1 reflector -38 36 11 -41       %Top reflector square portion with outgas tube.
cell 23 1 air 38 -39 11 -41             %Top reflector air gap between reflector and Al in the square portion.
cell 24 1 reflector -38 42 -12          %Bottom reflector square portion.
cell 25 1 air 38 -39 42 -12             %Bottom reflector air gap between reflector and Al in the square portion.

% Aluminium Can Dummy Fuel Assembly %
cell 75 3 coolant 2 -1 -15 16           %Coolant channel around assembly.
cell 76 3 aluminium -2 17 -13 14        %Reflector Al 6063 cladding (50 mils).
cell 77 3 reflector -39 -13 14          %Reflector.
cell 78 3 outside -16 32 -1             %Brings flux to zero outside of the core (sets boundary conditions).
cell 79 3 air -17 39 -13 14             %Air gap between reflector and Al cladding.
cell 80 3 aluminium -2 13 -15           %Top Al 6063 reflector cladding top end-cap(50 mils).
cell 81 3 aluminium -2 16 -14           %Bottom Al 6063 reflector cladding bottom end-cap(50 mils).

% Zircaloy Can Dummy Fuel Assembly %
cell 101 4 coolant 2 -1 -15 16          %Coolant channel around assembly.
cell 102 4 zircaloy 3 -2 -7 8           %Zircaloy 3 casing of assembly (25 mils).
cell 103 4 air 4 -3 -7 8                %Void within assembly (55 mils).
cell 104 4 reflector -4 -5 6            %Fuel within assembly (six 3.9"x3.9"x8" blocks stacked 48" high).
cell 105 4 zircaloy -4 5 -7             %Top Zr spacer (1/4").
cell 106 4 zircaloy -4 8 -6             %Bottom Zr spacer (1/4").
cell 107 4 zircaloy -2 7 -9             %Top Zircaloy 3 fuel end-cap (3/32").
cell 108 4 zircaloy -2 10 -8            %Bottom Zircaloy 3 fuel end-cap (3/32").
cell 109 4 aluminium -2 9 -11           %Top Al 6063 reflector cladding bottom end-cap(50 mils).
cell 110 4 aluminium -2 12 -10          %Bottom Al 6063 reflector cladding top end-cap(50 mils).
cell 111 4 reflector -39 41 -13         %Top assembly reflector (24").
cell 112 4 reflector -39 14 -42         %Bottom assembly reflector (24").
cell 113 4 aluminium -2 17 11 -13       %Top Reflector Al 6063 cladding (50 mils).
cell 114 4 aluminium -2 17 14 -12       %Bottom Reflector Al 6063 cladding (50 mils).
cell 115 4 aluminium -2 13 -15          %Top Al 6063 reflector cladding top end-cap(50 mils).
cell 116 4 aluminium -2 16 -14          %Bottom Al 6063 reflector cladding bottom end-cap(50 mils).
cell 117 4 outside -16 32 -1            %Brings flux to zero outside of the core (sets boundary conditions).
cell 118 4 air 39 -17 11 -13            %Top reflector air gap between reflector and Al.
cell 119 4 air 39 -17 -12 14            %Bottom reflector air gap between reflector and Al.
cell 120 4 reflector -38 11 -41         %Top reflector square portion.
```

```
cell 121 4 air 38 -39 11 -41          %Top reflector air gap between reflector and Al in the square portion.
cell 122 4 reflector -38 -12 42       %Bottom reflector square portion.
cell 123 4 air 38 -39 -12 42          %Bottom reflector air gap between reflector and Al in the square portion.

% Access Hole Fuel Assembly %

% Access Hole Dummy Fuel Assembly %

% Shielding Assembly %

% Thermocouple Fuel Assembly %

% Core %
cell 30 0 outside 15                  %Brings flux to zero outside of the core (sets boundary conditions).
cell 31 0 outside -32                 %Brings flux to zero outside of the core (sets boundary conditions).
cell 32 0 outside 20 -15 16           %Brings flux to zero outside of the core (sets boundary conditions).
cell 33 0 outside -16 32 18           %Brings flux to zero outside of the core (sets boundary conditions).
cell 34 0 fill 10 -18 32 -15          %Core.
cell 35 0 coolant 18 -19 -15 16       %Air gap between core and reflector. (not sure if there is a air gap)
cell 36 0 reflector 19 -20 -15 16     %Outside reflector.


% --- Lattice --- %
lat 10 1 0 0 19 19 10.16

3 3 3 3 3 3 3 3 3 3 3 3 3 3 3 3 3 3 3
3 3 3 3 3 3 3 3 3 3 3 3 3 3 3 3 3 3 3
3 3 3 3 3 3 4 4 4 3 4 4 4 3 3 3 3 3 3
3 3 3 3 3 4 1 1 1 4 1 1 1 4 3 3 3 3 3
3 3 3 3 4 1 1 1 1 1 1 1 1 1 4 3 3 3 3
3 3 3 4 1 1 1 2 1 1 1 5 1 1 1 4 3 3 3
3 3 4 1 1 1 1 1 1 1 1 1 1 1 1 1 4 3 3
3 3 4 1 1 2 1 1 1 1 1 1 1 2 1 1 4 3 3
3 3 4 1 1 1 1 1 1 1 1 1 1 1 1 1 4 3 3
3 3 3 4 1 1 1 1 1 1 1 1 1 1 1 1 4 3 3 3
3 3 4 1 1 1 1 1 1 1 1 1 1 1 1 1 4 3 3
3 3 4 1 1 2 1 1 1 1 1 1 2 1 1 4 3 3
3 3 4 1 1 1 1 1 1 1 1 1 1 1 1 1 4 3 3
3 3 3 4 1 1 1 2 1 1 1 2 1 1 1 4 3 3 3
3 3 3 3 4 1 1 1 1 1 1 1 1 1 4 3 3 3 3
3 3 3 3 3 4 1 1 1 4 1 1 1 4 3 3 3 3 3
3 3 3 3 3 3 4 4 4 3 4 4 4 3 3 3 3 3 3
3 3 3 3 3 3 3 3 3 3 3 3 3 3 3 3 3 3 3
3 3 3 3 3 3 3 3 3 3 3 3 3 3 3 3 3 3 3

%1=regular fuel assembly
%2=control rod fuel assembly
%3=zircaloy clad reflector assembly
%4=Al clad reflector assembly
%5=CR#1
%6=CR#2
%135 regular fuel elements
%+ 8 control rod elements
%= approximately 142 regular fuel elements


% --- Material Card --- %

therm gre gre6.00t

mat steel sum rgb <128> <128> <128>   %Steel (Gray)
26000.03c 8.51888875e-2               %Iron
25055.03c 8.46518204e-4               %Manganese

mat poison sum rgb <108> <0> <0>      %BC4 (Dark Red)
5010.03c 1.5567E-02                   %Boron-10
5011.03c 6.2660E-02                   %Boron-11
6000.03c 1.9557E-02                   %Carbon

mat fuel sum moder gre 6012 rgb <197> <92> <23>   %Fuel (Orange)
```

```
92234.03c 9.33150E-08                                %U-234
92235.03c 8.64137E-06                                %U-235
92236.03c 1.85836E-08                                %U-236
92238.03c 5.32131E-07                                %U-238
6012.03c 5.08811256E-02                              %Graphite
6000.03c 3.53580703E-02                              %Free Carbon
5010.03c 1.45913E-07                                 %Boron-10
5011.03c 5.83652E-07                                 %Boron-11
26000.03c 1.85516144e-5                              %Iron
23000.03c 6.1354E-07                                 %Vanadium
8016.03c 1.8590E-05                                  %Oxygen

mat coolant sum      rgb <100> <223> <249>           %Coolant (Light Blue)
7014.03c 4.3433e-5                                   %Nitrogen
8016.03c 1.0212e-5                                   %Oxygen

mat air sum rgb <230> <251> <255>                    %Air Gap (White Blue)
7014.03c 4.3433e-5                                   %Nitrogen
8016.03c 1.0212e-5                                   %Oxygen

Mat zircaloy sum rgb <128> <0> <255>                 %Zircaloy (Purple)
26000.03c 0.0001699236                               %Iron
50000.03c 0.000077674                                %Tin
40000.03c 4.2084792E-02                              %Zirconium
7014.03c 1.4266E-05                                  %Nitrogen
8016.03c 2.2604E-04                                  %Oxygen
1001.03c 8.5822E-05                                  %Hydrogen
5010.03c 3.6192E-08                                  %Boron-10
5011.03c 1.4568E-07                                  %Boron-11
3006.03c 2.1501E-08                                  %Lithium
21045.03c 4.3737E-06                                 %Scandium
47000.03c 5.468400E-06                               %Gold
49000.03c 2.397450E-07                               %Indium

Mat aluminium sum rgb <255> <255> <0>                %Al 6063 (Yellow)
13027.03c 0.0599572887                               %Aluminium
26000.03c .0004385235                                %Iron
22000.03c 1.654383E-05                               %Titanium
25055.03c 1.4716E-05                                 %Manganese
14000.03c 2.302895E-04                               %Silicone
12000.03c 4.490570E-04                               %Magnesium
24000.03c 1.554861E-05                               %Chromium
22000.03c 1.654383E-05                               %Titanium
27059.03c 6.8592E-06                                 %Cobalt

Mat reflector sum moder gre 6012 rgb <46> <50> <107> %Graphite (Blue)
6012.03c 0.08374907                                  %Graphite
5010.03c 3.7105968e-8                                %Boron-10
5011.03c 1.48423872e-7                               %Boron-11
26000.03c 1.801745e-5                                %Iron
22000.03c 2.521180E-07                               %Titanium
23000.03c 2.3690E-06                                 %Vanadium
3006.03c 7.3682E-09                                  %Lithium
1001.03c 2.2327E-05                                  %Hydrogen
8016.03c 1.1161E-05                                  %Oxygen
73181.03c 2.7790E-07                                 %Tantalum
22000.03c 2.521180E-07                               %Titanium
28000.03c 2.398884E-08                               %Nickel

mat test sum rgb 255 0 128                           %Test regions (Hot Pink)
7014.03c 4.3433e-5                                   %Nitrogen


%--- Mesh Generation --- %
%plot 3 5000 5000 [130.823]
%plot 3 5000 5000 [80.823]
%plot 3 1000 1000 [0]
%plot 3 5000 5000 [-80.823]
%plot 3 2000 2000 [-54.97]
%plot 2 8300 3920 [-40.64]
```

```
plot 2 8000 4000 [-42.818]
mesh 2 3150 2460
mesh 3 2000 2000 [0]


% --- Calculation Input --- %
set pop 70000 300 50 1.0 10
```

C.6 Revision p

The most recent revision I have made is p. In this revision I changed the orientation of the control rods so that a reflector runs through the core when the rods are withdrawn and they are inserted from above (except the transient rod). I also returned to the number densities I had calculated using ANL-6174. In this example it can be seen that I used “set his 1” in order to check fission source convergence.

```
% --- Treat Rev. p --- %                                  %133 fuel elements.


% --- Library File Path --- %
set acelib "/Users/serpent//SERPENT2/XSData/sss_endfb7u.xsdata"
set declib "/Users/serpent/SERPENT2/XSData/sss_endfb7.dec"
set nfylib "/Users/serpent/SERPENT2/XSData/sss_endfb7.nfy"


% --- Surface Card --- %

surf 1 sqc 0 0 5.08                     %Assembly including coolant gaps.
surf 2 octa 0 0 5.0292 6.318613         %Surface at the outside edge of the Zr.
surf 3 octa 0 0 4.9657 6.255113         %Surface at the outside edge of the void.
surf 4 octa 0 0 4.826 6.115413          %Surface at the outside edge of the fuel.
surf 5 pz 60.96                         %The top of the fuel.
surf 6 pz -60.96                        %The bottom of the fuel.
surf 7 pz 61.595                        %The top of the top Zr spacer.
surf 8 pz -61.595                       %The bottom of the bottom Zr spacer.
surf 9 pz 61.833125                     %The top surface between the zircaloy 3 cladding and Al 6063 cladding.
surf 10 pz -61.833125                   %The bottom surface between the zircaloy 3 cladding and Al 6063 cladding.
surf 11 pz 61.960125                    %The top inside surface between the Al 6063 cladding and graphite reflector.
surf 12 pz -61.960125                   %The bottom inside surface between the Al 6063 cladding and graphite reflector.
surf 13 pz 122.920125                   %The top outside surface between the Al 6063 cladding and graphite reflector.
surf 14 pz -122.920125          %The bottom outside surface between the Al 6063 cladding and graphite reflector.
surf 15 pz 123.047125                   %The top surface of the Al 6063 cladding (top of core).
surf 16 pz -123.047125                  %The bottom surface of the Al 6063 cladding (bottom of core).
surf 17 octa 0 0 4.9022 6.191613        %Surface between air gap and Al 6063 cladding of top and bottom reflector.
surf 18 sqc 0 0 96.52                   %Outer edge of the core.
surf 19 sqc 0 0 101.6                   %Inner edge of the reflector. Outside the 2" air gap.
surf 20 sqc 0 0 162.56                  %Outer edge of the reflector.
surf 21 cyl 0 0 2.2225                  %Control rod steel tube OD.
surf 22 cyl 0 0 1.905                   %Control rod steel tube ID.
surf 23 pz 228.6                        %Top of the control rod 1.
surf 24 pz 76.2                         %Surface between poison and zircaloy follower of control rod 1.
surf 25 pz -76.2                        %Surface between zircaloy follower and steel follower of control rod 1.
surf 26 pz 228.6                        %Top of the control rod 2.
surf 27 pz 76.2                         %Surface between poison and zircaloy follower of control rod 2.
surf 28 pz -76.2                        %Surface between zircaloy follower and steel follower of control rod 2.
surf 29 pz 228.6                        %Top of SD control rod.
surf 30 pz 76.2                         %Surface between poison and zircaloy follower of SD control rod.
surf 31 pz -76.2                        %Surface between zircaloy follower and steel follower of SD control rod.
surf 32 pz -228.6                       %Bottom boundary condition.
```

```
surf 33 cyl 0 0 2.54                    %Control rod assembly hole ANL-6173 pg 12.
surf 34 cyl 0 0 2.8575                  %ID of control rod fuel cladding. The cladding between the fuel and the control
rod. (From INL model-surf 477)
surf 35 cyl 0 0 2.9591                  %OD of control rod fuel cladding. The cladding between the fuel and the control
rod. (From INL model-surf 472)
surf 36 cyl 0 0 .9525                   %Outgas tube. (INL model-surf 300)
surf 37 pz 83.423125                    %Top of outgas tube. (INL model-surf 301)
surf 38 sqc 0 0 4.1656                  %Square section of top and bottom reflectors. (INL model-surf 200)
surf 39 octa 0 0 4.8006 6.020723628     %Surface between reflector and air gap of top and bottom reflector. (INL model-
surf 201)
surf 40 pz 228.6                        %Top boundary condition.
surf 41 pz 70.246875                    %Top reflector transition from octahedral to cuboid. (INL model-surf 250)
surf 42 pz -70.246875                   %Bottom reflector transition from octahedral to cuboid. (INL model-surf 250)


% --- Cell Card --- %

% Control Rod 1 %
cell 141 5 coolant 2 -1 -15 16          %Coolant channel around assembly.
cell 142 5 zircaloy 3 -2 -7 8           %Zircaloy 3 casing of assembly (25 mils).
cell 143 5 air 4 -3 -7 8                %Void within assembly (55 mils).
cell 144 5 fuel 35 -4 -5 6              %Fuel within assembly (six 3.9"x3.9"x8" blocks stacked 48" high).
cell 145 5 zircaloy 33 -4 5 -7          %Top Zr spacer (1/4").
cell 146 5 zircaloy 33 -4 8 -6          %Bottom Zr spacer (1/4").
cell 147 5 zircaloy 33 -2 7 -9          %Top Zircaloy 3 fuel end-cap (3/32").
cell 148 5 zircaloy 33 -2 10 -8         %Bottom Zircaloy 3 fuel end-cap (3/32").
cell 149 5 aluminium 33 -2 9 -11        %Top Al 6063 reflector cladding bottom end-cap(50 mils).
cell 150 5 aluminium 33 -2 12 -10       %Bottom Al 6063 reflector cladding top end-cap(50 mils).
cell 151 5 reflector 33 -39 41 -13      %Top assembly reflector (24").
cell 152 5 reflector 33 -39 14 -42      %Bottom assembly reflector (24").
cell 153 5 aluminium -2 17 11 -13       %Top Reflector Al 6063 cladding (50 mils).
cell 154 5 aluminium -2 17 14 -12       %Bottom Reflector Al 6063 cladding (50 mils).
cell 155 5 aluminium 33 -2 13 -15       %Top Al 6063 reflector cladding top end-cap(50 mils).
cell 156 5 aluminium 33 -2 16 -14       %Bottom Al 6063 reflector cladding bottom end-cap(50 mils).
cell 157 5 air -21 23                   %Void where the control rod would go through.
cell 158 5 steel -21 22 -23 24          %Control rod poison carbon steel housing.
cell 159 5 poison -22 -23 24            %Control rod poison.
cell 160 5 zircaloy -21 22 -24 25       %Control rod zircaloy follower housing.
cell 161 5 reflector -22 -24 25         %Control rod zircaloy follower reflector.
cell 162 5 steel -21 22 -25 32          %Control rod steel follower housing.
cell 163 5 reflector -22 -25 32         %Control rod steel follower reflector.
cell 164 5 outside 21 -16 32 -1         %Brings flux to zero outside of the core (sets boundary conditions).
cell 165 5 outside 21 15                %Brings flux to zero outside of the core (sets boundary conditions).
cell 166 5 air -33 21 -15 16            %Control rod assembly hole.
cell 167 5 air -35 34 -5 6              %Void between fuel and cladding (wraps around control rod).
cell 168 5 zircaloy -34 33 -5 6         %Fuel cladding (wraps around control rod).
cell 169 5 air 39 -17 11 -13            %Top reflector air gap between reflector and Al.
cell 170 5 air 39 -17 -12 14            %Bottom reflector air gap between reflector and Al.
cell 171 5 reflector 33 -38 11 -41      %Top reflector square portion.
cell 172 5 air 38 -39 11 -41            %Top reflector air gap between reflector and Al in the square portion.
cell 173 5 reflector 33 -38 -12 42      %Bottom reflector square portion.
cell 174 5 air 38 -39 -12 42            %Bottom reflector air gap between reflector and Al in the square portion.

% Control Rod 2 %
cell 241 6 coolant 2 -1 -15 16          %Coolant channel around assembly.
cell 242 6 zircaloy 3 -2 -7 8           %Zircaloy 3 casing of assembly (25 mils).
cell 243 6 air 4 -3 -7 8                %Void within assembly (55 mils).
cell 244 6 fuel 35 -4 -5 6              %Fuel within assembly (six 3.9"x3.9"x8" blocks stacked 48" high).
cell 245 6 zircaloy 33 -4 5 -7          %Top Zr spacer (1/4").
cell 246 6 zircaloy 33 -4 8 -6          %Bottom Zr spacer (1/4").
cell 247 6 zircaloy 33 -2 7 -9          %Top Zircaloy 3 fuel end-cap (3/32").
cell 248 6 zircaloy 33 -2 10 -8         %Bottom Zircaloy 3 fuel end-cap (3/32").
cell 249 6 aluminium 33 -2 9 -11        %Top Al 6063 reflector cladding bottom end-cap(50 mils).
cell 250 6 aluminium 33 -2 12 -10       %Bottom Al 6063 reflector cladding top end-cap(50 mils).
cell 251 6 reflector 33 -39 41 -13      %Top assembly reflector (24").
cell 252 6 reflector 33 -39 14 -42      %Bottom assembly reflector (24").
cell 253 6 aluminium -2 17 11 -13       %Top Reflector Al 6063 cladding (50 mils).
cell 254 6 aluminium -2 17 14 -12       %Bottom Reflector Al 6063 cladding (50 mils).
cell 255 6 aluminium 33 -2 13 -15       %Top Al 6063 reflector cladding top end-cap(50 mils).
cell 256 6 aluminium 33 -2 16 -14       %Bottom Al 6063 reflector cladding bottom end-cap(50 mils).
```

```
cell 257 6 air -21 26                       %Void where the control rod would go through.
cell 258 6 steel -21 22 -26 27              %Control rod poison carbon steel housing.
cell 259 6 poison -22 -26 27                %Control rod poison.
cell 260 6 zircaloy -21 22 -27 28           %Control rod zircaloy follower housing.
cell 261 6 reflector -22 -27 28             %Control rod zircaloy follower reflector.
cell 262 6 steel -21 22 -28 32              %Control rod steel follower housing.
cell 263 6 reflector -22 -28 32             %Control rod steel follower reflector.
cell 264 6 outside 21 -16 32 -1             %Brings flux to zero outside of the core (sets boundary conditions).
cell 265 6 outside 21 15                    %Brings flux to zero outside of the core (sets boundary conditions).
cell 266 6 air -33 21 -15 16                %Control rod assembly hole.
cell 267 6 air -35 34 -5 6                  %Void between fuel and cladding (wraps around control rod).
cell 268 6 zircaloy -34 33 -5 6             %Fuel cladding (wraps around control rod).
cell 269 6 air 39 -17 11 -13                %Top reflector air gap between reflector and Al.
cell 270 6 air 39 -17 -12 14                %Bottom reflector air gap between reflector and Al.
cell 271 6 reflector 33 -38 11 -41          %Top reflector square portion.
cell 272 6 air 38 -39 11 -41                %Top reflector air gap between reflector and Al in the square portion.
cell 273 6 reflector 33 -38 -12 42          %Bottom reflector square portion.
cell 274 6 air 38 -39 -12 42        %Bottom reflector air gap between reflector and Al in the square portion.

% Shutdown Control Rod Fuel Assembly %
cell 41 2 coolant 2 -1 -15 16               %Coolant channel around assembly.
cell 42 2 zircaloy 3 -2 -7 8                %Zircaloy 3 casing of assembly (25 mils).
cell 43 2 air 4 -3 -7 8                     %Void within assembly (55 mils).
cell 44 2 fuel 35 -4 -5 6                   %Fuel within assembly (six 3.9"x3.9"x8" blocks stacked 48" high).
cell 45 2 zircaloy 33 -4 5 -7               %Top Zr spacer (1/4").
cell 46 2 zircaloy 33 -4 8 -6               %Bottom Zr spacer (1/4").
cell 47 2 zircaloy 33 -2 7 -9               %Top Zircaloy 3 fuel end-cap (3/32").
cell 48 2 zircaloy 33 -2 10 -8              %Bottom Zircaloy 3 fuel end-cap (3/32").
cell 49 2 aluminium 33 -2 9 -11             %Top Al 6063 reflector cladding bottom end-cap(50 mils).
cell 50 2 aluminium 33 -2 12 -10            %Bottom Al 6063 reflector cladding top end-cap(50 mils).
cell 51 2 reflector 33 -39 41 -13           %Top assembly reflector (24").
cell 52 2 reflector 33 -39 14 -42           %Bottom assembly reflector (24").
cell 53 2 aluminium -2 17 11 -13            %Top Reflector Al 6063 cladding (50 mils).
cell 54 2 aluminium -2 17 14 -12            %Bottom Reflector Al 6063 cladding (50 mils).
cell 55 2 aluminium 33 -2 13 -15            %Top Al 6063 reflector cladding top end-cap(50 mils).
cell 56 2 aluminium 33 -2 16 -14            %Bottom Al 6063 reflector cladding bottom end-cap(50 mils).
cell 57 2 air -21 29                        %Void where the control rod would go through.
cell 58 2 steel -21 22 -29 30               %Carbon steel tube.
cell 59 2 poison -22 -29 30                 %Boron-carbide powder compacted to 1.6g/cc.
cell 60 2 zircaloy -21 22 -30 31            %Control rod Zircaloy follower housing.
cell 61 2 reflector     -22         -30 31  %Control rod Zircaloy follower reflector.
cell 62 2 steel -21 22 -31 32               %Control rod steel follower housing.
cell 63 2 reflector -22 -31 32              %Control rod steel follower reflector.
cell 64 2 outside 21 -16 32 -1              %Brings flux to zero outside of the core (sets boundary conditions).
cell 65 2 outside 21 15                     %Brings flux to zero outside of the core (sets boundary conditions).
cell 66 2 air -33 21 -15 16                 %Control rod assembly hole.
cell 67 2 air -35 34 -5 6                   %Void between fuel and cladding (wraps around control rod).
cell 68 2 zircaloy -34 33 -5 6              %Fuel cladding (wraps around control rod).
cell 69 2 air 39 -17 11 -13                 %Top reflector air gap between reflector and Al.
cell 70 2 air 39 -17 -12 14                 %Bottom reflector air gap between reflector and Al.
cell 71 2 reflector 33 -38 11 -41           %Top reflector square portion.
cell 72 2 air 38 -39 11 -41                 %Top reflector air gap between reflector and Al in the square portion.
cell 73 2 reflector 33 -38 -12 42           %Bottom reflector square portion.
cell 74 2 air 38 -39 -12 42         %Bottom reflector air gap between reflector and Al in the square portion.

% Standard Fuel Assembly %
cell 1 1 coolant 2 -1 -15 16                %Coolant channel around assembly.
cell 2 1 zircaloy 3 -2 -7 8                 %Zircaloy 3 casing of assembly (25 mils).
cell 3 1 air 4 -3 -7 8                      %Void within assembly (55 mils).
cell 4 1 fuel -4 -5 6                       %Fuel within assembly (six 3.9"x3.9"x8" blocks stacked 48" high).
cell 5 1 zircaloy -4 5 -7                   %Top Zr spacer (1/4").
cell 6 1 zircaloy -4 8 -6                   %Bottom Zr spacer (1/4").
cell 7 1 zircaloy -2 7 -9                   %Top Zircaloy 3 fuel end-cap (3/32").
cell 8 1 zircaloy -2 10 -8                  %Bottom Zircaloy 3 fuel end-cap (3/32").
cell 9 1 aluminium -2 36 9 -11              %Top Al 6063 reflector cladding bottom end-cap(50 mils).
cell 10 1 aluminium -2 12 -10               %Bottom Al 6063 reflector cladding top end-cap(50 mils).
cell 11 1 reflector -39 37 -13              %Top assembly reflector (24").
cell 12 1 reflector -39 14 -42              %Bottom assembly reflector (24").
cell 13 1 aluminium -2 17 11 -13            %Top Reflector Al 6063 cladding (50 mils).
cell 14 1 aluminium -2 17 14 -12            %Bottom Reflector Al 6063 cladding (50 mils).
```

```
cell 15 1 aluminium -2 13 -15                %Top Al 6063 reflector cladding top end-cap(50 mils).
cell 16 1 aluminium -2 16 -14                %Bottom Al 6063 reflector cladding bottom end-cap(50 mils).
cell 17 1 outside -16 32 -1                  %Brings flux to zero outside of the core (sets boundary conditions).
cell 18 1 air -36 9 -37                      %Outgas Tube.
cell 19 1 air 39 -17 11 -13                  %Top reflector air gap between reflector and Al.
cell 20 1 air 39 -17 -12 14                  %Bottom reflector air gap between reflector and Al.
cell 21 1 reflector -39 36 41 -37            %Top reflector octahedral portion with outgas tube.
cell 22 1 reflector -38 36 11 -41            %Top reflector square portion with outgas tube.
cell 23 1 air 38 -39 11 -41                  %Top reflector air gap between reflector and Al in the square portion.
cell 24 1 reflector -38 42 -12               %Bottom reflector square portion.
cell 25 1 air 38 -39 42 -12          %Bottom reflector air gap between reflector and Al in the square portion.
cell 26 1 outside 15                         %Brings flux to zero outside of the core (sets boundary conditions).

% Aluminium Can Dummy Fuel Assembly %
cell 75 3 coolant 2 -1 -15 16                %Coolant channel around assembly.
cell 76 3 aluminium -2 17 -13 14             %Reflector Al 6063 cladding (50 mils).
cell 77 3 reflector -39 -13 14               %Reflector.
cell 78 3 outside -16 32 -1                  %Brings flux to zero outside of the core (sets boundary conditions).
cell 79 3 air -17 39 -13 14                  %Air gap between reflector and Al cladding.
cell 80 3 aluminium -2 13 -15                %Top Al 6063 reflector cladding top end-cap(50 mils).
cell 81 3 aluminium -2 16 -14                %Bottom Al 6063 reflector cladding bottom end-cap(50 mils).
cell 82 3 outside 15                         %Brings flux to zero outside of the core (sets boundary conditions).

% Zircaloy Can Dummy Fuel Assembly %
cell 101 4 coolant 2 -1 -15 16               %Coolant channel around assembly.
cell 102 4 zircaloy 3 -2 -7 8                %Zircaloy 3 casing of assembly (25 mils).
cell 103 4 air 4 -3 -7 8                     %Void within assembly (55 mils).
cell 104 4 reflector -4 -5 6                 %Fuel within assembly (six 3.9"x3.9"x8" blocks stacked 48" high).
cell 105 4 zircaloy -4 5 -7                  %Top Zr spacer (1/4").
cell 106 4 zircaloy -4 8 -6                  %Bottom Zr spacer (1/4").
cell 107 4 zircaloy -2 7 -9                  %Top Zircaloy 3 fuel end-cap (3/32").
cell 108 4 zircaloy -2 10 -8                 %Bottom Zircaloy 3 fuel end-cap (3/32").
cell 109 4 aluminium -2 9 -11                %Top Al 6063 reflector cladding bottom end-cap(50 mils).
cell 110 4 aluminium -2 12 -10               %Bottom Al 6063 reflector cladding top end-cap(50 mils).
cell 111 4 reflector -39 41 -13              %Top assembly reflector (24").
cell 112 4 reflector -39 14 -42              %Bottom assembly reflector (24").
cell 113 4 aluminium -2 17 11 -13            %Top Reflector Al 6063 cladding (50 mils).
cell 114 4 aluminium -2 17 14 -12            %Bottom Reflector Al 6063 cladding (50 mils).
cell 115 4 aluminium -2 13 -15               %Top Al 6063 reflector cladding top end-cap(50 mils).
cell 116 4 aluminium -2 16 -14               %Bottom Al 6063 reflector cladding bottom end-cap(50 mils).
cell 117 4 outside -16 32 -1                 %Brings flux to zero outside of the core (sets boundary conditions).
cell 118 4 air 39 -17 11 -13                 %Top reflector air gap between reflector and Al.
cell 119 4 air 39 -17 -12 14                 %Bottom reflector air gap between reflector and Al.
cell 120 4 reflector -38 11 -41              %Top reflector square portion.
cell 121 4 air 38 -39 11 -41                 %Top reflector air gap between reflector and Al in the square portion.
cell 122 4 reflector -38 -12 42              %Bottom reflector square portion.
cell 123 4 air 38 -39 -12 42         %Bottom reflector air gap between reflector and Al in the square portion.
cell 124 4 outside 15                        %Brings flux to zero outside of the core (sets boundary conditions).

% Access Hole Fuel Assembly %

% Access Hole Dummy Fuel Assembly %

% Shielding Assembly %

% Thermocouple Fuel Assembly %

% Core %
cell 30 0 outside 40                         %Brings flux to zero outside of the core (sets boundary conditions).
cell 31 0 outside -32                        %Brings flux to zero outside of the core (sets boundary conditions).
cell 32 0 outside 20 -15 16                  %Brings flux to zero outside of the core (sets boundary conditions).
cell 33 0 outside -16 32 18                  %Brings flux to zero outside of the core (sets boundary conditions).
cell 34 0 fill 10 -18 32 -40                 %Core.
cell 35 0 coolant 18 -19 -15 16              %Air gap between core and reflector. (not sure if there is a air gap)
cell 36 0 reflector 19 -20 -15 16            %Outside reflector.
cell 37 0 outside 15 18                      %outside


% --- Lattice --- %
lat 10 1 0 0 19 19 10.16
```

```
3 3 3 3 3 3 3 3 3 3 3 3 3 3 3 3 3 3 3
3 3 3 3 3 3 3 3 3 3 3 3 3 3 3 3 3 3 3
3 3 3 3 3 3 4 4 4 3 4 4 4 3 3 3 3 3 3
3 3 3 3 3 4 1 1 1 4 1 1 1 4 3 3 3 3 3
3 3 3 3 4 1 1 1 1 1 1 1 1 1 4 3 3 3 3
3 3 3 4 1 1 1 2 1 1 1 5 1 1 1 4 3 3 3
3 3 4 1 1 1 1 1 1 1 1 1 1 1 1 4 3 3
3 3 4 1 1 2 1 1 1 1 1 1 1 2 1 1 4 3 3
3 3 4 1 1 1 1 1 1 1 1 1 1 1 1 1 4 3 3
3 3 3 4 1 1 1 1 1 1 1 1 1 1 1 4 3 3 3
3 3 4 1 1 1 1 1 1 1 1 1 1 1 1 1 4 3 3
3 3 4 1 1 2 1 1 1 1 1 1 2 1 1 4 3 3
3 3 4 1 1 1 1 1 1 1 1 1 1 1 1 1 4 3 3
3 3 3 4 1 1 1 2 1 1 1 2 1 1 1 4 3 3 3
3 3 3 3 4 1 1 1 1 1 1 1 1 1 4 3 3 3 3
3 3 3 3 3 4 1 1 1 4 1 1 1 4 3 3 3 3 3
3 3 3 3 3 3 4 4 4 3 4 4 4 3 3 3 3 3 3
3 3 3 3 3 3 3 3 3 3 3 3 3 3 3 3 3 3 3
3 3 3 3 3 3 3 3 3 3 3 3 3 3 3 3 3 3 3
```

%1=regular fuel assembly
%2=control rod fuel assembly
%3=zircaloy clad reflector assembly
%4=Al clad reflector assembly
%5=CR#1
%6=CR#2
%135 regular fuel elements
%+ 8 control rod elements
%= approximately 142 regular fuel elements

% --- Material Card --- %

therm gre gre6.00t

```
mat steel sum rgb <128> <128> <128>          %Steel (Gray)
26000.03c 8.51888875e-2                      %Iron
25055.03c 8.46518204e-4                      %Manganese

mat poison sum rgb <108> <0> <0>             %B4C (Dark Red)
5010.03c 1.39515714e-2                       %Boron-10
5011.03c 5.58062855e-2                       %Boron-11
6012.03c 1.74394642e-2                       %Carbon

mat fuel sum moder gre 6012  rgb <197> <92> <23>   %Fuel (Orange)
92234.03c 9.33150E-08                        %U-234
92235.03c 8.64137E-06                        %U-235
92236.03c 1.85836E-08                        %U-236
92238.03c 5.32131E-07                        %U-238
6012.03c 5.08811256E-02                      %Carbon
6000.03c 3.53580703E-02                      %Carbon
5010.03c 1.45913E-07                         %Boron-10
5011.03c 5.83652E-07                         %Boron-11
26000.03c 1.85516144e-5                      %Iron

mat coolant sum      rgb <100> <223> <249>   %Coolant (Light Blue)
7014.03c 4.3433e-5                           %Nitrogen
8016.03c 1.0212e-5                           %Oxygen

mat air sum          rgb <230> <251> <255>   %Air Gap (White Blue)
7014.03c 4.3433e-5                           %Nitrogen
8016.03c 1.0212e-5                           %Oxygen

Mat zircaloy sum rgb <128> <0> <255>         %Zircaloy (Purple)
26000.03c 0.0001699236                       %Iron
50000.03c 0.000077674                        %Tin
40000.03c 4.2084792E-02                      %Zirconium

Mat aluminium sum rgb <255> <255> <0>        %Al 6063 (Yellow)
```

```
13027.03c 0.0599572887                                  %Aluminium
26000.03c .0004385235                                   %Iron

Mat reflector sum moder gre 6012 rgb <46> <50> <107>    %Graphite (Blue)
6012.03c 0.08374907                                     %Carbon
5010.03c 3.7105968e-8                                   %Boron-10
5011.03c 1.48423872e-7                                  %Boron-11
26000.03c 1.801745e-5                                   %Iron

mat test sum rgb 255 0 128                              %Test regions (Hot Pink)
7014.03c 4.3433e-5                                      %Nitrogen


%--- Mesh Generation --- %
%plot 3 5000 5000 [130.823]
%plot 3 5000 5000 [80.823]
plot 3 5000 5000 [0]
%plot 3 5000 5000 [-80.823]
%plot 3 2000 2000 [-54.97]
%plot 3 1000 1000 [70]          %View outgas tube and square portion of reflector perpendicular to z.
%plot 3 1000 1000 [71]          %View outgas tube and octahedral portion of reflector perpendicular to z.
%plot 3 1000 1000 [84]          %View octahedral portion of reflector perpendicular to z.
%plot 3 1000 1000 [-70]         %View outgas tube and square portion of reflector perpendicular to z.
%plot 3 1000 1000 [-71]         %View outgas tube and octahedral portion of reflector perpendicular to z.
%plot 3 1000 1000 [-84]         %View octahedral portion of reflector perpendicular to z.
%plot 3 1000 1000 [123]         %View of Al end caps perpendicular to z (top).
%plot 3 1000 1000 [-123]        %View of Al end caps perpendicular to z (bottom).
plot 2 8300 3920 [-40.64]
plot 2 2000 1000
mesh 2 3150 2460
mesh 3 2000 2000 [0]


% --- Calculation Input --- %
set pop 30000 500 50 1.0 10
set his 1
```

REFFERENCES

1. S. K. Bhattacharyya, "Design Analysis of the Upgraded TREAT Reactor," *Proceedings of Thermal-Reactor Bernhmark Calculations, Techniques, Results, and Applications*, Uptown, New York (1982).
2. T. E. Booth, *A Sample Problem for Variance Reduction in MCNP*, LA-10363-MS, Los Alamos National Laboratory (1985).
3. F. B. Brown, A Review of Monte Carlo Criticality Calculations - Convergence, Bias, Statistics, LA-UR- 09-02377, Los Alamos National Laboratory (2009).
4. F. B. Brown, *Fundamentals of Monte Carlo Particle Transport*, LA-UR-05-4983, Los Alamos National Laboratory (2005).
5. J. Campbell, Materials and Fuels Complex Capabilities, URL: http:// http://www.inl.gov/research/mfc-capabilities/, Accessed Feb 2015
6. D. C. Crawford, R. W. Swanson, A. E. Wright, R. E. Holtz, "RIA Testing Capability of the Transient Reactor Test Facility," *Fuel Cycle Options for Light Water Reactors and Heavy Water Reactors*, pp. 99-109, IAEA (1999).
7. D. C. Crawford, L. W. Deitrich, R. E. Holtz, R. W. Swanson, A. E. Wright, *Experimental Capabilities of the Transient Reactor Test (TREAT) Facility*, American Nuclear Society (1998).
8. J. J. Duderstadt and L. J. Hamilton, *Nuclear Reactor Analysis*, John Wiley & Sons Inc. (1976).
9. T. Ehresman, Transient Reactor Test Facility, URL: http://www.inl.gov/research/transient-reactor-test-facility/, Accessed Jan 2015.

10. Engineering Toolbox, Coefficients of Linear Thermal Expansion, URL: http://www.engineeringtoolbox.com/linear-expansion-coefficients-d_95.html, Accessed Feb 2015, The Engineering Toolbox (2015a)
11. Engineering Toolbox, Molecular Mass of Air, URL: http://www.engineeringtoolbox.com/molecular-mass-air-d_679.html, Accessed Feb 2015, The Engineering Toolbox (2015b)
12. G. A. Freund, P. Elias, D. R. MacFarlane, J. D. Geier, J. F. Boland, *Design Summary Report on the Transient Reactor Test Facility TREAT,* Argonne National Laboratory Report 6034 (1960).
13. J. H. Handwerk and R. C. Lied, *The Manufacture of the Graphite-Urania Fuel Matrix for TREAT,* Argonne National Laboratory Report 5963 (1960).
14. M. Heman, Sigma: Evaluated Nuclear Data File (ENDF) Retrieval & Plotting, URL: http://www.nndc.bnl.gov/sigma/, Accessed Feb 2015, National Nuclear Data Center, Brookhaven National Laboratory (2011).
15. Idaho National Laboratory, *Future Transient Testing of Advanced Fuels,* INL report INL/EXT-09-16392 (2009).
16. H. P. Iskenderain, *Post Criticality Studies on the TREAT Reactor,* Argonne National Laboratory Report 6115 (1960).
17. M. H. Kalos, P. A. Whitlock, *Monte Carlo Methods*, 1986, Second Revised and Enlarged Edition, Wiley-VCH (2008).
18. F. Kirn, J. Boland, H. Lawroski, R. Cook, *Reactor Physics Measurements in TREAT,* Argonne National Laboratory Report 6173 (1960).

19. R. A. Knief, Nuclear Engineering: Theory and Technology of Commercial Nuclear Power, 1992, Second Edition, American Nuclear Society (2008).
20. G. F. Knoll, *Radiation Detection and Measurement*, 1980, fourth edition, John Wiley & Sons Inc. (2010).
21. J. R. Lamarsh and A. J. Baratta, *Introduction to Nuclear Engineering*, 1975, Third Edition, Prentice Hall (2001).
22. J. Leppänen, Source Convergence Serpent 2, URL: http://ttuki.vtt.fi/serpent/viewtopic.php?f=15&t=1968&p=4805&hilit=source+convergence+serpent+2&sid=277dc70f4770816333597d5f2ad1c349#p4805, Accessed Feb 2015, VTT Technical Research Centre of Finland (2013a).
23. J. Leppänen, Serpent – a Continuous-energy Monte Carlo Reactor Physics Burnup Calculation Code, VTT Technical Research Centre of Finland (2013b).
24. J. Leppänen, Implicit capture, URL: http://ttuki.vtt.fi/serpent/viewtopic.php?f=24&t=1689&p=3777&hilit=variance+reduction&sid=24d0e2c2df6da499f221b9f1289e2df1#p3777, Accessed Feb 2015, VTT Technical Research Centre of Finland (2013c).
25. J. Leppänen, Revised calculation of time constants (version 2.1.13), URL: http://ttuki.vtt.fi/serpent/viewtopic.php?f=24&t=1878&p=5383&hilit=adjoint+weighted+time+constants&sid=b54175e31a397811101e1c543ceb7716#p5383, Accessed Feb 2015, VTT Technical Research Centre of Finland (2013d).
26. D. Okrent, C. E. Dickerman, J. Gasidlo, D. M. O'Shea, D. F. Schoeberle, *The Reactor Kinetics of the Transient Reactor Test Facility (TREAT)*, Argonne National Laboratory Report 6174 (1960).

27. Oxford Dictionary, *Monte Carlo Method*, URL: http://www.oxforddictionaries.com/us/definition/american_english/Monte-Carlo-method, Accessed Feb 2015.
28. R. W. Swanson and L. J. Harrison, "The Effect of Carbon Crystal Structure on TREAT Reactor Physics Calculations", *Proceedings of International Reactor Physics Conference*, Jackson Hole, Wyoming (1988).
29. VTT, *Serpent*, URL: http://montecarlo.vtt.fi/, Accessed Feb 2015, VTT Technical Research Centre of Finland (2014).